Graduate Theses and Dissertations

2015

Optical responses at the nanoparticle-biological interface with an introduction to optical microscopy in undergraduate analytical chemistry curriculum

Ashley Elizabeth Augspurger
Iowa State University

Optical responses at the nanoparticle-biological interface with an introduction to optical microscopy in undergraduate analytical chemistry curriculum

by

Ashley Elizabeth Augspurger

A dissertation submitted to the graduate faculty

in partial fulfillment of the requirements for the degree of

DOCTOR OF PHILOSOPHY

Major: Analytical Chemistry (Specialization – *Chemical Education*)

Program of Study Committee:
Ning Fang, Major Professor
Thomas J. Greenbowe
Emily Smith
Pat Thiel
Theresa Windus
Jake Petrich

Iowa State University

Ames, Iowa

2015

DEDICATION

I would like dedicate my dissertation to my amazing husband, Paul. You have been my biggest supporter and I love you.

TABLE OF CONTENTS

NOMENCLATURE

LSPR	Localized surface plasmon resonance
RI	Refractive Index
PRET	Plasmon Resonance Energy Transfer
FRET	Förster's Resonance Energy Transfer
DIC	Differential interference contrast
MSN	Mesoporous silica nanoparticle
NA	Numerical aperture
FWHM	Full Width at Half Maximum
DTT	Dithiothreitol
GSH	Glutathione
SWH	Science Writing Heuristic
COMA	Chemical Optical Microscopy Assessment

ACKNOWLEDGMENTS

ABSTRACT

Plasmonic nanoparticles have been gaining attention in the medical field for their use as chemical and biological sensors, drug delivery vectors and contrast agents for cellular imaging; however, the ability to monitor the chemical binding events and drug delivery kinetics is limited. The majority of this body of work explores nanoparticles optical responses as they undergo energy transfer processes for biological sensing. The latter portion of this dissertation discusses optical microscopy in undergraduate analytical chemistry.

In the first experiment, plasmon resonance energy transfer between gold nanospheres and cytochrome c was investigated. As cytochrome c adsorbs to the surface of a nanoparticle, the plasmonic energy is transferred from the nanoparticle to cytochrome c, as a result there are spectral dips in the extinction spectrum of the gold nanoparticle. This optical phenomenon was studied in Hi-Fi microchannels and HeLa cells undergoing ethanol induced apoptosis.

The second set of experiments encompasses the observations of the optical changes of gold-capped mesoporous silica nanoparticles (MSNs) undergoing uncapping by dithiothreitol and glutathione. The uncapping process was studied in flow cells with dithiothreitol as the uncapping agent, and also in lung cancer cells using glutathione as the cleaving agent. Differential interference contrast (DIC) microscopy was employed to image the optical changes as gold is cleaved from MSNs.

As part of the chemical education project, an optical microscopy laboratory experiment was created, implemented and assessed in an instrumental analysis course for junior and senior level undergraduate chemistry students. Students were introduced to optical microscopy and nanoparticles through the use of a dark field microscope to image a reaction between copper wire

and silver nitrate in the first section. In the second portion of the experiment, students imaged gold, silver and silica nanospheres with the aid of bandpass filters and were also introduced to the concept of localized surface plasmon resonances. There were two formats for the experiment, traditional and inquiry based. Students were split into two groups, each group performing one format of the experiment and their learning gains were monitored with the Chemical Optical Microscopy Assessment (COMA) that was created for this purpose. The learning outcomes based on the COMA and laboratory report scores were compared to determine with which instructional method students had higher learning gains.

CHAPTER 1. INTRODUCTION

In the last 20 years, nanoparticles have gained a lot of attention for their potential applications in biosensing, drug delivery and cellular imaging.[1-4] The recent growth in nanoparticle research has come about due to several innovations. Synthesis methods are now able to better control the size and shape of nanoparticles, leading to more homogeneity of colloidal solutions. Instrumentation is now able to monitor nanoparticles at the single particle level, in real time and below the diffraction limit. The motivation behind this dissertation was to study nanoparticles' unique optical properties to better understand their application as contrast agents for cellular imaging and biosensing.

This dissertation also encompasses a project in chemical education research. As a teaching assistant and analytical chemist I wanted to create a laboratory experiment for undergraduate analytical chemists, to update analytical chemistry curriculum and bring what "real analytical chemists" do in research to the students. Only 3% of academic institutions in the United States teaches optical microscopy in lecture or lab, but when chemical industry was surveyed they said that knowledge of optical microscopy is desired.[5,6] I wanted to do this project as a way to have students understand what chemists are doing in the field and to motivate them about chemistry and prepare them for their future chemistry careers.

This rest of this chapter will continue with an introduction to nanoparticles, their optical properties and applications in biosensing. Two common optical microscopy methods, differential interference contrast and dark field, used to observe the process of biosensing are discussed. There is also a brief background on the theory used for the chemical education project - the

learning cycle as well as the Science Writing Heuristic, an alternative laboratory report format that incorporates the learning cycle.

Chapter 2 discusses the optical phenomena of plasmon resonance energy transfer (PRET) detected with DIC Microscopy. The PRET process encompasses the energy transfer process between cytochrome c and gold nanospheres as cytochrome c binds and dissociates from the surface of gold nanospheres. As this happens, the cytochrome c absorbs the plasmonic energy from the nanoparticle resulting in spectral dips where the two spectra overlap.

Chapter 3 delves into the world of mesoporous silica nanoparticles (MSNs) as drug delivery agents. MSNs are able to have cargo loaded into the pores, have the pores capped with gold nanoparticles, then subsequently uncap the pores due to change in a cellular environment to release the cargo into a cell. One of the factors that limit the application of MSNs as drug delivery agents is the lack of being able to monitor the entire delivery process from cellular uptake, to pore uncapping and cargo release. In this chapter the kinetics and imaging of the uncapping process of gold-capped MSNs is discussed.

Chapters 4 and 5 focus on the creation, implementation and assessment of an inquiry and traditional optical microscope experiment for undergraduate analytical chemists. A dark field microscope experiment for undergraduate analytical students was created, in which the students image a replacement reaction between silver nitrate and copper wire, students also image nanospheres and investigate the concept of localized surface plasmon resonances. The laboratory experiment was created in two formats – inquiry and traditional. To measure the student learning gains from their experience with the experiment, an assessment was created that covers the basics of optical microscopy.

Chapter 6 includes the concluding remarks on the research presented and insights into further research that can be done in analytical chemical education, biological sensing and drug delivery.

Introduction to Nanoparticles

Nanoparticles are, generally speaking, any particle that is in the nanoscale, 10-100 nm in size. Nanoparticles can be composed of a variety of materials, but for the purposes of this dissertation gold and silica nanoparticles will be discussed. Noble metal nanoparticles are the most commonly used as contrast agents for non-fluorescence imaging. When choosing a probe for chemical and biological sensing, gold nanoparticles are ideal probes. They are biocompatible, for cellular imaging, they have well understood surface chemistry to conjugate ligands for chemical sensing and they are also photostable for long imaging times.[2,7,8]

Plasmonic nanospheres, such as gold, have a strong optical signal in the visible and near-IR range. Their optical spectra can be determined from Mie Theory, an exact solution of Maxwell's equations.[9,10] A quasi-static approximation to Mie Theory is used when discussing plasmonic nanospheres much smaller than the wavelength of light; this approximation allows us to only consider dipolar contributions in determining the scattering and absorption cross sections.[10-12] The roles of higher modes as well as phase retardation have a small contribution to the absorption and scattering cross sections and are not included.[10] The scattering (σ_{sc}) and absorption (σ_{abs}) cross sections, when combined, give the extinction spectra of a nanoparticle over all electric and magnetic oscillations and are described by the following equations[11,12]:

$$\sigma_{(sc)} = \frac{128\,\pi^5}{3\lambda^4} a^6 \left|\frac{m^2-1}{m^2+1}\right|^2 \qquad (1)$$

$$\sigma_{(abs)} = \frac{8\pi^2}{\lambda} a^3 Im\left(\frac{m^2-1}{m^2+1}\right) \qquad (2)$$

Where λ is the wavelength of light, a is a particle's radius, Im is the imaginary portion of the equation and m is the relative refractive index. The relative refractive index is the particle's refractive index divided by the medium's refractive index. When the scattering and absorption cross sections are added together we arrive at the extinction cross section, this gives rise to the optical spectra for the nanoparticle. At small diameters, less than 10 nm, the extinction spectrum is dominated by absorption, but as the diameter increases the scattering contribution also increases.[10,11] Spheres are isotropic nanoparticles, meaning they only produce a single dipolar localized surface plasmon resonance (LSPR). As the diameter of the particle increases, the LSPR will red-shift while also undergoing broadening.

The optical properties that noble metal nanoparticles possess come from an optical phenomenon known as LSPR.[13] LSPR is the collective oscillation of the conducting electrons in the nanoparticle. This occurs when particles are irradiated with light within a narrow band of wavelengths. The wavelengths that excite the conducting electrons the greatest is determined by several factors, such as size, shape and composition of the nanoparticle. The dielectric medium (surrounding environment) also has an effect on the LSPR position and can produce a shift in the LSPR. The nanoparticle produces a signal at wavelengths other than the LSPR wavelength – non-resonance wavelengths.[14]

Nanoparticles that do not produce an LSPR are termed non-plasmonic nanoparticles. One of the most commonly used non-plasmonic nanoparticles are mesoporous silica nanoparticles (MSNs). These dielectric nanoparticles are able to scatter light, but do not have a dipole producing an LSPR.

MSNs are nanoparticles synthesized from silica with pores that go through the particle. They are commonly used to study drug delivery because the pores can be loaded with drugs or fluorescent dyes and then capped to trap the loaded cargo.[1,15] For drug delivery studies, the dye diffusion is monitored to study the release behavior and kinetics.[15-18] MSNs are advantageous for drug delivery because they have large surface areas due to their pores. They are also easy to synthesize and functionalize, are biocompatible, and photostable.[1,19,20]

The optical properties of MSNs are vastly different than that of gold nanoparticles. Silica nanoparticles are known to predominately scatter light in the visible and IR ranges when the particles are on the nanometer scale.[21,22] Silica is a non plasmonic, dielectric material; therefore, there is no LSPR so the optical spectrum does not contain any peaks – it is electronically inert.[10,23]

The optical properties of silica nanoparticles can be altered with the aid of noble metals such as gold. Gold nanospheres can be deposited on the surface of the MSNs to cap pores. When gold is added to silica the optical properties of the resulting system are altered. As more gold spheres are added to the MSNs, they interact more (termed plasmon coupling) and the LSPR peak will broaden until the optical spectrum resembles that of a core-shell particle.[24] Gold can also be added to silica as a shell rather than nanoparticles. When this occurs, the thicker the shell the more the LSPR peak is red-shifted and broadens.[25,26]

Chemical and Biological Sensing with Nanoparticles

Chemical and biological sensing with nanoparticles can be performed with single nanoparticles or an array of nanoparticles on a surface.[3,27] During chemical and biological sensing, the optical signal from the nanoparticles changes as the analyte of interest binds to the

surface of the nanoparticle(s).[13] Sensing with nanoparticles is preferred over sensing with bulk metals because the volume of required analyte sample is decreased.[28] The measurement time is also decreased, while the detection accuracy is increased. When sensing with plasmonic nanoparticles, it is often the LSPR wavelength spectral location, signal intensity, or both that are monitored.[3,13] There are many different theories and methods used to investigate chemical sensing. The ones covered in this dissertation include Förster Resonance Energy Transfer (FRET); PRET, and refractive index (RI) sensing. There are many others, but they are beyond the scope of this research.

As an analyte binds to the surface of a nanoparticle, the local dielectric field (medium) is altered which changes the RI of the surrounding solution at the surface of the nanoparticle. This change of RI causes a spectral shift of the LSPR due to its dependence on RI. The dependence of the spectral location of the LSPR for a nanoparticle is predicted by Mie theory. The molecular layer around the nanoparticle surface alters the refractive index which will cause either a red or blue shift in the LSPR. The spectral shift then deviates from the Mie theory prediction of an unmodified nanoparticle. This is due to the analyte layer that interacts with the surface electron cloud.[27,29,30]

Refractive index sensing takes advantage of the nanoparticles' LSPR dependence on local RI and dielectric medium. As the analyte of interest binds to the surface of the nanoparticle the local RI changes and, therefore, causes a change in the spectral position of the LSPR. With RI sensing it is possible to monitor the binding events of organic molecules in real time as they have a higher RI than buffers.[30] As organic molecules bind to the surface there is a red shift in the LSPR spectral location.

FRET is a commonly used method for biological and chemical sensing as well as cellular imaging. The excitation energy is transferred through a distance dependent (1-10 nm), non-radiative (no photon is emitted and reabsorbed), dipole-dipole interaction of a donor molecule and an acceptor molecule.[31-33] The donor emission spectrum must overlap with the excitation spectrum of the acceptor in order for successful energy transfer to occur.[33]

There is a parametric proportionality between the rate of energy transfer and radiative rate constant; the resonant coupling emission and absorption dipoles compete with other radiative and non-radiative processes for deactivation.[32] The efficiency of FRET is mainly affected by the distance dependence between the donor and acceptor molecules. It is the ratio of the number of energy transfer occurrences from the donor to the acceptor divided by the total number of excitations of a donor molecule. This leads to a rate proportional of $1/R^6$ where R is the distance between the donor and acceptor.[33]

FRET does have a few drawbacks though. It can suffer from autofluorescence, optical noise and photobleaching due to the use of organic dyes, low quantum yields, narrow excitations and broad emissions.[31] It is usually performed with organic dyes, but to enhance the fluorescence signal, noble metal nanoparticles can be used as the energy donor to the dye's acceptor.[34] When the dye binds to the surface of the nanoparticle and the nanoparticle's energy is transferred to the dye, whose absorption spectrum overlaps with the nanoparticles' extinction spectrum, the excitation energy has a high probability of being transferred. It is due to the radiating plasmons of the nanoparticles that cause the dye to enhance its fluorescence signal.[34] When plasmonic nanoparticles are used as donors, the process becomes known as Plasmon Resonance Energy Transfer (PRET).

PRET uses a noble metal nanoparticle as the donor and a resonant molecule as the acceptor.[35] Like FRET, PRET is a non-radiative, distance dependent energy transfer process through a dipole-dipole interaction.[36] Rather than looking at the fluorescence of an organic dye to monitor the PRET process, as in FRET, the intensity from the nanoparticle donor is monitored.[35] As the acceptor molecule binds to the surface of the nanoparticle, and the nanoparticle's plasmon is excited by light irradiation, the signal decreases because the acceptor molecule is absorbing the plasmonic energy from the nanoparticle.[37,38] The decrease results in spectral dips where the donor extinction spectrum overlaps with the acceptor absorbance spectrum.[35] PRET is a reversible process; unlike FRET, which can photobleach over time.[39,40] PRET is also more biocompatible as organic dyes can be cytotoxic.

Predominately, intensity changes (enhancement, or quenching) and LSPR spectral changes are monitored at the single particle level with microscopy. One of the more common imaging techniques is dark field microscopy, another that offers more advantages is differential interference contrast (DIC) microscopy.

DIC Microscopy

DIC microscopy is based on interferometry. There are many variations of DIC, but the most popular, and commercially available, is Nomarski DIC. The setup of a Nomarski DIC microscope can be seen in figure 1. Using Nomarski DIC we are able to image in the visible and near-IR range. The popularity of Nomarski DIC comes from its reliance on a large condenser aperture. This provides a higher lateral resolution with a shallower depth of field than other popular types of microscopy such as dark field. DIC is also able to image and differentiate plasmonic nanoparticles in complex environments such as cells.[40-43]

In DIC microscopy, light passes through a polarizer and light becomes plane polarized. Light then passes through the first Nomarski prism where it is split into two orthogonal beams separated by a shear distance (100-200 nm). The Nomarski prism also introduces birefringence to the light paths. Each beam of light is at a 45° angle relative to the polarizer. The two light beams pass through the sample and interacts with the sample's RI. The light then passes through the objective where the image is created and onto the second Nomarski prism where the light beams are recombined. The light then passes though an analyzer. When the two beams are recombined their constructive and destructive interference pattern are put together which creates the black and white images with a grey background – shadow cast image. The shadow cast image is created from a phase shift in either of the two beams that is introduced from nanoparticles and other features on the sample plane.[41-43]

Dark Field Microscopy

Dark field microscopy is one of the more common modes of microscopy for non-fluorescent imaging. It relies on the collection of scattered light, specifically Rayleigh scattering, to create an image. The physical set up of a dark field microscope with the light path is shown in figure 2.

In standard dark field, a dark background is created by an annular (light) stop in the condenser that blocks light from directly going through from the light source to the sample plane. Only light that goes around the edges of the annular stop is allowed to pass onto the sample plane. Objects on the sample plane scatter the transmitted light at oblique angles which is then collected by the objective and passed on to the detector. If there are no objects to scatter light, the oblique light rays will not enter the objective. This is due to the numerical aperture (NA) of the

objective being at a lower setting than the condenser NA. The light that is successfully collected by the objective will appear as a white or colored feature against the dark background. When there are complex structures, such as cells, many of the components scatter light. This creates problems such as large background noise and interference with nanoparticle differentiation for cellular imaging.[41,42]

Often dark field microscopes have additional components to aid with spectroscopy. If multiple wavelengths are of interest, a monochromator or grating is placed between the objective and detector to give a high resolution spectral profile of nanoparticles.[41] When a specific wavelength of light is of interest, a bandpass filter can be placed before the condenser in the light path.

Inquiry Based Learning with the Learning Cycle

Inquiry based learning as an instructional method that came about in the 1950's with the National Science Foundation's support for science curriculum reform.[44] The scientific method is based on inquiry therefore, science should be taught with an inquiry method and be consistent with the nature of science to be able to successfully model the scientific process to students.[45] There are different levels of inquiry based learning, from open inquiry where students are given materials and they create the experimental question and procedure to investigate their question, to structured inquiry in which students are given the question to investigate and procedure but the outcome is withheld from the student.[46,47]

As an instructional strategy, concepts should be divided into phases that fit into an instructional process. Specifically, these include the identification of the concept, demonstration of the concept and application of the concept.[48-50] These three phases are the basis of the learning

cycle; an inquiry oriented approach. The three phases of the learning cycle are known as "exploration" where students are exposed to data that demonstrates the concept to be learned; "concept invention" in which students derive the concepts from the data; "application" where students apply the concept to other phenomena.[51,52] The learning cycle has been mapped out in figure 3.

The learning cycle is derived from constructivist ideas of the nature of science and developmental theory from Jean Piaget.[53,54] Constructivism and Piaget's theory are beyond the scope of this dissertation. The purpose of inquiry based learning and the learning cycle is to not only teach students science concepts, but also how to think like a scientist.

The Science Writing Heuristic

To further aid students' engagement with science instruction, the Science Writing Heuristic (SWH) is an instructional method that utilizes inquiry based learning and incorporates the learning cycle.[50,55] The SWH is an alternative laboratory report format and instructional method that helps students learn conceptually and improve their attitude toward chemistry; unlike a traditional format where students may gain laboratory techniques, but may have little else.[55,56] The main problem with traditional style laboratory instruction is that students will spend most of their time following the instructions and will arrive at the end of the laboratory period with data, which they will proceed to "plug and chug" into equations they are given and not fully understand what they are calculating.[55] When students arrive at an answer that is a large percentage off of the expected value the students will blame human error, chance, and even poor laboratory equipment; students do not go back to their procedure, their data, or the concepts

covered in the experiment to understand where the error occurred and why it did.[55] When SWH is used as an instructional method the instructor's role changes from a lecturer to a facilitator.[57,58]

From the student perspective, the biggest change is in the laboratory report notebook. Rather than have students write in the five traditional report sections (purpose, procedure, observations, data, conclusions) students are prompted in such a way as to elicit a deeper understanding and engagement with the laboratory content.[55] The deeper understanding of concepts comes from the students writing about the new information connecting it to their prior knowledge.[59]

The SWH laboratory report will include beginning questions, data and observations, claims, evidence, reading and reflection.[60] The beginning questions are student generated, based upon their reading of the laboratory manual; the questions shape what the student wants to investigate during the laboratory exercise. The students are required to state claims after completing the experiment. The claims are to answer their beginning questions, and are to be supported by their data and observations. Students also write a reflection section in which they compare their conclusions to other students, textbooks and literature, as well as reflecting on how their ideas have changed. It is this writing portion that helps students create a deeper understanding of science concepts.[50,61]

Other than a change in laboratory report formatting, the key difference between traditional laboratory instruction and SWH is the amount of control the students are given of the laboratory experiment. SWH uses guided inquiry, meaning a specific procedure is not given to the students.[55] This does not mean that students get to do whatever they want; they are bound by guidelines from the instructor.[55] This approach promotes student discussion within groups and creates a friendly and engaging learning environment.

REFERENCES

(1)   Slowing, I. I.; Trewyn, B. G.; Giri, S.; Lin, V. S. Y. *Adv. Funct. Mater.* **2007**, *17*, 1225.

(2)   Saha, K.; Agasti, S. S.; Kim, C.; Li, X.; Rotello, V. M. *Chemical Reviews* **2012**, *112*, 2739.

(3)   Zeng, S.; Yong, K.-T.; Roy, I.; Dinh, X.-Q.; Yu, X.; Luan, F. *Plasmonics* **2011**, *6*, 491.

(4)   Gu, Y.; Sun, W.; Wang, G.; Fang, N. *J. Am. Chem. Soc.* **2011**, *133*, 5720.

(5)   Fahey, A.; Tyson, J. *Anal. Chem.* **2006**, 4249.

(6)   Tyson, J. F. *Management of Modern Laboratories* **1996**, *2*, 55.

(7)   Park, C.; Youn, H.; Kim, H.; Noh, T.; Kok, Y. H.; Oh, E. T.; Park, H. J.; Kim, C. *J. Mater. Chem.* **2009**, *19*, 2310.

(8)   Sun, W.; Wang, G.; Fang, N.; Yeung, E. S. *Anal. Chem.* **2009**, *81*, 9203.

(9)   Mie, G. *Annalen der Physik* **1908**.

(10)   Kreibig, U.; Vollmer, M. *Optical Properties of Metal Clusters*; Springer: New York, 1995.

(11)   Kooij, E. S.; Poelsema, B. *Phys. Chem. Chem. Phys.* **2006**.

(12)   Bohren, C. F.; Huffman, D. R. *Absorption and Scattering of Light by Small Particles*; Wiley: New York, 1983.

(13)   Willets, K. A.; Van Duyne, R. P. In *Annu. Rev. Phys. Chem.*; Annual Reviews: Palo Alto, 2007; Vol. 58, p 267.

(14)   Daniel, M.-C.; Astruc, D. *Chemical Reviews* **2004**, 293.

14

(15)   Cauda, V.; Argyo, C.; Schlossbauer, A.; Bein, T. *J. Mater. Chem.* **2010**, *20*, 4305.

(16)   Lai, J.; Shah, B. P.; Garfunkel, E.; Lee, K.-B. *ACS Nano* **2013**, *7*, 2741.

(17)   Lai, C.-Y.; Trewyn, B. G.; Jeftinija, D. M.; Jeftinija, K.; Xu, S.; Jeftinija, S.; Lin, V. S.-Y. *Journal of American Chemical Society* **2003**, *125*, 4451.

(18)   Tan, S. Y.; Ang, C. Y.; Li, P.; Yap, Q. M.; Zhao, Y. *Chemistry* **2014**, *20*, 11276.

(19)   Vivero-Escoto, J. L.; Slowing, II; Trewyn, B. G.; Lin, V. S. *Small* **2010**, *6*, 1952.

(20)   Ma, X.; Nguyen, K. T.; Borah, P.; Ang, C. Y.; Zhao, Y. *Advanced Healthcare Materials* **2012**, *1*, 690.

(21)   Blaber, M. G.; Arnold, M. D.; Ford, M. J. *Journal of Physics* **2010**, *22*, 143201.

(22)   Stuart, H. R.; Hall, D. G. *Appl. Phys. Lett.* **1998**, *73*, 3815.

(23)   Liz-Marzan, L. M.; Giersig, M.; Mulvaney, P. *Langmuir* **1996**, *12*, 4329.

(24)   Preston, T. C.; Signorell, R. *ACS Nano* **2009**, 3696.

(25)   Oldenburg, S. J.; Averitt, R. D.; Westcott, S. L.; Halas, N. J. *Chem. Phys. Lett.* **1998**, *288*, 243.

(26)   Yang, C. K.; Chang, J. S.; Chao, S. D.; Wu, K. C. *Journal of Applied Physics* **2008**, *103*.

(27)   Sannomiya, T.; Voeroes, J. *Trends in biotechnology* **2011**, *29*, 343.

(28)   Mortazavi, D.; Kouzani, A. Z.; Kaynak, A.; Duan, W. In *Internation Conference on Complex Medical Engineering* Harbin, China, 2011, p 31.

(29)   Anker, J. N.; Hall, W. P.; Lyandres, O.; Shah, N. C.; Zhao, J.; Van Duyne, R. P. *Nature Materials* **2008**, *7*, 442.

(30)   Choi, I.; Choi, Y. *IEEE* **2011**.

(31)   Sekar, R. B.; Periasamy, A. *J. Cell Biol.* **2003**, *160*, 629.

(32)   Jares-Erijman, E. A.; Jovin, T. M. *Curr. Opin. Chem. Biol.* **2006**, *10*, 409.

(33)   Clegg, R. M. In *Laboratory Techniques in Biochemistry and Molecular Biology, FRET and FLIM Techniques*; Gadella, T. W. J., Ed.; Elsevier B.V.: 2009; Vol. 33, p 1.

(34)   Lakowicz, J. R. *Anal. Biochem.* **2005**, 171.

(35)   Liu, G. L.; Long, Y.-T.; Choi, Y.; Kang, T.; Lee, L. P. *Nat. Methods* **2007**, *4*, 1015.

(36)   Liu, L. In *Plasmon Resonance Energy Transfer Nanospectroscopy*; McGraw-Hill: 2010, p 313.

(37)   Qu, W.-G.; Deng, B.; Zhong, S.-L.; Shi, H.-Y.; Wang, S.-S.; Xu, A.-W. *Chem. Commun.* **2011**, *47*, 1237.

(38)   Juluri, B.; Lu, M.; Zheng, Y.; Huang, T.; Jensen, L. *J. Phys. Chem. C* **2009**, *113*, 18499.

(39)   Choi, Y.; Kang, T.; Lee, L. P. *Nano Lett.* **2009**, *9*, 85.

(40)   Augspurger, A. E.; Stender, A. S.; Han, R.; Fang, N. *Anal. Chem.* **2014**, *86*, 1196.

(41)   Stender, A. S.; Marchuk, K.; Liu, C.; Sander, S.; Meyer, M. W.; Smith, E. A.; Neupane, B.; Wang, G.; Li, J.; Cheng, J.-X.; Huang, B.; Fang, N. *Chemical Reviews* **2013**, *113*, 2469.

(42)   Wang, G.; Stender, A. S.; Sun, W.; Fang, N. *Analyst* **2010**, *135*, 215.

(43)   Stender, A. S.; Augspurger, A. E.; Wang, G.; Fang, N. *Anal. Chem.* **2012**, *84*, 5210.

(44)   DeBoer, G. E. *A history of ideas in science education*; Teachers College Press: New York, 1991.

(45)   Abraham, M. R. In *Chemists' Guide to Effective Teaching*; Pienta, N. J., Cooper, M. M., Greenbowe, T. J., Eds.; Pearson: New Jersey, 2005; Vol. 1.

(46)   Fay, M. E.; Bretz, S. L. *The Science Teacher* **2008**, 38.

(47)   Fay, M. E.; Grove, N. P.; Towns, M. H.; Bretz, S. L. *Chemistry Education Research and Practice* **2007**, *8*, 212.

(48)   Karplus, R.; Thier, H. D. *A new look at elementary school science*; Rand McNally: Chicago, 1967.

(49)   Renner, J. W. *Science Education* **1982**, *66*, 709.

(50)   I, J. A. R.; Greenbowe, T. J.; Hand, B. M.; Legg, M. J. *Journal of College Science Teaching* **2001**, *12*, 1680.

(51)   Lawson, A. E.; Abraham, M. R.; Renner, J. W. *A theory of instruction: Using the learning cycle to teach science concepts and thinking skills*; National Association for Research and Science Teaching: Kansas State University, 1989.

(52)   Lawson, A. E. *Science teaching and the development of thinking*; Wadsworth Publishing Company: Belmont, CA, 1995.

(53)   Piaget, J. *Structuralism*; Harper and Row: New York, 1970.

(54)   Bodner, G. M. *Journal of Chemical Education* **1986**, *10*, 873.

(55)   Greenbowe, T. J.; Hand, B. In *Chemists' Guide to Effective Teaching*; Pienta, N. J., Cooper, M. M., Greenbowe, T. J., Eds.; Pearson: Upper Saddle River, NJ, 2005; Vol. 1, p 140.

(56)   Lazarowitz, R.; Tamir, P. In *Handbook of Research on Science Teaching and Learning*; Gable, D. L., Ed.; MacMillian: New York, 1990.

17

(57)   Poock, J.; Burke, K. A.; Cantonwine, D.; Greenbowe, T. J.; Hand, B. M. In *National Meeting of the American Chemical Society* New Orleans, LA, 2004.

(58)   Burke, K. A.; Poock, J.; Greenbowe, T. J.; Hand, B. M. In *National Meeting of the American Chemical Society* New Orleans, LA, 2004.

(59)   Campbell, B.; Kaunda, L.; Allie, S.; Buffler, A.; Lubben, F. *Journal of Research in Science Teaching* **2000**, *37*, 839.

(60)   Rudd II, J. A. Dissertation, Iowa State University, 2001.

(61)   Prain, V.; Hand, B. *Teaching and Teacher Education* **1996**, *12*, 609.

(62)   Augspurger, A. E.; Stender, A. S.; Marchuk, K.; Greenbowe, T. J.; Fang, N. *Journal of Chemical Education* **2014**, *91*, 908.

FIGURES
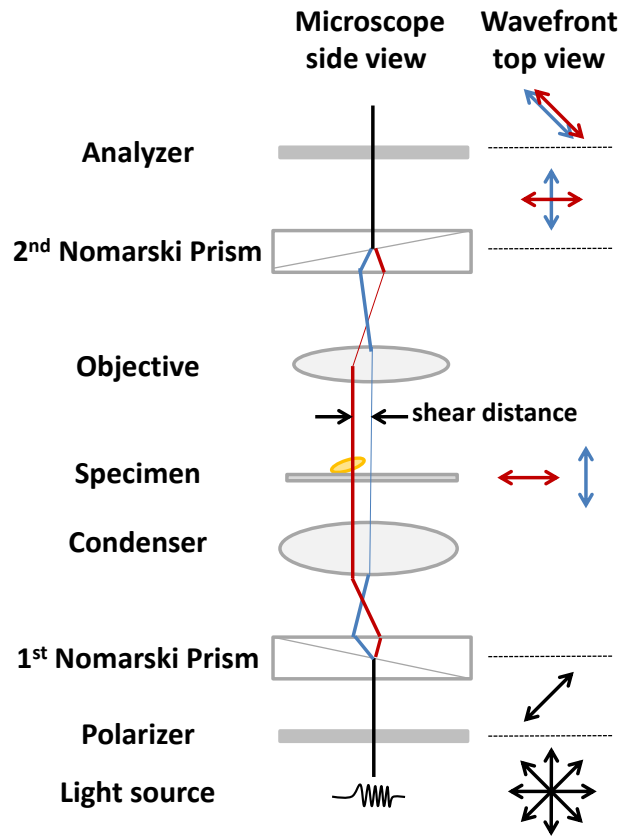
Figure 1. Nomarski DIC Microscope with corresponding light path.
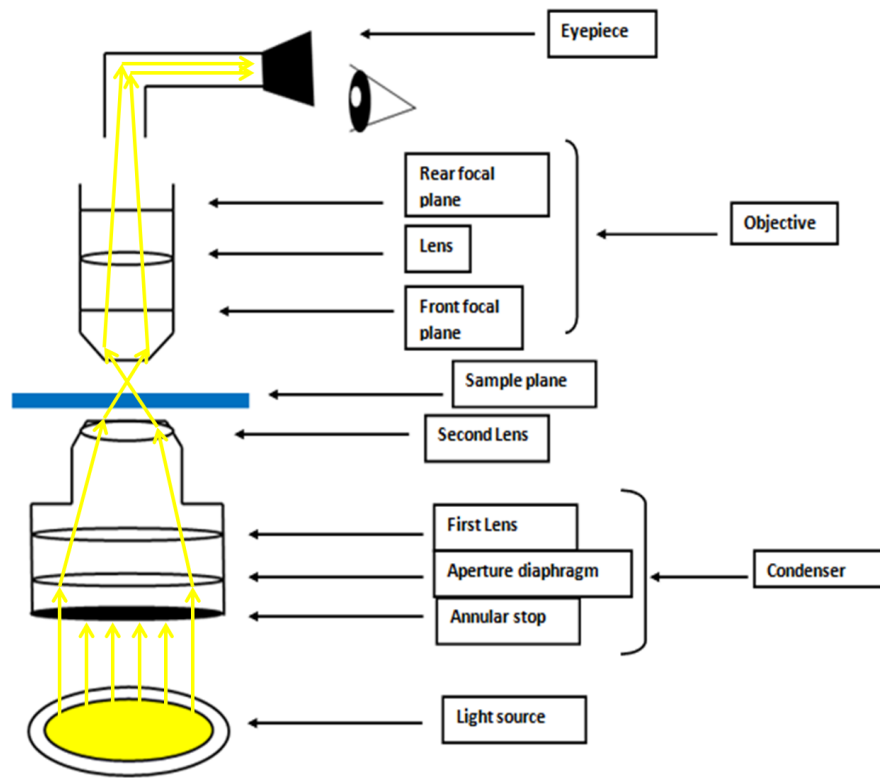
Figure 2. Dark field microscope with light path and components labeled.[62]
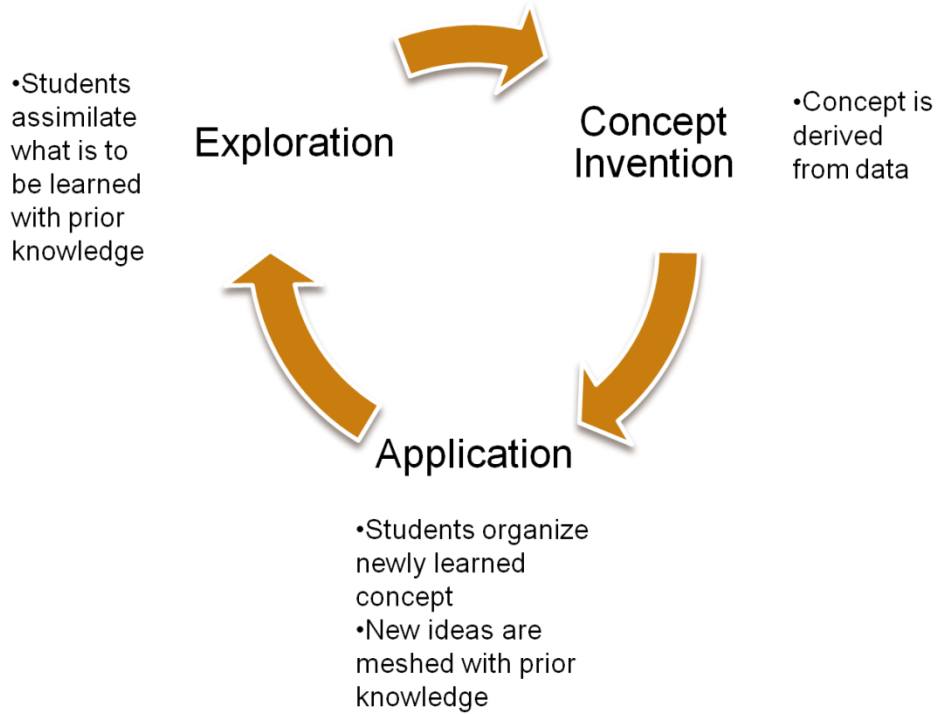
Figure 3. The learning cycle shown in three steps: exploration, concept invention and application.

CHAPTER 2. DETECTING PLASMON RESONANCE ENERGY TRANSFER WITH DIFFERENTIAL INTERFERENCE CONTRAST (DIC) MICROSCOPY

Ashley E. Augspurger[†], Anthony S. Stender[†], Rui Han[†], Ning Fang[†]

Abstract

Gold nanoparticles are ideal probes for studying intracellular environments and energy transfer mechanisms due to their plasmonic properties. Plasmon resonance energy transfer (PRET) relies on a plasmonic nanoparticle to donate energy to a nearby resonant acceptor molecule, a process which can be observed due to the plasmonic quenching of the donor nanoparticle. In this study a gold nanosphere was used as the plasmonic donor, while the metalloprotein cytochrome c was used as the acceptor molecule. Differential Interference Contrast (DIC) microscopy allows for simultaneous monitoring of complex environments and noble metal nanoparticles in real time. Using DIC and specially designed microfluidic channels, we were able to monitor PRET at the single gold particle level and observe the reversibility of PRET upon the introduction of phosphate buffered saline to the channel. In an additional experiment, single gold particles were internalized by HeLa cells and were subsequently observed undergoing PRET as the cell hosts underwent morphological changes brought about by ethanol-induced apoptosis.

Introduction

Noble metal nanoparticles have been shown to be an excellent and versatile option for optical imaging because of their signature optical property known as the localized surface plasmon resonance (LSPR).[42,63-66] These plasmonic nanoparticles have high absorption and scattering cross-sections at the LSPR wavelengths, and the optical signal does not suffer from photobleaching. The optical properties of plasmonic nanoparticles are tunable with different particle size and shape. Furthermore, the surface of noble metal nanoparticles can be readily modified with ligands or surfactants, making it easy to tailor the individual nanoprobes for a specific chemical interaction.

Biosensing with noble metal nanoparticles is typically accomplished by monitoring changes in the LSPR of individual nanoparticles.[67] Detection of molecular binding to the surface of the nanoparticles can be observed by a shift in the LSPR peak,[68] or by significant changes in the intensity of the LSPR peak. The latter case is most prominent when coupling occurs between biomolecules and metallic nanoparticles, which is further described below. This coupling has been termed plasmon resonance energy transfer (PRET).[65,68-70]

PRET involves the coupling of molecular and plasmonic resonances between a plasmonic donor and a resonant acceptor molecule; it is most easily explained by making a comparison with Förster's resonance energy transfer (FRET). FRET describes a non-radiative energy transfer process between two dipoles – a donor molecule and a resonant acceptor molecule. In comparison, PRET is a non-radiative process in which the plasmon energy from a nanoparticle is transferred to adjacent acceptor molecules that have matching electronic transition energy.[69,70]

Therefore, PRET is highly dependent on the degree of spectral overlap between the donor plasmon spectrum and the acceptor molecule's absorption spectrum. Greater overlap results in stronger quenching of the plasmon resonance, which is characterized by dips in signal intensity within the plasmon spectrum of the donor particle. The position of the signal intensity dips directly corresponds to the absorption wavelengths of the resonant molecule.[69,70]

In this study gold nanoparticles were used as plasmonic donors and cytochrome c as the resonant acceptor molecule. Cytochrome c has two electronic states, oxidized and reduced. In the oxidized state there is a broad absorption peak between 540-560 nm. In the reduced state there are two absorption peaks, one at 525 nm and a more dominant peak at 550 nm.[68]

Cytochrome c is a metalloprotein found in the mitochondria of a cell; it plays a significant role in multiple biological processes, including metabolism and apoptosis.[71] Apoptosis is a set of individual processes that lead to the programmed death of cells. Once such pathway arises when the membranes of mitochondria become permeable, and in response, cytochrome c is released from the mitochondria into the cytosol.[72] As cytochrome c moves into the cytosol it quickly becomes reduced.[72] The process of apoptosis is initiated when reduced cytochrome c is coupled to inositol-3-phosphate receptor, a calcium channel mediator located on the outer membrane of the endoplasmic reticulum. This coupling causes calcium ions to be released into the cytosol and results in apoptosis of the affected cell.[73] This apoptotic pathway can easily be induced in the lab with the proper stimulants such as ethanol.[74]

PRET has previously been studied with dark field microscopy.[68,69,75] Dark field microscopy relies on the principle of light scattering. An annular stop in the light path prevents the directly transmitted light from passing through the condenser and objective to the detector. Instead, only the scattered light from the sample enters the objective. Dark field microscopy is a

popular technique for studying nanoparticles because of its simplicity and high sensitivity.[42] However, anything on the sample plane that scatters light will be detected, and it is possible for unwanted debris to cause an increase in the background noise.[76]

It is important to reinvestigate PRET with differential interference contrast (DIC) microscopy as it offers the ability to image PRET within complex environments at high resolution.[42] DIC has the capability to observe specific cells continuously over long periods of time. With DIC it is also possible to differentiate nanoprobes from cellular and intracellular organelles. High image resolution and a shallow depth of field are attained because a full aperture is used unlike dark field microscopy.[77] Furthermore, DIC microscopy is essentially two-beam interferometry; therefore, it is less sensitive to scattered light from surrounding cellular components when compared to dark field microscopy.

The principles of DIC microscopy have been discussed at length in earlier papers,[42,78] but we provide a brief overview here. DIC is a mode of microscopy that utilizes polarization and interferometry to generate an image. Plane polarized light passes through a Nomarski prism that splits the polarized light into two orthogonal polarization beams. As the light passes through the sample, a phase shift is introduced to the two beams by objects in the sample plane. The phase shift is caused by a change in the refractive index around the sample.[77] After the light exits the sample plane, it is collected by the objective, and the two light beams are recombined with a second Nomarski prism. The phase shift in the two beams and their resultant interference pattern generates a shadow cast image of the sample against a grey background.[78]

In a series of experiments discussed below, PRET was detected with DIC and with the aid of microchannels. The microchannels enabled a study of the PRET process over time, both as cytochrome c adsorbs to individual gold nanospheres and as the PRET effect was reversed due to

the addition of phosphate buffered saline. Because DIC provides a good platform to study complex environments,[42] PRET was also studied within HeLa cells that were treated with ethanol to induce apoptosis. During apoptosis, the release of reduced cytochrome c was monitored with the aid of cysteamine modified gold spheres. Cytochrome c is known to electrostatically bind to charged carboxylic acid and amine functional groups; cysteamine contains a thiol group which covalently binds to the surface of gold and an amine group which electrostatically binds to cytochrome c.[79]

Materials and Methods

DIC microscopy. A Nikon Eclipse 80i upright microscope was used for collecting images. In DIC mode a 100× 1.4 numerical aperture (NA) Plan Apo oil immersion objective and a 1.4 NA oil immersion condenser were used. Filters with full width at half maximum of 10 nm were purchased from Thorlabs. Movies and images were taken with a CMOS Hamamatsu Orca Flash2.8 (1920 × 1440 imaging array with 3.63 μm × 3.63 μm individual pixels). Movies and images collected were analyzed with ImageJ.

Modification of gold spheres on glass slides. Cleaned glass slides (Electron Microscopy Sciences, Hatfield, PA) were modified with 1-mM 3-mercaptopropyltrimethoxysilane (MPTMS) in acetone for 24 hours. Slides were then rinsed with acetone and dried with nitrogen gas.[69] 60 nm gold spheres were cast onto MPTMS modified slides, and the solution was allowed to evaporate; spheres were immobilized by the thiol group on the MPTMS.

Spheres were modified with 0.1 mM cysteamine (Sigma Aldrich) in deaerated water for two hours. Afterward the slide was washed with water to remove excess cysteamine. Cystemaine bonds with gold spheres via the thiol group leaving cysteamine's amine group available to bond

with cytochrome c. It is well known that cytochrome c bonds with amine and carboxylic acid functional groups.[79] Cysteamine modified spheres were modified with 10-µM horse heart oxidized cytochrome c or with reduced cytochrome c (Sigma Aldrich) in phosphate buffered saline (PBS, 1X, pH 6.8) for 40 min. Cytochrome c is purchased in the oxidized form; reduced cytochrome c was prepared in deoxygenated PBS with excess sodium dithionate (Sigma Aldrich).

Modifying spheres in solution. 60 nm gold spheres were purchased from BBI Solutions (Madison, WI). Gold spheres are stabilized in solution with citrate ions with a concentration of 2.6×10^{10} nanoparticles per mL. 200 µL of spheres were sonicated for 15 minutes and 4 µL of 26-mM cysteamine in de-aerated water was added to the centrifuge tube. The solution was refrigerated for 2 hours. The colloid had a resulting concentration of 2.6×10^{10} nanoparticles per mL.

Microchannel Fabrication and Imaging. Microchannels were fabricated by a previously published method using polydimethylsiloxane (PDMS) gel and a quartz slide.[80] The dimensions of the straight channel were 45 mm long, 2.69 mm wide and 267 µm deep**;** flow rate = 5.5296 µL min^{-1}; volume flow rate = 1.71×10^{-10} µL min^{-1} µm^{-3}. The Y-shaped microchannel dimensions were 80 µm wide in the arms, 160 µm wide in the main channel, 100 µm deep, and 2.5 cm long. Flow rate = 2.3 µL min^{-1}; volume flow rate = 5.76×10^{-8} µL min^{-1} µm^{-3}.

In the Y-shaped microchannel, 15 µL of 60-nm cysteamine modified gold spheres were injected into the channel and allowed to flow through the channel and attach to the coverslip. Imaging was done with 540, 550 and 560 nm filters with a vertical scan of the stage by hand every 5 minutes for 45 minutes.

In the straight channel, 40 µL of 60 nm cysteamine modified gold spheres were injected allowed to flow through to cover the channel. 250 µL of 10 µM reduced cytochrome c in deoxygenated PBS was flowed through the channel for 45 minutes followed by 250 µL of PBS for another 45 minutes. 540, 550 and 560 nm filters were used to image the channel. Vertical scanning was done by hand for each wavelength every five minutes for 45 minutes for each solution.

Culturing and Imaging HeLa cells. HeLa cells were cultured using previously published methods using cell culture medium.[76] To image cells, culturing medium was removed and cells were washed with 1X PBS. 200 µL of cysteamine modified 60-nm gold spheres (gold spheres were modified as before in solution with cysteamine) were added to the petri dish with 1 mL of new culturing medium. Cells were then incubated for 2.5 hours to naturally internalize the gold spheres.[81] After incubation with modified gold spheres, culturing medium and excess gold sphere solution was removed and cells were washed again with 1X PBS and prepared for imaging.

After cells were washed with PBS after incubation with cysteamine modified gold spheres, a slide was prepared for imaging. Two pieces of double sided tape were placed across a cleaned glass slide parallel to one another. Between the two pieces of tape some culturing medium was pipetted and the glass coverslip was secured on the glass slide with the tape.

Cells with ethanol treatment were imaged at 550 and 560 nm before ethanol was added to the slide. Ethanol was added by injecting ~100 µL of dilute ethanol in cell culturing medium between the slide and coverslip. The dilute ethanol was drawn across the coverslip with filter paper. Cells without ethanol treatment were imaged at 550 and 560 nm every ten minutes for the same amount of time as ethanol treated cells.

During imaging the cell sample was scanned vertically with a computer controlled vertical stage scanner (Sigma Koki, model no. SGSP-60YAM) attached to the fine tune knob of the microscope. 550 and 560 nm filters were used to image cells; the stage was scanned for each wavelength every ten minutes until cells died, approximately 2.5 hours after ethanol was added. The exposure time was adjusted to maintain a constant background value between wavelengths.

Results and Discussion

PRET in DIC Microscopy. To determine if PRET can be detected with DIC, a replication of a previously published study[69] was first performed. Gold spheres capped with citrate were initially imaged and found to have an LSPR at 550 nm. Spheres modified with cysteamine, the crosslinker between the gold spheres and cytochrome c, through a covalent bond were then imaged. The contrast spectra are provided in Figure S1 of the Supporting Information. Contrast is defined as the difference between the maximum and minimum particle intensities divided by the average background intensity. No change in the LSPR wavelength was observed, but a slight damping effect across the entire spectrum was observed.

After the spheres were modified with oxidized cytochrome c a spectral dip appears from 540 nm to 560 nm, where oxidized cytochrome c is known to have an absorption peak. When 60 nm gold spheres are modified with reduced cytochrome c spectral dips appeared at the corresponding absorption peaks – one at 525 nm and a more dominant one at 550 nm. In both cases of cytochrome c modification, the LSPR of the gold spheres shifted from 550 nm to 560 nm due to a change of the local refractive index at the surface of the sphere.[13] The data is seen in Figure 1.

For the rest of the study reduced cytochrome c was used because it initiates one pathway of apoptosis,[72] and the wavelength of 550 nm was chosen to monitor PRET between reduced cytochrome c and gold spheres.

Real-time PRET in Microchannels. PRET was detected during the course of reversible cytochrome c adsorption to gold spheres within a Hi-Fi optical imaging microchannel. The microfluidic channels were fabricated from a microscope slide, an ultrathin layer of PDMS and a microscope coverslip sandwiched together.[82] The microfluidic sandwich results in a microchannel that is thin enough to produce high contrast and high resolution images in transmitted-light DIC microscopy. 60 nm gold spheres modified with cysteamine were injected into the channel and allowed to move through the channel and attach to the positively charged, poly-L-lysine (PLL) coated channel surface. After a sufficient number of gold spheres were attached to the slide, the 10-μM reduced cytochrome c solution was pumped through the channel. Cytochrome c adsorbed to the gold spheres, causing a decrease in the image contrast of gold spheres at the PRET wavelength of 550 nm.

After the completion of cytochrome c adsorption onto gold spheres, the microchannel was flushed with PBS. The original contrast of gold spheres was recovered as the cytochrome c desorbed from the gold spheres.

Figure 2 A shows a gold sphere that experiences the adsorption of cytochrome c over the course of 45 minutes, followed by the desorption of cytochrome c with PBS over the subsequent 45 minutes. As cytochrome c adsorbs, the contrast decreases at 550 nm. This trend begins at 15 minutes and becomes constant after approximately 30 minutes from the beginning of cytochrome c adsorption. A similar trend can be seen for the contrast at 540 nm and 560 nm, but instead of decreasing the contrast increases, which is likely due to the change of the local refractive index.[13]

As cytochrome c desorbs, the contrast trends reverse and the original signals are obtained. This trend can be seen in the latter part of Figure 2A, 45 – 90 minutes. More examples are provided in Figure 23 of the Supporting Information.

Figure 2B shows a contrast ratio of the gold sphere graphed in 2A. The contrast ratio is the signal at 550 nm divided by the 560 nm signal. As reduced cytochrome c adsorbs to the gold sphere the contrast ratio decreases; the signal at 550 nm decreases while the signal at 560 nm increases. As reduced cytochrome c desorbs from the surface of the gold sphere, the contrast ratio increases; the signal at 550 nm increases while the signal at 560 nm decreases.

An easier way to see the contrast intensity changes would be to look at the line intensity profile of the gold sphere as cytochrome c adsorbs and desorbs from the surface. The line intensity of a sphere is simply the measurement across the diameter of the sphere from the brightest half to the darkest half. This was done for four time points during the adsorption and desorption process; 10 minutes, 30 minutes, 60 minutes and 90 minutes. The data can be seen in Figure 2 C – E. As cytochrome c adsorbs the line intensity at 550 nm decreases, while at 540 nm and 560 nm the line intensity increases. As cytochrome c is desorbed from the surface of the gold sphere, with the aid of PBS, the line intensity increases at 550 nm and decreases at 540 nm and 560 nm. These are the same trends that can be seen in the contrast spectra, Figure 2A.

A Y-shaped Hi-Fi optical imaging microchannel was employed in another similar experiment. In one arm of the Y-shaped channel, PBS was pumped through and in the other arm, the 10-μM reduced cytochrome c solution was pumped instead. Laminar flow was achieved to reduce mixing of the two solutions; this allowed for half of the spheres in the channel to act as an experimental group, the half with cytochrome c, and the other half to act as a control (the half with PBS). The results are shown in Figure S3 of the Supporting Information.

From the microchannel experiments it is established that the PRET process as well as the reversibility of PRET can be successfully monitored with DIC microscopy. Both processes occurred gradually over the course of several minutes, and the change in signal contrast was sufficient to support the finding that energy was transferred between the nanoparticle and biomolecule. Next, we investigated whether PRET could be detected with DIC microscopy in an intracellular environment.

Intracellular PRET Experiments. To study PRET intracellularly, HeLa cells were treated with dilute ethanol after the cells internalized gold spheres. Only a dilute treatment of ethanol, 100 mM, is necessary to induce apoptosis, and once this process begins, the mitochondria will release cytochrome c into the cytosol.[68,74] Once cytochrome c is in the cytosol of the cell internalized cysteamine modified gold spheres will be able to detect the cytochrome c and changes in the contrast of the gold spheres should result. When cells are not treated with ethanol cytochrome c is not released and no changes in nanoparticle contrast should occur.

Ethanol treated cells were incubated with 60 nm cysteamine modified gold spheres until they were naturally internalized. Cells were then imaged at 550 nm and 560 nm. These two wavelengths gave the strongest signals as demonstrated in the previous microchannel experiments. An initial image was taken at each wavelength before the ethanol treatment. After ethanol treatment, images at each wavelength were taken every 10 minutes until the cells had progressed through the entire apoptotic process, approximately 2.5 hours.

During apoptosis cells shrink and detach from the coverslip. Cytoplasmic membranes undergo blebbing (i.e. the organelles' membranes begin to swell).[83] Cells were imaged for the same duration and in the same manner as cells with ethanol treatment. The morphological signs

of apoptosis are not seen as readily as in cells with ethanol treatment because the apoptotic process is not speeded up with the aid of ethanol; although, cytoplasmic blebbing still occurs.

The cells were imaged over the apoptotic process. Figure 3 shows a HeLa cell before the ethanol treatment and ~2.5 h after. As the cells were imaged, the stage was vertically scanned to have each gold sphere analyzed in focus. Each sphere that was analyzed was tracked very carefully to ensure that the same sphere was analyzed throughout the apoptosis process. The images below highlight gold spheres that were analyzed. The red boxes outline the spheres graphed in Figure 4A and B, while the green boxes outline additional spheres that were analyzed; the additional spheres' graphs can be found in Figure S4 of the Supporting Information. Because the stage was scanned, not all of the gold spheres are in full focus in Figure 3. Previous work by our group has shown that it is possible to decipher an internalized gold sphere from intracellular structures.[76]

Figure 4A show contrast ratio changes of gold spheres in ethanol treated cells. After ethanol treatment the "contrast ratio" (i.e. the contrast at 550 nm divided by the contrast at 560 nm) begins to decrease and continues to do so throughout the apoptotic process. The contrast ratio decreases because the contrast at 550 nm decreases and the 560 nm contrast increases. A total of 20 spheres internalized in ethanol treated HeLa cells were analyzed in different locations of the cell. Some were closer to mitochondria than others. Even though the location of the analyzed spheres was different, all showed the same decrease in contrast ratio trend. Additional contrast ratio spectra can be found in Figure S4 in the supporting information.

Cells that were not given an ethanol treatment were imaged for the same amount of time as the ethanol treated cells (2.5 hours). Gold spheres in cells not given ethanol treatment maintained a contrast ratio above 1 for the entire period; meaning that cytochrome c was not

adsorbed. This can be seen in Figure 4B. The change of the contrast ratio in ethanol treated cells, shows that PRET was detected in cells undergoing ethanol induced apoptosis, but PRET was obviously absent from untreated cells. Additional NPs that show similar results can be found in the Supporting Information.

Conclusions

We have shown in this study that PRET can be detected and monitored with DIC microscopy in real time. This is possible in both Hi-Fi microchannels and within cells undergoing a changing morphology due to apoptosis. PRET was first studied over the course of cytochrome c adsorption on 60 nm gold spheres with the use of a microchannel. The reversibility of PRET was also studied with the aid of microchannels. In both sets of experiments the contrast changes of a gold sphere at 540 nm, 550 nm and 560 nm were monitored. As cytochrome c adsorbs, the contrast at 550 nm decreases because of the PRET interaction between cytochrome c and the gold nanoparticle. The more cytochrome c that is adsorbed, the more the contrast is decreased. Similarly, contrast at 560 nm increases as more cytochrome c adsorbs; a red shift of the LSPR from 550 nm to 560 nm is a result of the change in the local refractive index at the surface of the gold sphere.

The most significant finding from this study is the detection of PRET in a complex and changing environment, specifically HeLa cells as they undergo ethanol induced apoptosis. As cells underwent the apoptosis process, cytochrome c was released from the mitochondria into the cytosol where internalized cysteamine modified gold spheres were able to couple with cytochrome c. The coupling caused a decrease in contrast at 550 nm and an increase in contrast at 560 nm. Cells that were not treated with ethanol showed no changes in contrast at 550 nm or

560 nm. In order to elucidate details behind complex cellular behavior, it is important to be able to utilize techniques that impose minimal interruption to the cell's natural activity while achieving high resolution. As we have shown with this study, one such technique capable of accomplishing this goal is incorporating PRET experiments with DIC microscopy.

REFERENCES

(1) Willets, K. A.; Van Duyne, R. P. *Annu. Rev. Phys. Chem.* 2007, *58*, 267.

(2) Tong, L.; Wei, Q.; Wei, A.; Cheng, J.-X. *Photochem. Photobiol.* 2009, *85*, 21.

(3) Wang, G.; Stender, A. S.; Sun, W.; Fang, N. *Analyst* 2010, *135*, 215.

(4) Li, Y.; Jing, C.; Zhang, L.; Long, Y.-T. *Chem. Soc. Rev.* 2012, *41*, 632.

(5) Aaron, J.; Nitin, N.; Travis, K.; Kumar, S.; Collier, T.; Park, S. Y.; Jose-Yacaman, M.; Coghlan, L.; Follen, M.; Richards-Kortum, R.; Sokolov, K. *J. Biomed. Opt.* 2007, *12*, 034007.

(6) Anker, J. N.; Hall, W. P.; Lyandres, O.; Shah, N. C.; Zhao, J.; Van Duyne, R. P. *Nat. Mater.* 2008, *7*, 442.

(7) Choi, Y.; Kang, T.; Lee, L. P. *Nano Lett.* 2009, *9*, 85.

(8) Liu, G. L.; Long, Y.-T.; Choi, Y.; Kang, T.; Lee, L. P. *Nat. Methods* 2007, *4*, 1015.

(9) Liu, L. In *Plasmon Resonance Energy Transfer Nanospectroscopy*; McGraw-Hill: 2010, p 313.

(10) Wuttke, D. S.; Bjerrum, M. J.; Winkler, J. R.; Gray, H. B. *Science* 1992, *256*, 1007.

(11) Ripple, M. O.; Abajian, M.; Springett, R. *Apoptosis* 2010, *15*, 563.

(12) Willig, K. I.; Rizzoli, S. O.; Westphal, V.; Jahn, R.; Hell, S. W. *Nature* 2006, *440*, 935.

(13) Hirata, H.; Machado, L. S.; Okuno, C. S.; Brasolin, A.; Lopes, G. S.; Smaili, S. S. *Neurosci. Lett.* 2006, *393*, 136.

(14) Qu, W.-G.; Deng, B.; Zhong, S.-L.; Shi, H.-Y.; Wang, S.-S.; Xu, A.-W. *Chem. Commun.* 2011, *47*, 1237.

(15) Sun, W.; Wang, G.; Fang, N.; Yeung, E. S. *Anal. Chem.* 2009, *81*, 9203.

(16) Stender, A. S.; Marchuk, K.; Liu, C.; Sander, S.; Meyer, M. W.; Smith, E. A.; Neupane, B.; Wang, G.; Li, J.; Cheng, J.-X.; Huang, B.; Fang, N. *Chem. Rev.* 2013, *113*, 2469.

(17) Stender, A. S.; Augspurger, A. E.; Wang, G.; Fang, N. *Anal. Chem.* 2012, *84*, 5210.

(18) Frasconi, M.; Mazzei, F.; Ferri, T. *Anal. Bioanal. Chem.* 2010, *398*, 1545.

(19) Luo, Y.; Sun, W.; Liu, C.; Wang, G.; Fang, N. *Anal. Chem.* 2011, *83*, 5073.

(20) Gu, Y.; Di, X. W.; Sun, W.; Wang, G. F.; Fang, N. *Anal. Chem.* 2012, *84*, 4111.

(21) Willets, K. A.; Van Duyne, R. P. In *Annu. Rev. Phys. Chem.*; Annual Reviews: Palo Alto, 2007; Vol. 58, p 267.

(22) Luo, Y.; Sun, W.; Liu, C.; Wang, G. F.; Fang, N. *Anal. Chem.* 2011, *83*, 5073.

(23) Liu, X. S.; Kim, C. N.; Yang, J.; Jemmerson, R.; Wang, X. D. *Cell* 1996, *86*, 147.

FIGURES
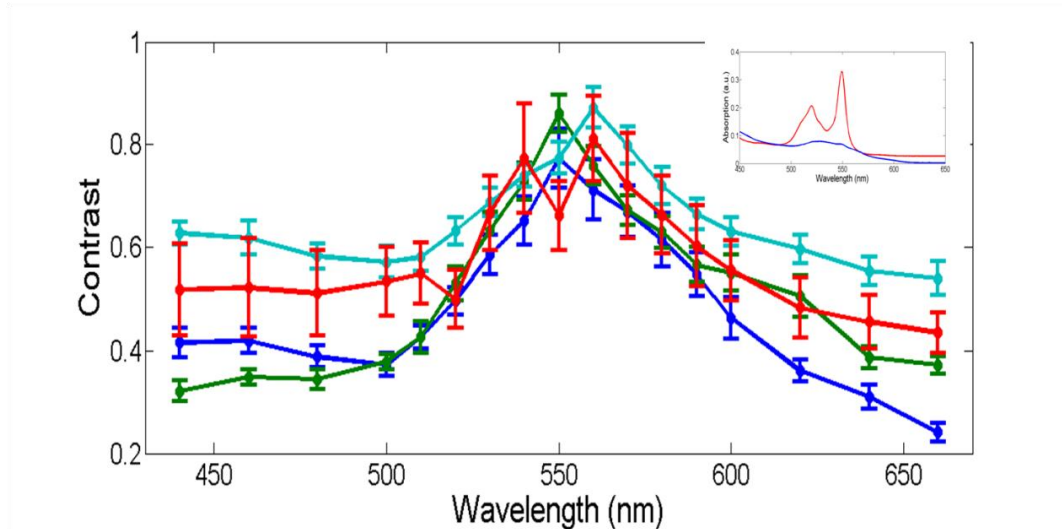
Figure 4. Contrast spectra of citrate capped gold spheres (green line), cysteamine modified gold spheres (blue line), oxidized cytochrome c modified gold spheres (aqua line), and reduced cytochrome c modified gold spheres (red line). Each line is an average of 20 spheres and the data is normalized. The inset is absorption spectra of oxidized (blue line) and reduced cytochrome c (red line).
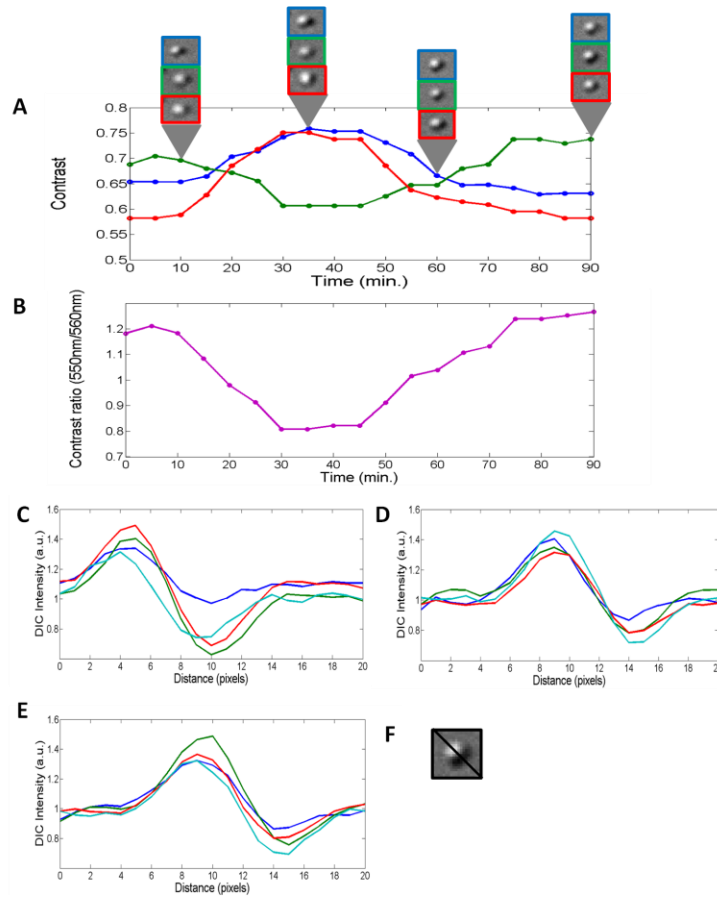
Figure 5. A) Contrast spectra of a gold sphere as reduced cytochrome c adsorb and desorbs from the surface of the sphere. The Blue line is 540 nm, green line is 550 nm and red line is 560 nm. DIC images of the gold spheres at select times are outlined in the corresponding line color. B) Contrast ratio of 550 nm/ 560 nm of the gold sphere graphed in Figure 2A. C) Line intensity profile at 540 nm of the gold sphere as cytochrome c adsorbs and desorbs from the surface. D) Line intensity profile at 550 nm of the gold sphere as cytochrome c adsorbs and desorbs from the surface. E) Line intensity profile at 560 nm of the gold sphere as cytochrome c adsorbs and desorbs from the surface. F) Example of a line intensity measurement of a sphere. The line measurement is taken across the diameter of the sphere from the brightest half to the darkest half. For C-E: blue line is 10 minutes, green line is 30 minutes, red line is 60 minutes and aqua line is 90 minutes.
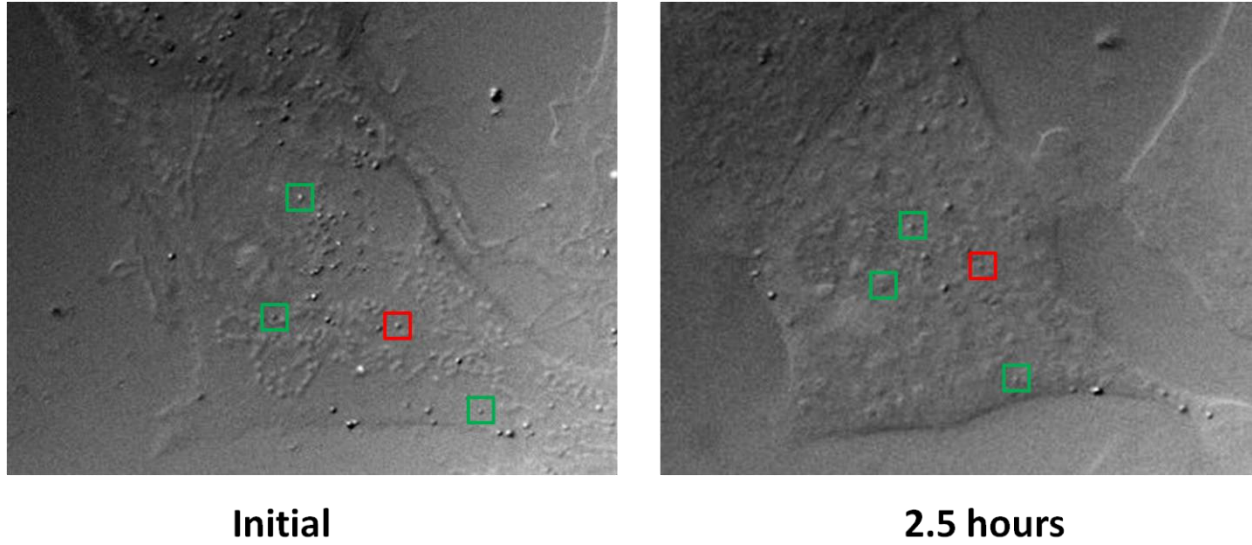
Figure 6. Ethanol treated HeLa cells undergoing apoptosis. Green and red squares highlight internalized gold spheres; red squares highlight gold spheres graphed in Figure 4.
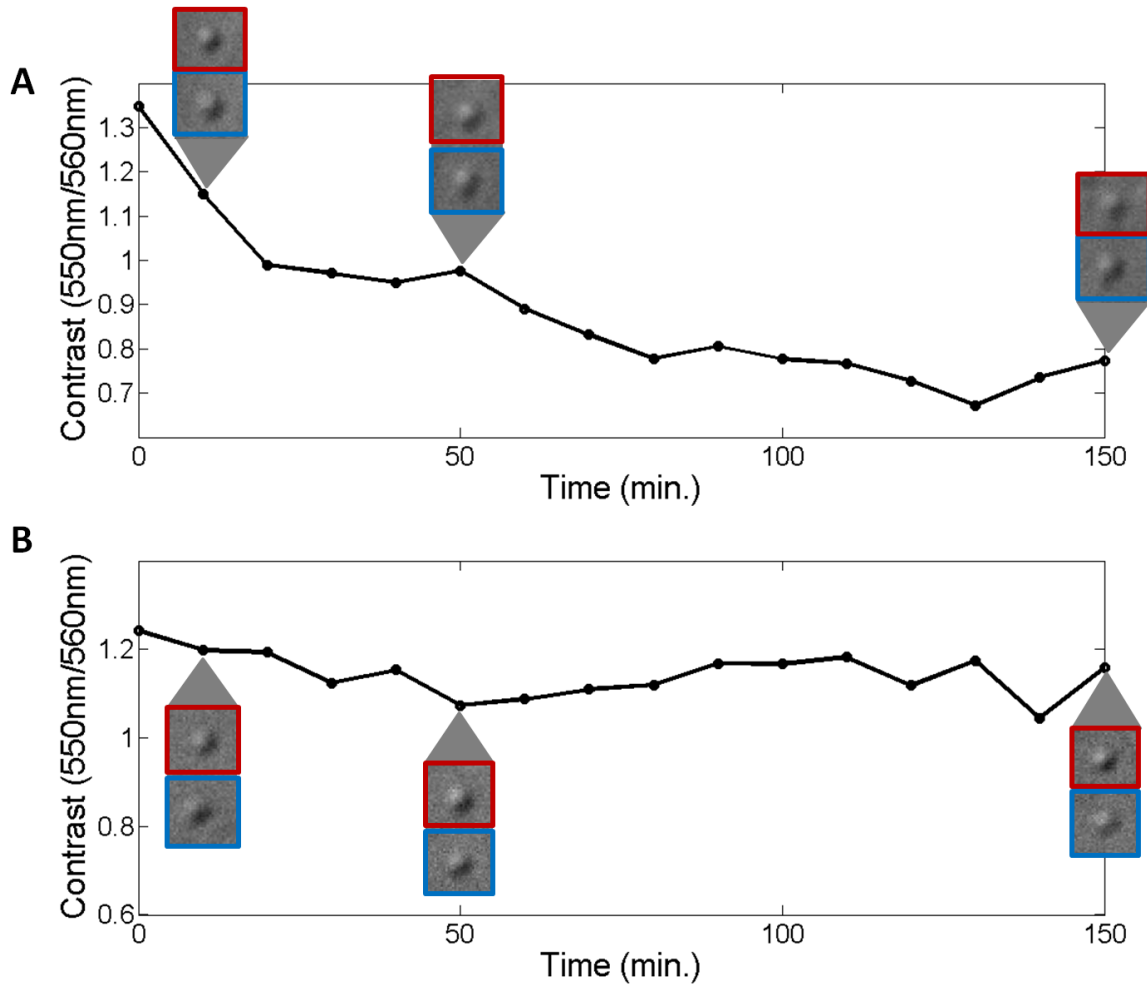
Figure 4. A) Contrast spectrum of a gold sphere in a cell with ethanol treatment with sample images of an internalized gold sphere. B) Contrast spectrum of a gold sphere in a cell without ethanol treatment with sample images of an internalized gold sphere. For both graphs, the sphere images are outlined in red (550 nm) and blue (560 nm) boxes.

APPENDIX. SUPPORT. INFORMATION
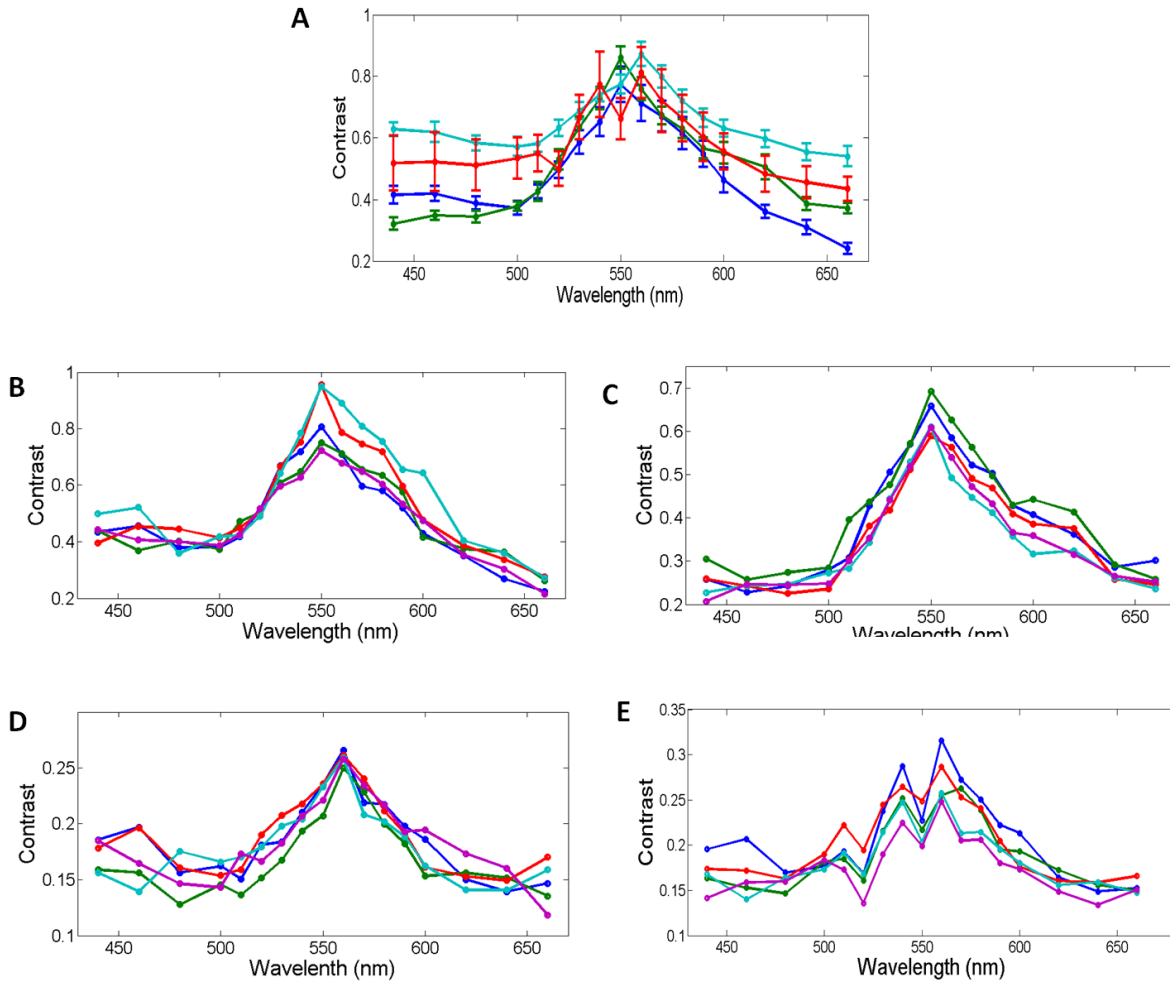
Figure S1. Contrast spectra of 4 types of gold spheres.
A) Average contrast spectra of 4 types of gold spheres: citrate capped gold spheres (green line), cysteamine modified gold spheres (blue), oxidized cytochrome c modified gold spheres (aqua), reduced cytochrome c modified gold spheres (red). B) Contrast spectra of 5 citrate capped gold spheres. C) Contrast spectra of 5 cysteamine modified gold spheres. D) Contrast spectra of 5 oxidized cytochrome c modified gold spheres. E) Contrast spectra of 5 reduced cytochrome c modified gold spheres.
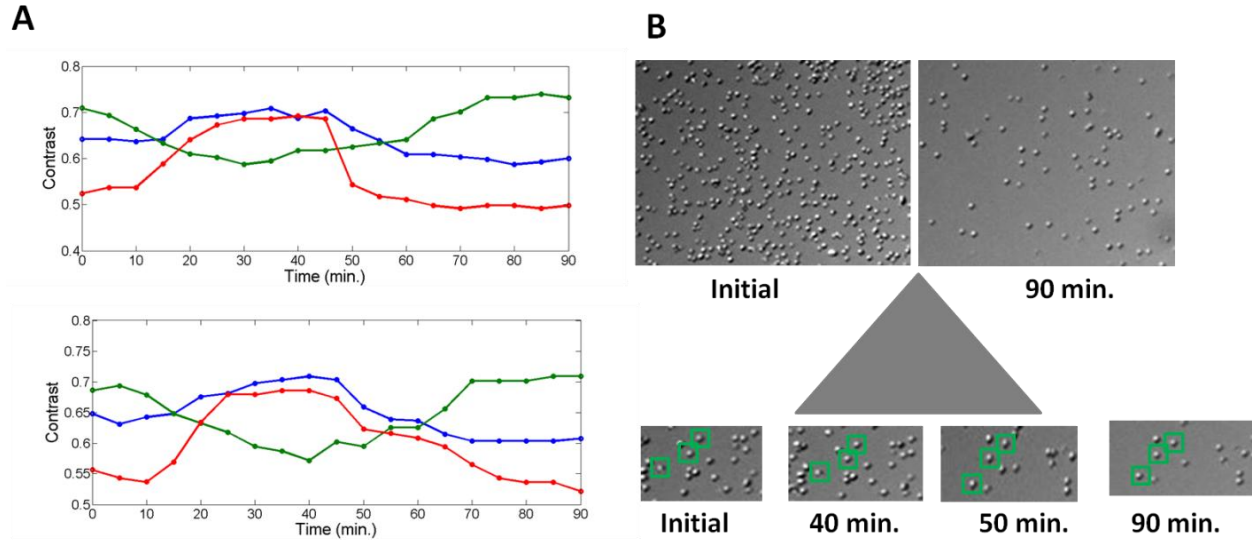
Figure S2. Detecting PRET reversibility with a straight microchannel.
A) Contrast spectra of a cysteamine modified gold sphere in a straight microchannel as reduced cytochrome c adsorbs to the surface. The green line is 550 nm, blue is 540 nm, and red is 560 nm. As cytochrome c adsorbs the contrast at 550 nm decreases while 540 nm and 560 nm increase. B) Sample images of the microchannel as cytochrome c and PBS flow through the channel.

It should be noted that as the cytochrome c and PBS solutions flow through the channel, some of the cysteamine modified spheres attached to the coverslip are washed away with the solutions due to the continusou laminar flow. Analyzed spheres were identified at the end of the experiment and tracked backward to the beginning of the experiment to ensure that the same sphere was analyzed through the cytochrome c and PBS exposures.
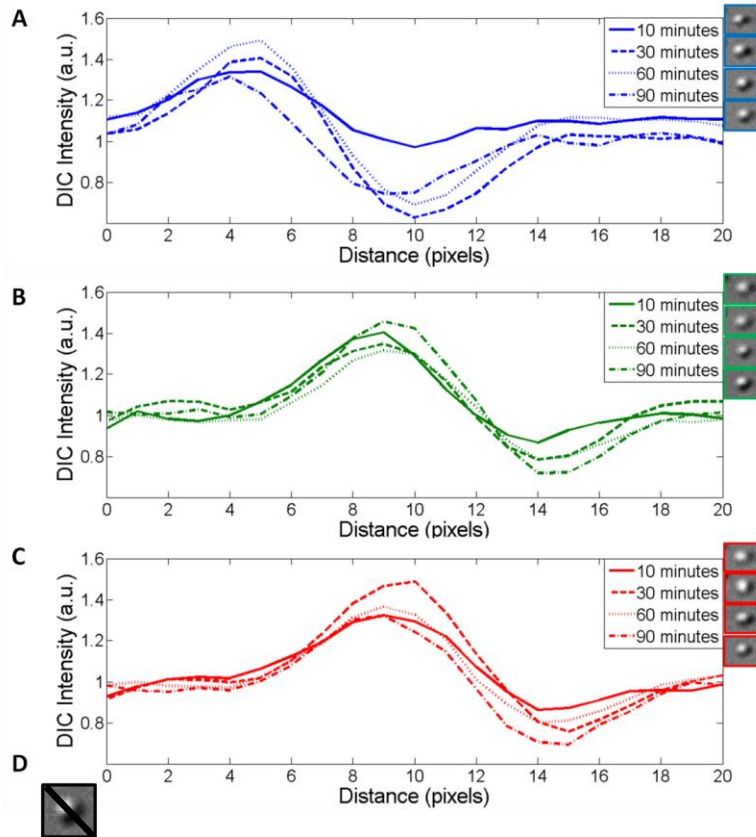
Figure S3. DIC line intensity profiles of a gold sphere during cytochrome c adsorption and desorption.

The line intensity profile is the measurement of the signal intensity across the diameter of the sphere from the brightest portion to the darkest portion of the sphere. The intensity is then graphed as a function of distance in pixels. The line intensity for gold spheres was measured as cytochrome c was adsorbed and desorbed in a Hi-Fi microchannel, at 10, 30, 60 and 90 minutes. As cytochrome c adsorbs the intensity at 550 nm decreases and then increases as cytochrome c desorbs from the surface. The opposite is true for 540 nm and 560 nm; the line intensity increases as cytochrome c adsorbs and then decreases as cytochrome c desorbs. Each wavelength was graphed seperately to better see the line intensity changes over time. The corresponding images of the sphere are highlighted next to the corresponding graph.

A) Line intensity profile at 540 nm of the gold sphere as cytochrome c adsorbs and desorbs from the surface.
B) Line intensity profile at 550 nm of the gold sphere as cytochrome c adsorbs and desorbs from the surface.
C) Line intensity profile at 560 nm of the gold sphere as cytochrome c adsorbs and desorbs from the surface.
D) Example of a line intensity measurement of a sphere. The line measurement is taken across the diameter of the sphere from the brightest half to the darkest half.

For A-C: blue line is 10 minutes, green line is 30 minutes, red line is 60 minutes and aqua line is 90 minutes. The images of spheres at the corresponding time points and wavlengths are outlined next to the corresponding line intensity graph. For each group of four images, the top image is the sphere at 10 minutes, next is the sphere at 30 minutes, then 60 minutes and the bottom image is the sphere at 90 minutes.
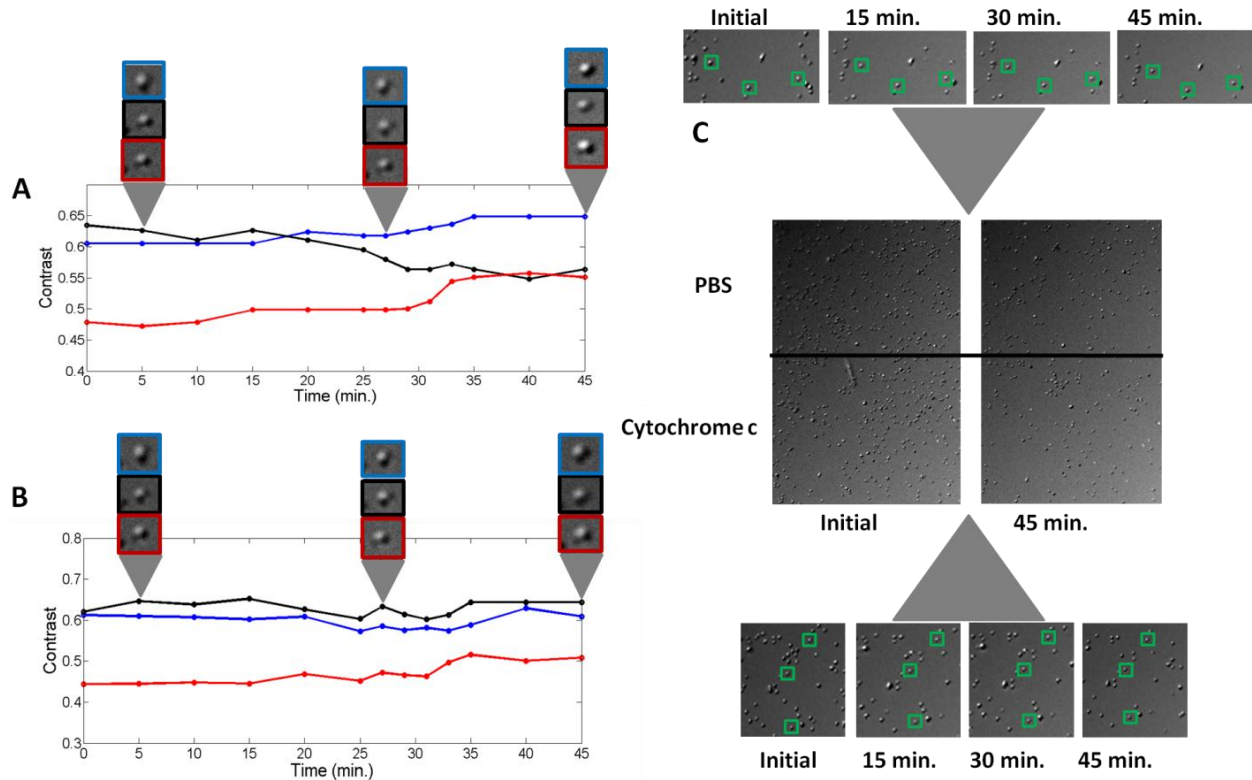
Figure S4. Detecting PRET overtime with a Y-shaped microchannel.

A) Contrast spectrum of a cysteamine modified gold sphere while reduced cytochrome c adsorbs to the surface in a Y-shaped microchannel. The black line is 550 nm, blue line is 540 nm. Red line is 560 nm. As cytochrome c adsorbs contrast at 550 nm decreases while 540 nm and 560 nm increases. Sample images of the sphere at 5, 27 and 45 minutes are highlighted. The box colors correspond to the wavelength.

B) Contrast spectrum of cysteamine modified gold spheres exposed to PBS in the microchannel. Over time the contrast at the three wavelengths remains constant.

C) Sample images of the microchannel over time as PBS and reduced cytochrome c flows through the channel. The top portion of the channel had PBS flowing and the bottom half had the reduced cytochrome c solution flowing. The solutions were pumped at flow rates to achieve laminar flow. Sample images of the sphere at 5, 27 and 45 minutes are highlighted. The box colors correspond to the wavelength.

It should be noted that as the cytochrome c and PBS solutions flow through the channel, some of the cysteamine modified spheres attached to the coverslip are washed away with the solutions due to the continuous laminar flow. Analyzed spheres were identified at the end of the experiment and tracked backward to the beginning of the experiment to ensure the same sphere was being analyzed through out the experiment.
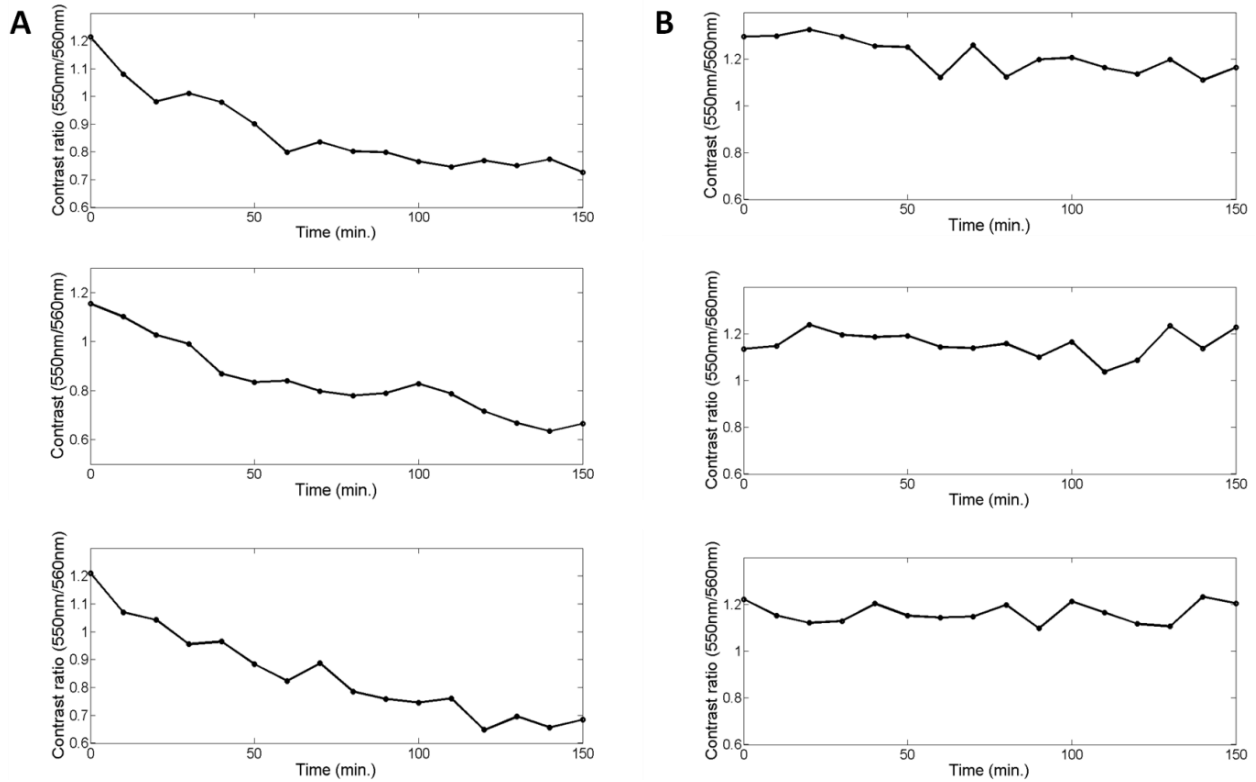
**Figure S5.** Detecting PRET during ethanol induced apoptosis.

    A) Contrast ratio (550 nm / 560 nm) spectra of cysteamine modified gold spheres in a HeLa cell undergoing ethanol induced apoptosis. As the cell goes through the apoptosis process the contrast ratio decreases – 550 nm decreases while 560 nm increases.

    A) Contrast ratio (550 nm / 560 nm) spectra of gold spheres in a HeLa cell serving as a control – not given an ethanol treatment. Over the same amount of time as the ethanol treated cell, the contrast ratio does not fall below 1. Because the ratio does not fall below 1, the contrast at 550 nm and 560 nm remains constant.
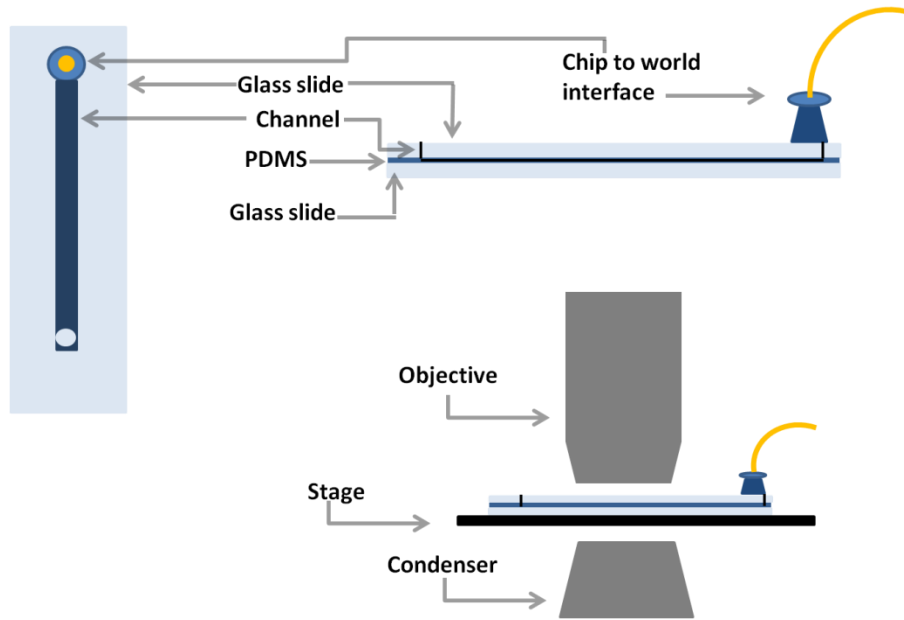
Figure S6. Microscope with a Hi-Fi channel.

A Hi-Fi microchannel imaging set up is shown with a straight channel and microscope. The channel is placed on the stage between the condenser and objective for imaging. The channel is composed of a glass slide with a PDMS layer that has the channel etched into it between the slide and coverslip. The glass slide has holes drilled into the two ends that correspond to the two ends of the channel. At one hole there is a chip – to – world interface that allows a capillary to attach and flow the solution through the channel. The hole at the other end of the channel allows the solution to leave the channel.

CHAPTER 3. IMAGING THE RELEASE PROCESS OF GOLD NANOPARTICLES FROM CAPPED MESOPOROUS SILICA NANOPARTICLES IN REAL-TIME

Ashley E. Augspurger[†], Anthony S. Stender[†,§], Brian Trewyn[‡], and Ning Fang[†]

Abstract

Mesoporous silica nanoparticles (MSNs) have been extensively studied as drug delivery agents, but to date only the release kinetics of a fluorescent dye from the pores has been studied. Herein we describe the optical responses of the uncapping process of MSNs capped with gold spheres. The gold nanospheres are cleaved from the MSNs with the use of disulfide reduction agents such as dithiothrieitol and glutathione.

Introduction

Mesoporous silica nanoparticles (MSNs) have been widely tested for applications within drug delivery and biosensing for more than a decade.[1,4,5,13,14] MSNs are a popular choice for these applications for many reasons: they are photo-stable, biocompatible, easy to synthesize, and easy to functionalize. Moreover, because of their porous structure, they have a larger surface area than non-porous nanoparticles of the same size, and they also have a larger capacity for delivering a therapeutic load than other nanoparticle options.[19,84,85] When used as delivery agents, drugs (or fluorescent dyes) are directly loaded into the pores via diffusion, and the pores must then be capped in order to retain the payload.[1] Possible options for capping agents include supramolecular assemblies,[86] inorganic nanoparticles,[17] nucleic acids, polymers, and organic molecules.

Once the MSNs arrive at their biological target, it is essential that the capping agents are removed in order to release the cargo contained inside. Typically, the capping agent is cleaved

by external stimuli, and the loaded molecules are subsequently able to diffuse out of the pores at that location, thereby delivering the cargo upon loss of significant capping agent. There are several categories of stimuli that can be utilized to uncap the pores such as photo-irradiation, enzymes, competitive binding, temperature change, pH change, or redox reactions.[15,16,18,87-89]

When choosing a capping agent several criteria should be carefully considered: biocompatibility, targeting ability, means of cleaving the agent, selectivity, stability, and facile surface chemistry.[90,91] Inorganic nanoparticles such as gold nanospheres meet the above desirable criteria for capping agents.[8,40,42] Gold nanospheres also have tunable optical properties that make them versatile probes for imaging in complex cellular environments.

Characterizing the uncapping kinetics and drug releasing kinetics is essential in designing effective delivery agents. While the release kinetics has been measured by monitoring the fluorescence signals from loaded dyes,[15-19,85,86,89] the uncapping kinetics has not been quantified experimentally due to the technical challenges of "seeing" individual gold nanospheres as they are cleaved from MSNs in real time. Studying the uncapping process is crucial in the understanding of stimuli responsive release of loaded cargo from potential drug carriers as it is often the rate limiting step in the release process.[16,92]

The main objective of the present study was to develop a novel approach to measure the uncapping kinetics directly in real time.[19,85] Bare MSNs and gold-capped MSNs were found to have different absorptive and scattering properties; and therefore, monitoring the changing optical properties of the MSNs provides a new approach to determine the rate at which gold nanoparticles are cleaved from the MSNs once the particles come into contact with a chemical uncapping agent.

Materials and Methods

DIC Microscopy. A Nikon Eclipse 80i upright microscope was used for collecting images. In DIC mode a 100× 1.4 numerical aperture (NA) Plan Apo oil immersion objective and a 1.4 NA oil immersion condenser were used. With our Nikon DIC microscope, bandpass filters are used to image at wavelengths of interest. Filters (440 nm – 700 nm) with full width at half maximum of 10 nm were purchased from Thorlabs. Movies and images were taken with a CMOS Hamamatsu Orca Flash2.8 (1920 × 1440 imaging array with 3.63 μm × 3.63 μm individual pixels). Movies and images collected were analyzed with NIH ImageJ.

Microchannel Fabrication and Imaging. Microchannels were fabricated with a cleaned standard glass slide (Electron Microscopy Sciences) sandwiched together with poly-l-lysine (PLL) (Sigma-Aldrich) modified 24 x 50 mm coverslip (Corning) by 25 μm high adhesive tape in between the slide and coverslip. The coverslips were modified with a 10% PLL solution; the coverslips were incubated in at room temperature in the PLL solution for 15 minutes then dried under a stream of nitrogen.

To prepare the gold-capped MSN solution, 3 mg of dry gold-capped MSNs were weighed out on a balance. They were then put into a centrifuge tube with 1 mL of Milliq water (18 Ω) and sonicated for 2 hours. Immediately before being injected into the channel, the MSN solution was sonicated for 15 minutes.

After the channel has been prepped, 20 μL of gold-capped MSNs (3mg/ml) were injected into the channel and allowed to sit for 15 minutes before imaging. This allowed the nanoparticles to electrostatically bind with the PLL modified coverslip. During imaging, the solution, either DTT (Biorad) or GSH (Sigma-Aldrich), was pumped through the channel in a pressure driven manner through a fused silica capillary.

Immediately after the 15 minute waiting period, the slide was placed on the microscope stage and an initial scan was taken of the area of interest. After this the cleaving agent was flowed through the channel and a movie of a vertical scan of the stage was taken every 15 minutes until the contrast of the MSNs remained constant for 30 minutes. This took up to 3.5 hours for 1mM DTT; 2.5 hours for 10 mM DTT; 2 hours for 100 mM DTT; 3 hours for 5 mM GSH. To vertically scan the stage, a computer controlled vertical stage scanner (Sigma Koki, model no. SGSP-60YAM) was attached to the fine tune knob of the microscope. A constant exposure time was used to maintain a constant background.

Culturing and Imaging HeLa cells. A549 cells were cultured 48 hours before imaging using previously published methods using cell culture medium.[4] To image cells, culturing medium was removed and cells were washed with 1X phosphate buffered saline (PBS). 24 hours prior to imaging and incubation with gold-capped MSNs, 500μM α-Lipoic acid (Sigma-Aldrich) in cell culture medium replaced the acid free medium.[16] Cells were kept in the α-Lipoic acid culturing medium for 24 hours, until gold-capped MSNs were added. The acid containing medium was used to create a higher intracellular concentration of GSH. 200 μL of gold-capped spheres (2mg/mL) were added to the petri dish with 1 mL of new culturing medium. Cells were then incubated for 2 hours to naturally internalize the gold-capped MSNs.[81] After incubation with gold-capped MSNs, culturing medium and excess MSN solution were removed and cells were washed again with 1X PBS and prepared for imaging.

After cells were washed with PBS after incubation with gold-capped MSNs, a slide was prepared for imaging. Two pieces of double sided tape were placed across a cleaned glass slide parallel to one another. Between the two pieces of tape some culturing medium was aliquoted onto the slide and the glass coverslip was secured on the glass slide with the tape.

The same procedure was followed for scanning the stage while taking a movie from the channel experiments for the cell imaging experiment. A 540 nm filter was used to image cells; the stage was scanned for each wavelength every ten minutes for 3 hours. The cells were imaged for 3 hours to capture the gold-capped MSNs release from endosomes and enter the intracellular matrix and encounter GSH for cleaving. After 3 hours the cells began to die. A movie of each vertical scan was taken at a constant exposure time to maintain a constant background.

Results and Discussion

MCM-41 MSNs were chosen in the present investigation, because of their widespread study regarding drug delivery. Individual MSNs were spherical in shape with a diameter of ~200 nm and pore diameters of approximately 3 nm for the release kinetics, except where noted below. We followed the published protocol of capping the MSN pores with 10 nm gold nanospheres.[85] Transmission electron microscopy (TEM) images of the bare and gold-capped MSN used in this work are provided as Fig. S1 in the Supporting Information.

To facilitate the uncapping process, the MSNs are exposed to a specific reducing agent that selectively cleaves the disulfide bond within the linker molecule. Such reducing agents include dithiothreitol (DTT), cysteine, and glutathione (GSH). In our experiments, the reducing agent was either GSH or DTT. The linker molecule, 3-(propuldisulfanyl) ethylamine, is thus cleaved at its disulfide bridge via a redox reaction.[1,84,85]

GSH was selected as a cleaving agent for this study because of its important connection to cancer at the cellular level. GSH is a tripeptide that is normally produced in mammalian cells, but it exists at higher concentrations in cancerous cells than in non-cancerous cells, with a typical concentration of 5-10 mM in cancerous cells.[16,93] Additionally, GSH has been shown to be a

reliable agent for cleaving disulfide linker molecules, which is a necessary step to uncap pores on MSNs and release drugs into the cytosol of cells.[16,86,93-95] Finally, when working with cells in vitro, GSH can be artificially enhanced with the addition of α-lipoic acid to the cell culturing medium.[93]

The uncapping process was monitored in two different environments. In order to gauge the uncapping behavior in a highly controlled environment, the capped MSNs were first introduced into a microchannel and imaged as a range of concentrations of DTT were flowed through the channel. For the second stage of experiments, cultured A549 human lung cancer cells were incubated with the capped MSNs and monitored for several hours. To track the uncapping process in both environments, we used a Nikon Eclipse 80i microscope in differential interference contrast (DIC) mode, coupled with a Hamamatsu Orca-Flash 2.8 CMOS camera and a set of bandpass filters with 10-nm FWHM each.

DIC microscopy has been thoroughly discussed in our previous papers.[42,43] The key advantages for using DIC microscopy for this type of experiment include the ability to observe live cells non-intrusively over several hours, no halo effects with phase contrast, high contrasts, and shallow depth of field.[42] Plasmonic nanoparticles can be readily differentiated from cellular components by comparing images taken at resonance and non-resonance wavelengths. DIC creates an interferometry pattern for objects under the microscope, and the resulting image consists of objects with a shadow-cast appearance (i.e. a dark side and a bright side) against a grey background. The difference between the bright and dark signals is divided by the local background to give the contrast value of the nanoparticle, relative to the background. The contrast between the bright and the dark sides of the nanoparticle DIC image is what we report

here, with a focus on differences in contrast between bare and capped MSN as well as capped MSN before and after treatment with a cleaving agent.

Gold Loaded MSNs. Having noticed differences in contrast between bare MSNs and gold-capped MSNs, we studied the optical responses of MSNs with different gold loadings at the single particle level. MSNs with a larger pore size of 10 nm were used in this set of experiments for having a better control over the amount of gold coating.[90,91] By controlling the amount of gold loading on the MSNs, it is possible to monitor the change in optical properties and responses as gold is added to the system. This allowed us to be able to later differentiate between bare MSNs and gold-capped MSNs for the uncapping kinetics study.[90,91] Through a series of synthetic steps, gold becomes embedded on the interior surfaces of the MSNs (i.e. within the pores) as well as on the exterior surface of the MSNs.[91] No linker molecules are required. The number of gold decoration steps ranged from one to nine, thus the samples are accordingly labeled 1x, 3x, 6x, 9x. An aliquot of each sample was fixed to a microscope slide, immersed in an oil medium with a refractive index of 1.5, and a contrast-versus-wavelength spectral profile was developed. The data represented in Figure 1 shows spectra for single nanoparticles from each sample. These spectra were generated by taking DIC images with a set of optical filters at discrete wavelengths within the visible range. The CMOS camera's quantum yield falls below 20% at wavelengths longer than 750 nm.

In the visible range, silica nanoparticles in our size range are known to primarily scatter light.[21-23,96] Therefore, the spectral profiles change dramatically upon the introduction of gold to the MSNs, because the gold nanoparticles are highly absorptive. Upon the initial addition of a few gold nanoparticles (1x), the MSNs have a dramatic change in scattering intensity below 500 nm. At low levels of gold decoration, the gold nanoparticles are well-separated, and the particles

do not interact with each other; because silica is electronically inert, it does not have an electronic effect on the gold nanoparticles and their interactions.[23] Thus, the gold nanoparticles act mostly as isolated beacons and produce an intense absorption peak around 520 nm. By adding more gold to the MSNs, the absorption peak grows in intensity, broadens, and red shifts to 560 nm for the 3x sample. This is indicative of an ideal loading, in terms of imaging purposes, because the optical profile is most distinct from bare silica at this level. The shifting of the peak also indicates that enough gold is present that some of the gold particles are aggregating, and as a result, their plasmonic frequency is shifting. Further decoration of the MSNs with gold from this point leads to a weaker signal, as fewer of the gold particles can act as isolated absorbers (6x, 9x). Instead, they are located close enough to one another to form clusters, and eventually they form a nearly complete coating on the macroscopic-sized MSN's many surfaces. The result predictably leads to a visible absorption profile more of a gold shell.[25,97] The profile at this point is somewhat similar to that of light gold decoration (1x), except that the 6x and 9x peaks are much broader than the 1x sample.

Gold Capped MSNs. The properties just described were seen as providing us with a unique approach to sensing within cells, and more importantly, within cancerous cells without the need for a fluorescent agent. By capping the 3 nm pores of standard MSNs with gold and then exposing the particles to an environment where the gold will cleave off, we can study the kinetics of the uncapping process by monitoring the change in overall contrast of the MSNs. Because individual 10 nm gold nanospheres are too small to be observed dynamically with a light microscope in a complex cellular environment and because of resolution limitations in optical microscopy, we are unable to witness individual particles being released from the MSNs.

In the following series of experiments, we measured the contrast differences between gold coated MSNs both before and after uncapping the MSN pores. For the purposes of our control experiments in microchannels, we cleaved the gold with DTT and GSH, as stated below. We also incubated gold capped MSNs into A549 cells to serve as a proof of concept that we can monitor the uncapping process of gold capped MSNs in live cells, because the higher concentration of GSH in these cells is sufficient to uncap a significant amount of gold from the MSN, thereby releasing any cargo inside to the cancerous cells. For the microchannel experiments, MSNs were deposited inside of a microchannel, and then a variety of solutions were flowed through to determine their individual abilities to aid in the uncapping of gold nanoparticles. Figure 2 shows the spectra both before and after cleaving gold spheres from the MSNs with 1 mM DTT. The DTT was flowed for 3.5 hours in a pressure driven system. The contrast significantly decreases after the pores have been uncapped, particularly at shorter wavelengths. This indicates the loss of gold nanoparticles during the experiment.

However, we wanted to be certain that the flow of water alone would not cause a change in particle contrast. As a control experiment, another channel was prepared with MSNs, and water was pumped through. Because no disulfide cleaving agent is present in the solution, there is no change in contrast; the data are shown in Figure S2 in the Supporting Information.

Having proven that 1 mM DTT was responsible for cleaving the gold from the MSNs, a series of channel experiments were performed with a range of DTT (1 mM, 10 mM and 100 mM). Single particle data for these channels are shown in Figure 3. As with the first channel experiment, contrast changed during the course of each experiment, but at different rates. The kinetic data from these channels are plotted in Figure S3 in the Supporting Information, and they show that the cleaving follows a first order reaction rate. The change in contrast was measured

by taking the final contrast minus the initial contrast and divided it by the amount of time it took for the contrast to change. The natural log of these values was then taken to arrive at a first order reaction rate with a rate constant of 0.019 hours^{-1}.

Uncapping Gold in Cells. Gold-capped MSNs were then uncapped with 5 mM GSH; the data is shown in Figure S4. MSNs were next incubated with A549 cells. To ensure there was enough GSH in the cell, the cells were also incubated with α-lipoic acid, a GSH production enhancer, for 24 hours prior to MSN addition. The gold capped MSNs were incubated with cells for 3 hours prior to imaging. Once the incubation was completed, the cells were then imaged for 3 hours with a vertical scan taken every ten minutes using a 540 nm filter, because of the strong absorbance associated with gold nanospheres at that wavelength. Figure 4 shows the contrast changes over time. Cellular images and additional cleaving is shown in Figure S5.

MSNs being cleaved in the cells were found to have the same behavior as they did with DTT in the channels. Over the three hour time span, the MSNs first had to be released from the endosomes, before they could be exposed to the cytosol where GSH is actually located. For the first hour, contrast remained very steady, but the gradual decrease at that point suggests that some MSNs had entered the cytosol at that point and were losing their gold caps. The most significant drop in contrast for this target MSN occurred at the 2-hour mark, after which the contrast plateaued once more. Thus, little to no gold was cleaved after the 2-hour mark.

Conclusions

In conclusion, we have shown that it is possible to monitor the uncapping process of gold capped MSNs with DIC microscopy, which is especially beneficial for circumstances where the use of fluorescent dyes needs to be avoided. The gold was cleaved from MSNs with both DTT

and GSH, the latter of which is significant due to its connection to cancer. In view of these findings, we believe that gold-capped MSNs can serve as single particle sensors in live cells.

REFERENCES

(1)   Vivero-Escoto, J. L.; Slowing, II; Trewyn, B. G.; Lin, V. S. *Small* **2010**, *6*, 1952.

(2)   Sun, X.; Zhao, Y.; Lin, V. S.; Slowing, II; Trewyn, B. G. *J Am Chem Soc* **2011**, *133*, 18554.

(3)   Torney, F.; Trewyn, B. G.; Lin, V. S.; Wang, K. *Nat Nanotechnol* **2007**, *2*, 295.

(4)   Slowing, I. I.; Trewyn, B. G.; Giri, S.; Lin, V. S. Y. *Adv. Funct. Mater.* **2007**, *17*, 1225.

(5)   Kim, H.; Kim, S.; Park, C.; Lee, H.; Park, H. J.; Kim, C. *Adv Mater* **2010**, *22*, 4280.

(6)   Lai, C. Y.; Trewyn, B. G.; Jeftinija, D. M.; Jeftinija, K.; Xu, S.; Jeftinija, S.; Lin, V. S. *J Am Chem Soc* **2003**, *125*, 4451.

(7)   Sauer, A. M.; Schlossbauer, A.; Ruthardt, N.; Cauda, V.; Bein, T.; Brauchle, C. *Nano Lett* **2010**, *10*, 3684.

(8)   Colilla, M.; González, B.; Vallet-Regí, M. *Biomater. Sci.* **2013**, *1*, 114.

(9)   Tan, S. Y.; Ang, C. Y.; Li, P.; Yap, Q. M.; Zhao, Y. *Chemistry* **2014**, *20*, 11276.

(10)   Cauda, V.; Argyo, C.; Schlossbauer, A.; Bein, T. *J. Mater. Chem.* **2010**, *20*, 4305.

(11)   Lai, J.; Mu, X.; Xu, Y.; Wu, X.; Wu, C.; Li, C.; Chen, J.; Zhao, Y. *Chem Commun (Camb)* **2010**, *46*, 7370.

(12)   Lai, J.; Shah, B. P.; Garfunkel, E.; Lee, K. B. *ACS Nano* **2013**, *7*, 2741.

(13)   Martin-Ortigosa, S.; Valenstein, J. S.; Sun, W.; Moeller, L.; Fang, N.; Trewyn, B. G.; Lin, V. S.-Y.; Wang, K. *Small* **2012**, *8*, 413.

(14)   Martin-Ortigosa, S.; Valenstein, J. S.; Lin, V. S.-Y.; Trewyn, B. G.; Wang, K. *Adv. Funct. Mater.* **2012**, 1.

(15)   Wang, G.; Stender, A. S.; Sun, W.; Fang, N. *Analyst* **2010**, *135*, 215.

(16)   Augspurger, A. E.; Stender, A. S.; Han, R.; Fang, N. *Anal Chem* **2014**, *86*, 1196.

(17)   Sun, W.; Wang, G.; Fang, N.; Yeung, E. S. *Anal Chem* **2009**, *81*, 9203.

(18)   Gomez-Gaete, C.; Tsapis, N.; Besnard, M.; Bochot, A.; Fattal, E. *Int J Pharm* **2007**, *331*, 153.

(19)   Gu, Y.; Sun, W.; Wang, G.; Fang, N. *J Am Chem Soc* **2011**, *133*, 5720.

(20)   Gu, Y.; Di, X. W.; Sun, W.; Wang, G. F.; Fang, N. *Anal. Chem.* **2012**, *84*, 4111.

(21)   Deng, R.; Xie, X.; Vendrell, M.; Chang, Y. T.; Liu, X. *J Am Chem Soc* **2011**, *133*, 20168.

(22)   Cheng, R.; Feng, F.; Meng, F.; Deng, C.; Feijen, J.; Zhong, Z. *Journal of controlled release : official journal of the Controlled Release Society* **2011**, *152*, 2.

(23)   Muniesa, C.; Vicente, V.; Quesada, M.; Sáez-Atiénzar, S.; Blesa, J. R.; Abasolo, I.; Fernández, Y.; Botella, P. *RSC Advances* **2013**, *3*, 15121.

(24)   Stender, A. S.; Augspurger, A. E.; Wang, G.; Fang, N. *Anal Chem* **2012**, *84*, 5210.

(25)   Liz-Marzan, L. M.; Giersig, M.; Mulvaney, P. *Langmuir* **1996**, *12*, 4329.

(26)   Blaber, M. G.; Arnold, M. D.; Ford, M. J. *J Phys Condens Matter* **2010**, *22*, 143201.

(27)   Stuart, H. R.; Hall, D. G. *Appl. Phys. Lett.* **1998**, *73*, 3815.

(28)   Pillai, S.; Catchpole, K. R.; Trupke, T.; Green, M. A. *Journal of Applied Physics* **2007**, *101*, 093105.

(29)   Oldenburg, S. J.; Averitt, R. D.; Westcott, S. L.; Halas, N. J. *Chem. Phys. Lett.* **1998**, *288*, 243.

(30)   Shi, W.; Sahoo, Y.; Swihart, M. T.; Prasad, P. N. *Langmuir* **2005**, *21*, 1610.
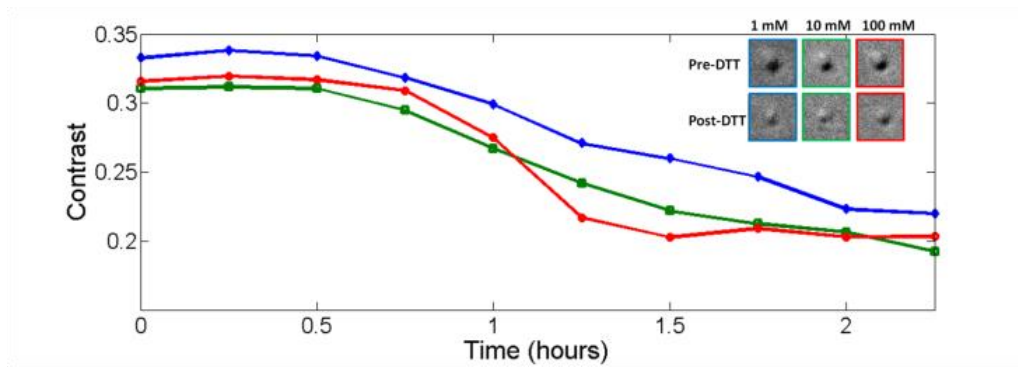
FIGURES
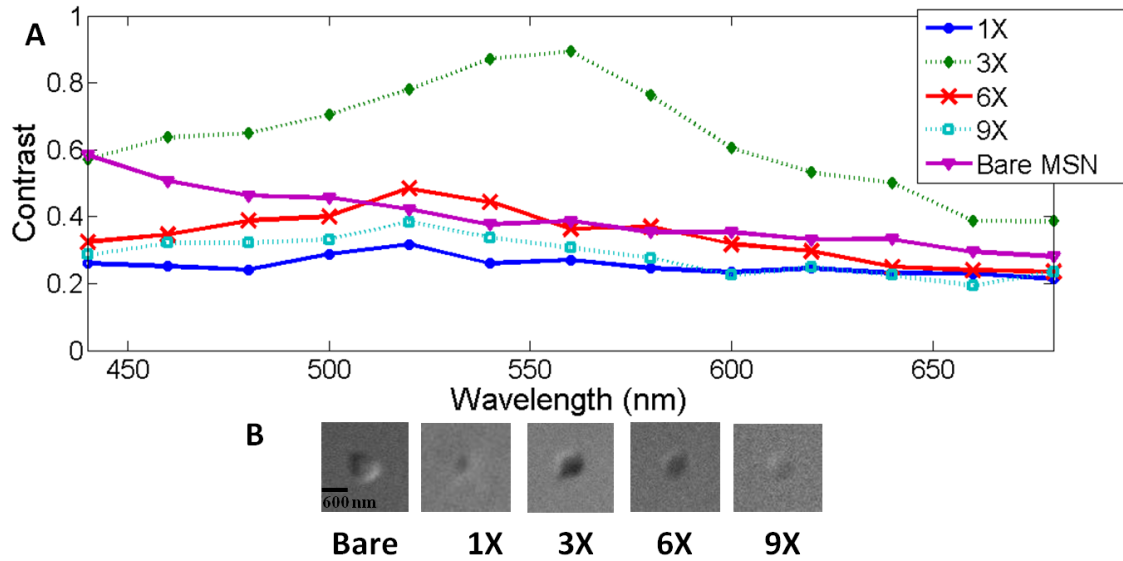
Figure 7. A) Contrast spectra of LPMSNs with varying amounts of gold loading. Each data series has been normalized to itself and is an average of 20 particles. B) Representative DIC images of each LPMSN with different gold loading at 440 nm.
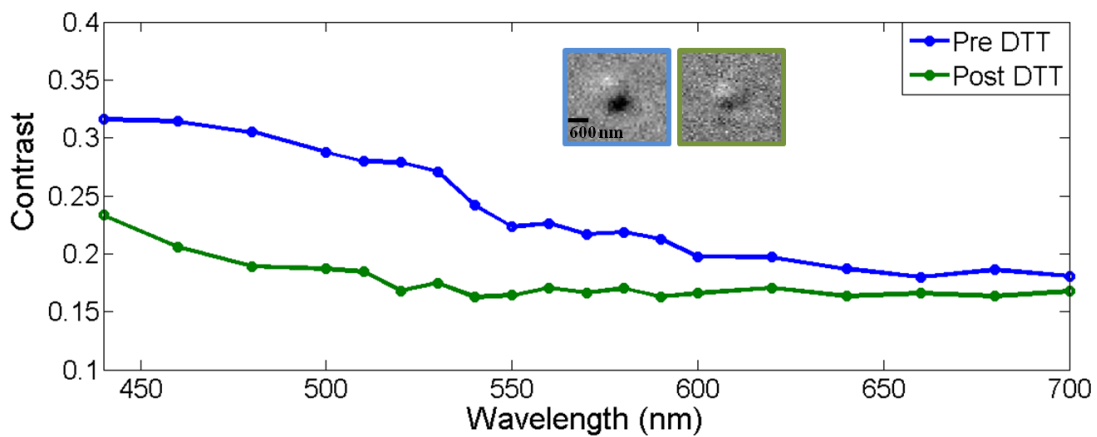
Figure 8. DIC contrast spectra of a gold-capped MSN before and after gold cleaving with DTT.

Figure 3. The blue line shows the cleaving of gold from MSNs with 1 mM DTT. The total time it took to cleave the gold was approximately 2.5 hours. The green line shows cleaving with 10 mM DTT, which took approximately 2 hours to cleave gold. The red line shows cleaving with 100 mM DTT which took approximately 1.5 hours to cleave the gold from the MSNs. The inset are the corresponding particles showing DIC contrast images before and after cleaving with DTT.
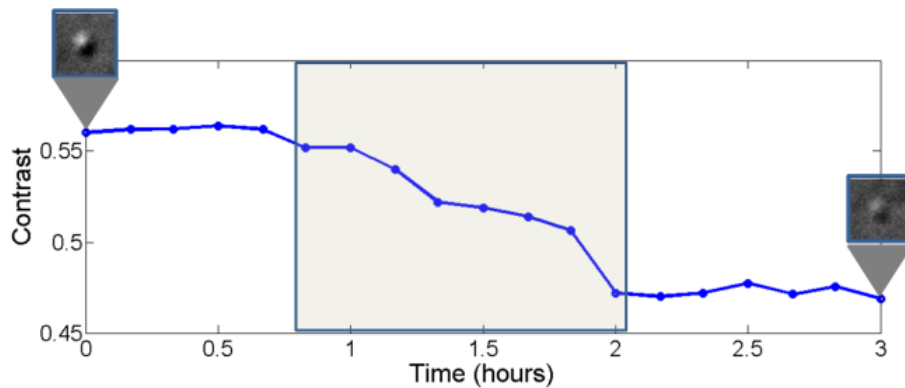
Figure 4. Contrast changes of gold-capped MSNs being uncapped by intracellular GSH over the course of 3 hours. The highlighted area shows the cleaving reaction of gold from the MSN as it comes in contact with GSH.

APPENDIX. SUPPORT. INFORMATION
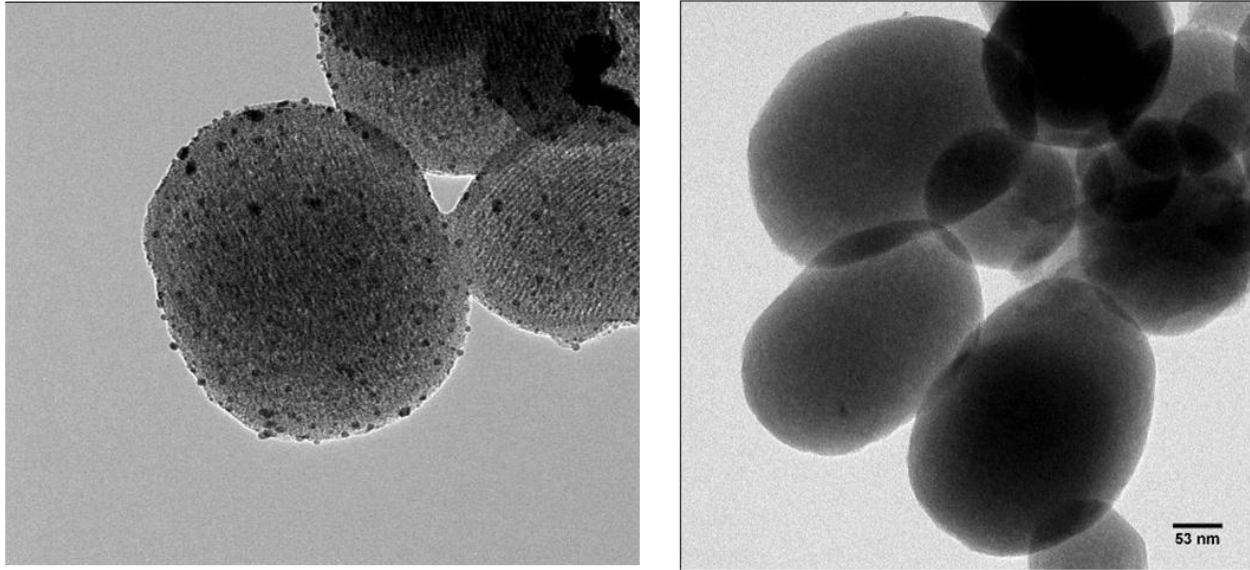
Figure S1. TEM images of gold capped MSNs before and after gold cap cleaving with DTT

MSNs capped with 10 nm gold spheres on the left, before cleaving with DTT. On the right are MSNs after cleaving with DTT; the majority of the gold has been removed.
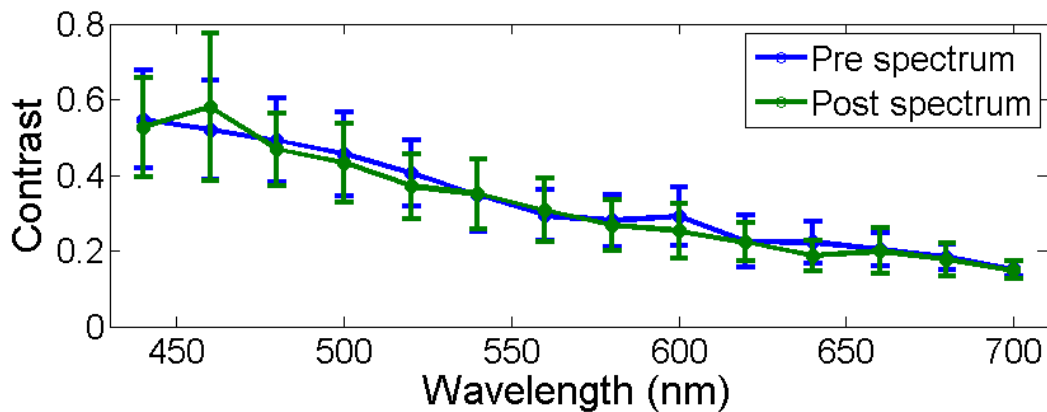
Figure S2. Water channel data, control experiment
Average DIC contrast data of 10 gold-capped MSNs, a spectrum (440 nm – 700 nm) was taken before and after water was flowed through the channel for 3 hours. There is no change in the spectra showing that gold was not cleaved from MSNs.
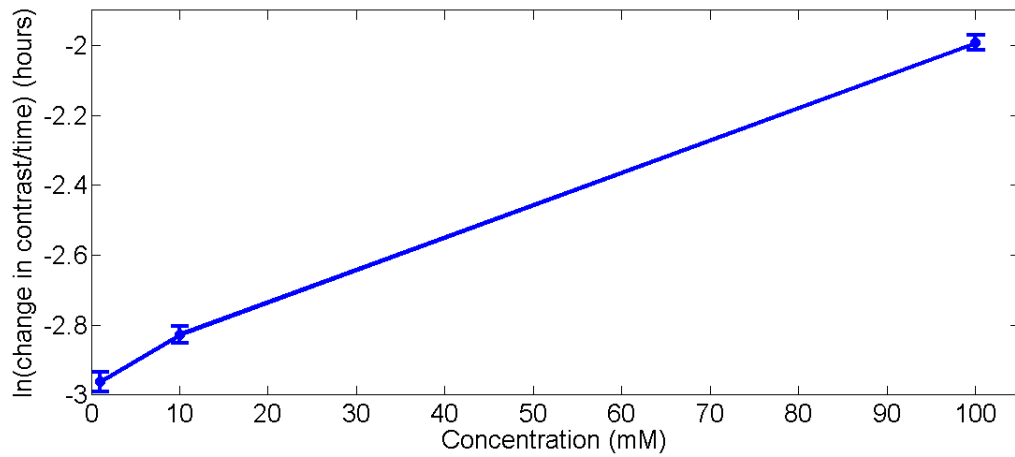
Figure S3. Kinetic graph of cleaving gold spheres from MSNs with DTT. The error bars show two standard deviations.
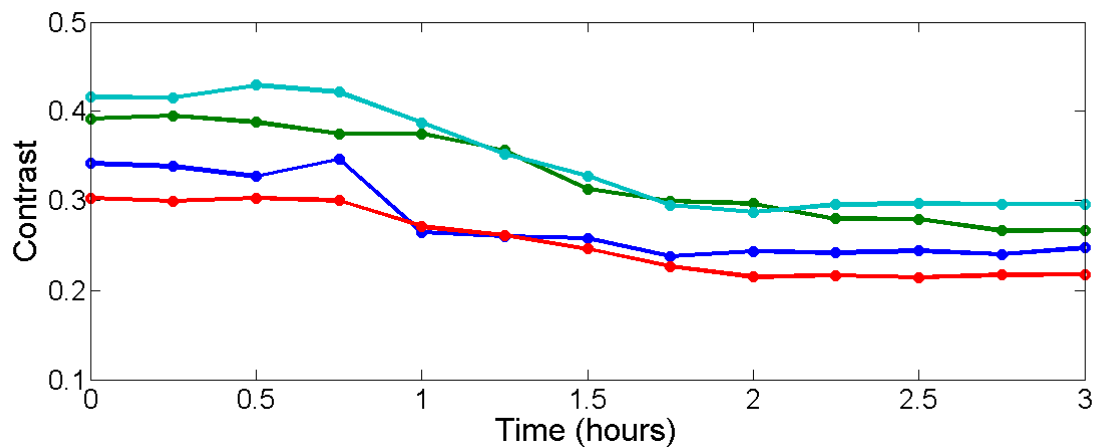
Figure S4. Gold nanoparticles cleaved from MSNs with glutathione.
DIC contrast data of five single particles, each particle has a different line color, having gold cleaved from MSNs with 5 mM GSH. The cleaving process took approximately 2 hours before reaching a constant contrast value.
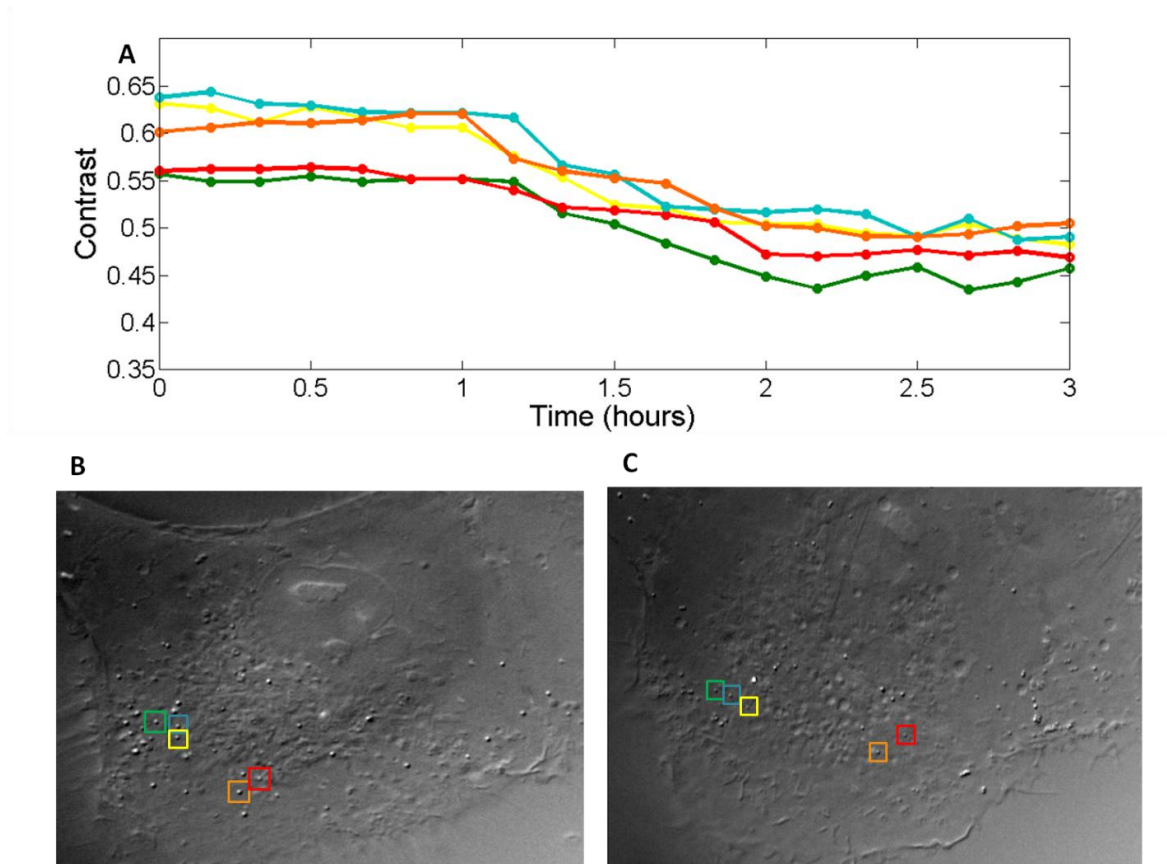
Figure S5. Intracellular cleaving of gold-capped MSNs.
A) Single particle cleaving of gold-capped MSNs with intracellular GSH. The contrast reaches a constant value about 2 hours showing that gold was cleaved from the MSNs. Each line represents one MSN. The colors in A and B correspond to the same MSN. B and C) DIC images of an A549 lung cancer cell with internalized gold-capped MSNs before and after cleaving with internal GSH after 3 hours.

CHAPTER 4. DARK FIELD MICROSCOPY FOR ANALYTICAL LABORATORY COURSES

Ashley E. Augspurger[†], Anthony S. Stender[†], Kyle Marchuk[†§], Ning Fang[†] and Thomas J. Greenbowe[*]

Abstract

An innovative and inexpensive optical microscopy experiment for a quantitative analysis, or an instrumental analysis chemistry course is described. The laboratory experiment allows students the opportunity for a hands-on experience to work with a dark field microscope, and to investigate the wavelength dependence of plasmons in gold and silver nanospheres. In another part of the experiment, students are given the opportunity to observe and measure individual crystal growth during a replacement reaction between copper and silver nitrate. The experiment allows for quantitative, qualitative and image data analyses for undergraduate students.

Introduction

It is important to give undergraduate chemistry students exposure to current research techniques being used in the field to prepare them for industry and academic research laboratory work.[5] Undergraduate laboratory experiments for conventional separation and spectroscopy techniques have been very well documented and implemented. However, optical microscopy has received little attention in undergraduate curriculum,[5] even though it has received an increase in analytical chemistry and related fields due to the rise of nanoparticle research.[98,99]

Currently, there are few laboratory experiments for chemists in optical microscopy and the most recent of those published date back to the early 1990s. What has been done in these experiments with optical microscopy simply utilizes the microscope as a platform for studying chemical reactions. Within the experiments, the optical microscope was used simply as a platform for studying chemical reactions. For example, Beste used a polarized light microscope with which students could look at electrolysis reactions of alkali metals and explore the effects of temperature and electrode potential.[100] Also, Winokur et al. used a dissecting microscope to have students study reactions between magnesium and hydrochloric acid where magnesium particles are active with Brownian motion as hydrogen gas is formed; a second reaction between copper metal and silver nitrate allowed for the observation of crystal growth.[101]

Most recently, Flowers used optical microscopy by employing the microscope as a microscpectrophotometer and students were able to explore the effects of path length, effective spectral aperture, transillumination, stray light and various magnification settings.[102] Others have used low magnification light microscopes to study fusion reactions in which a flux was performed to detect cations and anions in solution,[103] and replacement reactions to study the reactivity of metals such as calcium, silver, and magnesium.[104] The experiment described in this manuscript introduces students to a dark field microscope, an instrument commonly used in analytical research, to study several nanomaterials.

This optical microscopy experiment allows students to engage in a variety of current analytical research techniques. Students work with a dark field microscope to watch and measure crystal growth of a replacement reaction between copper wire and a silver nitrate solution. Students also work with bandpass filters and investigate what makes a "good" filter while

simultaneously looking at nanospheres of different size (100 nm – 200 nm) and composition (gold, silver and silica) in an attempt to compare the particles' light scattering properties.

The experiment was successfully pilot studied with students who had completed quantitative analysis and instrumental analysis courses. Students took two hours to complete the experiment while working alone.

Background

Dark Field Microscopy

Dark field microscopy relies on the principles of light scattering. This is accomplished by illuminating the sample with light at oblique angles due to a light stop in the center of the condenser. The blocking of the direct light to the sample and the creation of the large light angles creates a dark background on which the sample appears bright. Anything that is able to scatter light located on the sample plane will scatter light, which is then collected by the objective; only light scattered in the direction of the objective is able to be detected. Once the light is collected by the objective, it is directed toward a charge coupled device (CCD) where it is then converted into a digital signal. The signal is then sent to a computer that can project the data as a visual image.[41,42] Figure 1 shows the working principles of a dark field microscope.

Nanoparticles and Plasmons

Nanoparticles are defined as any structure between 10 and 100 nm. Interestingly, the optical properties of nanoparticles are typically quite different than their bulk counterparts, due to their small size. Noble metal nanoparticles will have localized surface plasmon resonance (LSPR). When a nanoparticle is irradiated with specific wavelengths of light, its electron cloud will oscillate. This enables the nanoparticle to scatter and absorb light.

Changing the nanoparticles' composition will vary the optical properties. For example, the LSPR wavelength location and intensity is material dependent as well as reliant on the dielectric value of the surrounding medium. Gold spheres have an LSPR at approximately 550 nm, while silver spheres have an LSPR at approximately 500 nm.[13]

Methods and Results

Materials and Chemicals

The dark field microscope (ID: 9500600; Model No: M834-A191) and digital CCD camera (ID: 5628124; Model No : A35140U) were purchased from microscope.net (Tustin, CA). The silver nitrate (catalog# S181-25, 25g) and copper wire (16 AWG, 1 lb; catalog# 15-545-2A) were purchased from Fisher Scientific (Pittsburgh, PA).

All of the nanoparticles were purchased from Sigma Aldrich (St. Louis, MO). Gold nanospheres (3.8×10^9 particles/mL; 100 nm diameter; stabilized suspension in citrate buffer; catalog# 742031); silver nanospheres (3.8×10^9 particles/mL; 100 nm diameter; stabilized suspension in citrate buffer; catalog# 730777); mesoporous silica nanospheres (200 nm diameter; catalog# 748161) The silica spheres were suspended in de-ionized water with a concentration of 0.01 mg/mL.

Filters were bandpass filters with 70% transmittance and variable wavelength ranges: 580 – 660 nm; 350 - 510 nm; 340 – 500 nm; 380 – 540 nm; 510 – 590 nm.

The glass microscope slides (3x1', 1.0mm thick; catalog# 71879-15 and 71867-10) were purchased from Electron Microscopy Science (Hatfield, PA). Coverslips (22x22mm; catalog# G1592B)were purchased from Daigger (Vernon Hills, IL). The clear nail polish (Sally Hansen; 4860-01 Invisible) was purchased from Wal-Mart.

Hazards

Silver nitrate can cause respiratory, eye and skin irritation. Gold, silver, and silica nanoparticles can cause skin irritation if absorbed through skin; use gloves to avoid contact. Eye and respiratory tract irritation can also occur if nanoparticles are inhaled. Nanoparticles may also be harmful if they are ingested.

Part 1

Students place a 1 cm piece of copper wire on a glass slide that has already been placed on the microscope stage. Students are then instructed to check the alignment of the condenser and objective by way of setting the Köhler illumination. This ensures even illumination and optimizes the spatial resolution. The copper wire is then brought into focus and a few drops of a 0.025M silver nitrate solution is added to the copper wire. As the crystals grow, students bring the crystals into focus, rather than the copper wire, and take an image of the crystals every 30 seconds over the course of the reaction – approximately 2 minutes. The reaction is run a few times with variable gain and exposure time settings.

After the reaction has taken place, students are able to measure the length of individual crystals with the aid of ImageJ, a free software packaged available for download from the National Institute of Health. The length of individual crystals is then graphed over time. Figure 2 shows student collected data from this section of the experiment.

Part 2

In the second section of the experiment, students make three samples of nanospheres (gold, silver and silica) to look at under the microscope. Each sample is prepared by casting 6 µl of a nanospheres solution onto the slide. The sphere solution is then covered with a glass coverslip and the edges of the coverslip are sealed with clear nail polish. The nail polish is

allowed to dry for approximately 30 minutes. After a slide has been prepared, it is placed on the stage and the spheres are brought into focus; the Köhler illumination is checked again to ensure proper alignment of the condenser and objective.

Each sample is imaged without a filter and followed subsequently with the five filters. Each time a filter is placed in the light path between the light source and condenser, the amount of light passing through the microscope is limited. Therefore, the students are forced to reset the gain and exposure time to obtain the cleanest image for each sample with each filter. This enables the students to investigate the relationship between gain and exposure time, the wavelength dependence of plasmons for each type of sphere, and spatial resolution. Figure 3 shows student data from this section of the experiment.

Part 3

After each nanosphere sample is imaged, students are asked to decide which filters have the cleanest image for each type of sphere, for a total of three filters. They are then asked to take a transmission spectrum of the three filters to determine, more accurately, the wavelength ranges of each filter. The students are then given the absorption spectra of each sphere and they are asked to find the relationship between the LSPR of each sphere sample and the corresponding filter.

Conclusion

In the laboratory experiment students are given a dark field microscope, which allows them to watch crystal growth during a replacement reaction between copper wire and a silver nitrate solution. Students also look at nanospheres and their wavelength dependency with the aid of plasmons.

This experiment gives students an opportunity to work with an instrument commonly used in analytical research labs, and it also provides students experience with experimental design that is currently being performed in analytical research. This dark field microscopy experiment is also an innovative and inexpensive experiment that can be implemented easily into any analytical or instrumental analysis laboratory curriculum.

REFERENCES

(1)   Fahey, A.; Tyson, J. Instrumental analysis in the undergraduate vuriculum. *Anal. Chem.* **2006**, *78*, 4249–4254.

(2)   Shah, I.; Reid, N. The rols of laboratory work in university chemistry *Chem. Educ. Res. Pract.* **2007**, *8*, 172-185.

(3)   Mellon, E.K.; Pulliam, E.; Berger, T.G.B. J. Report from the 11th Biennial Conference on Chemical Education; *J. Chem. Educ.*: Georgia Institute of Technology, Atlanta, GA, **1990**.

(4)   Thiessen, G.W.; Beste, L.F. An application of the polarizing microscope to reaction study. *J. Chem. Educ.* **1942**, *11*, 331.

(5)   Winokur, R.; Monroe, M. Using a dissecting microscope in teaching introductory chemistry. *J. Chem. Educ.* **1985**, *62*, 157.

(6)   Flowers, P. A. Incorporating basic optical microscopy in the instrumental analysis laboratory. *J. Chem. Educ.* **2011**, *88*, 1716-1719.

(7)   Benedetti-Pichler, A.A.; Vikin, Joe. Fusion reaction under the microscope. *J. Chem.l Educ.* **1966**, *42*, 421.

(8)   Lam-Erwin, Chuk-Yin; Sprague, J. Replacement reactions using a dissecting microscope. *J. Chem. Educ.* **1992**, *69*, 855.

(9)   Wang, G.; Stender, A. S.; Sun, W.; Fang, N. Optical imaging of non-fluorescent nanoparticle probes in live cells. *Analyst* **2010**, *135*, 215-221.

(10)   Stender, A. S.; Marchuk, K.; Liu, C.; Sander, S.; Meyer, M. W.; Smith, E. A.; Neupane, B.; Wang, G.; Li, J.; Cheng, J.-X.; Huang, B.; Fang, N. Single cell optical imaging and spectroscopy. *Chem. Rev.* **2013**, *113*, 2469-2527.

(11)   Willets, K. A.; Van Duyne, R. P. Localized surface plasmon resonance spectroscopy and sensing. *Annu. Rev. Phys. Chem.*; Annual Reviews: Palo Alto, **2007**; Vol. 58, p 267-297.

FIGURES
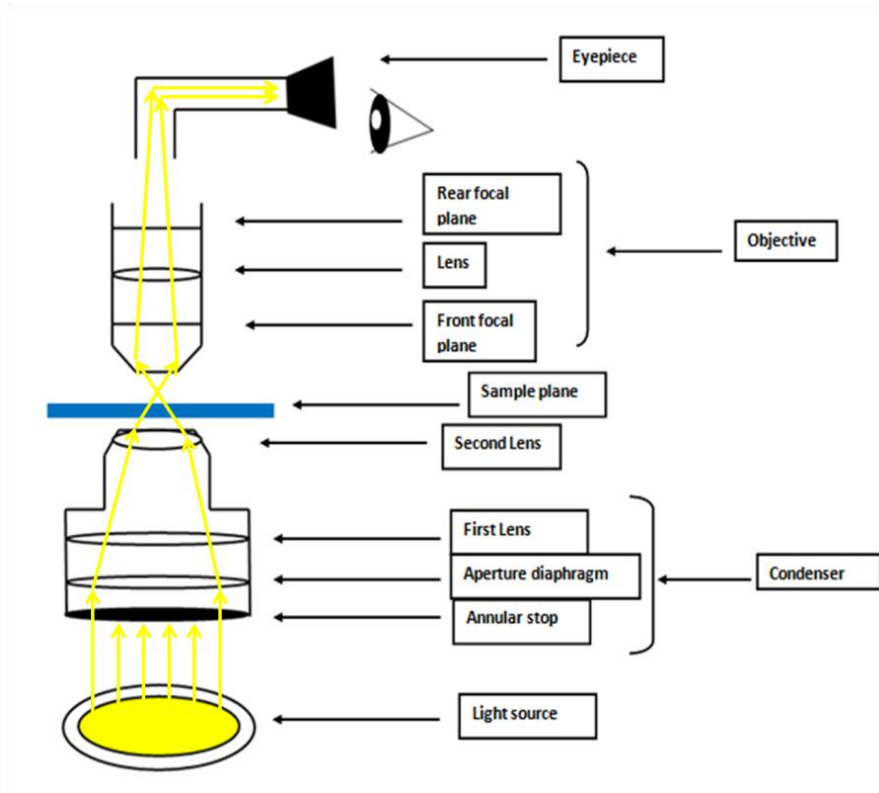
Figure 9. A dark field microscope with the light path. As light passes through the system most of the light passing directly to the sample plane is blocked by the annular stop, and only light hitting the sample plane from large angles is allowed to pass. The light is then collected by the objective where the image is created and passed on to the detector – either the observer's eye, or a CCD.
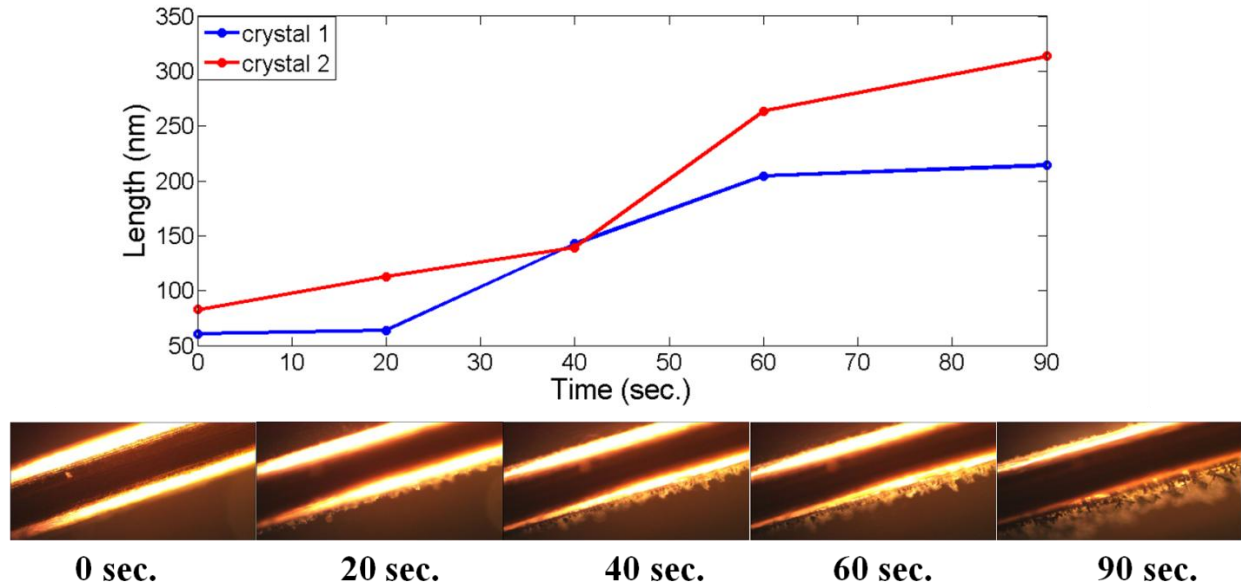
Figure 10. Copper wire and silver nitrate replacement reaction. As the silver crystals grow students are able to image the growth and then graph the length of individual crystals.
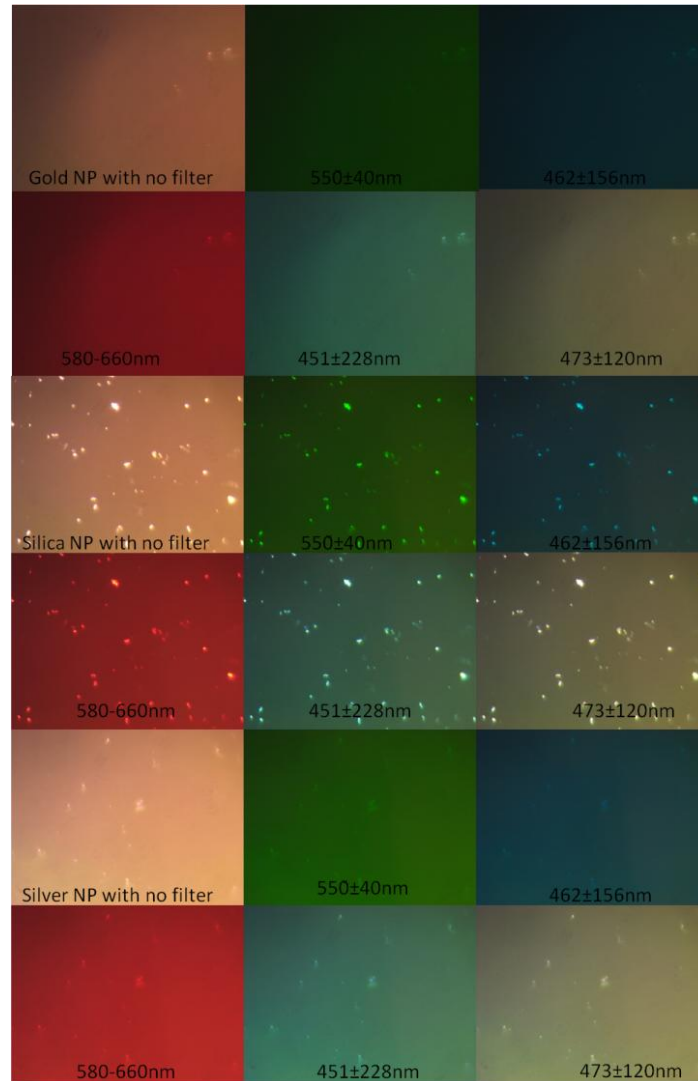
Figure 11. Gold, silica and silver nanospheres imaged with and without bandpass filters. Students are able to see how different wavelengths of light excite the plasmons in the nanostructures. The composition of the nanostructure affects the spectral position of the LSPR.

CHAPTER 5. ASSESSING AN INQUIRY VERSUS TRADITIONAL APPROACH IN DESIGNING A LABORATORY EXPERIMENT TO TEACH OPTICAL MICROSCOPY

Ashley E. Augspurger,[†] Anthony S. Stender[¥], and Thomas J. Greenbowe[†]

Abstract

Optical microscopes are an important tool in industry and academic research, but they are rarely discussed as part of an undergraduate curriculum in chemistry. In a previous paper, we presented a set of microscopy experiments that we implemented in an undergraduate instrumental analysis course. In this follow up paper, we compare and discuss the learning gains of two formats of the microscopy laboratory exercise: a traditional and an inquiry format. To gather data for our analysis, students in an instrumental analysis course were divided into two groups – one to perform the inquiry experiment and one to perform the traditional experiment. Both groups scored similarly on their laboratory reports, but students in the inquiry group displayed higher learning gains on the Chemical Optical Microscopy Assessment: the assessment created to monitor learning gains on optical microscopy for this study.

Introduction

Providing students with an innovative and cutting edge laboratory curriculum is a critical aspect to keeping them engaged in chemistry while also making them competitive in finding employment after graduation. One way to get students excited about chemistry is by introducing them to real-world research. Such an approach allows students to get hands on experience with tools, techniques, and materials that are actually used by industry and academic research laboratories.

Optical microscopy tends to be a topic for which undergraduate chemistry students have no exposure, but it is a skill that many employers want from their bench chemists.[5,6] What is desired includes UV-vis absorption, HPLC, autotitration and atomic absorption to name a few.[5] According to a recent survey, optical microscopy is only taught in 3% of academic institutions in the United States.[5] Optical microscopy is more often taught in undergraduate biology classes. Barclay and Fraser created a light microscopy experiment to teach geotropism with plant cells.[105] Gray *et al* created an optical microscopy assay to study exocytosis and phagocytosis in cell biology.[106] Omoto and Folwell discuss the conversion of a bright field microscope to a dark field microscopy for high school and college biology classes.[107]

Upon a literature review of undergraduate chemistry optical microscopy experiments, the microscopes are typically used as a static tool to watch reactions at the microscopic level.[100,108-110] One of the more advanced experiments utilized the microscope as a spectrophotometer and provided students with hands on experience manipulating the instrument by measuring the absorbance of a range of food dye concentrations.[102]

To overcome this current inadequacy in training students about optical microscopy, we created a laboratory experiment that uses a dark field microscope, which can be found in the *Journal of Chemical Education*.[62] The structure of the experiment was based in the Learning Cycle, where students have the opportunity to explore chemistry concepts through: 1) the pre-laboratory material and performing the experiment, 2) concept invention through answering analysis questions based on their laboratory generated data, and 3) application through writing the laboratory report; specifically the discussion section where they are forced to make connections to other experiments they've performed, lecture material and other classes they have taken.[45,51,111] Inquiry based learning has been implemented in general chemistry and organic

chemistry through the use of the Learning Cycle the Science Writing Heuristic (SWH); discussed below.[50,112]

It is important to engage students about chemistry with innovative "real-world" curriculum. However, creating new curriculum isn't sufficient. The teaching methodology is also important because, as instructors, we want students to gain as much from the curriculum as possible. To know if what is being taught and how it's being taught is effective, the learning gains have to be monitored. The optical microscopy experiment presented here was created in two formats – a traditional and a structured inquiry format. An optical microscopy assessment was also created to measure student learning gains. The present study investigates whether students will have higher learning gains from an inquiry or traditional approach for an optical microscopy experiment.

The traditional approach provides students with a series of clear steps for completing an experiment. Furthermore, a traditional manual describes the concepts, gives an explicit procedure for data collection, details a set of instructions for analyzing the data, and provides the students with explained conclusions. However, there are different levels of inquiry – open, guided and structured – with each level defined by the amount of information given to the students[47]. An open inquiry manual gives students suggestions for what to investigate during the laboratory period, but no procedures or methods are given to the student.[46] Guided and structured inquiry manuals provide students with more procedural details than the open approach, but they still expect the students to arrive at their own conclusions. Inquiry based learning is an instructional strategy used to simulate the scientific process for students.[45,58] The purpose of inquiry based learning is to provide opportunities for students to think like a scientist in addition to learning science concepts. [45]

For our laboratory exercises, the traditional format was strictly comprised of a verification laboratory experiment; students were given all of the information they needed to understand the concepts of the experiment and the goals of the experiment were explained in the introduction section. Students were provided with sample data. Students could use this sample data as a pattern to base how they were to analyze their data. The traditional format included post lab questions about the topics covered in the lab experiment.

The alternative version of the experiment was a structured inquiry approach, using the same chemicals and instruments as the traditional approach. Both formats have the same procedure and analysis questions, but the inquiry format does not have post lab questions. For the inquiry approach, the introductory material was given in the form of an interactive worksheet. Five diagrams with minimal background information were given with follow up questions for the students to answer. The students were not given sample data.

Because instrumental analysis courses are often described as writing-intensive, we chose to evaluate the students' thinking processes by analyzing laboratory reports. As a part of the laboratory reports for both groups, the students had to complete an identical pre-laboratory exercise. The pre-laboratory activity asked students several questions about optical microscopy from the different modes of microscopy to how an image is created and detected. Students were also required to write a post-laboratory report. The students in the traditional group wrote a traditional style report, while the students in the inquiry group wrote a report in the style of the SWH. The traditional style laboratory report consisted of a purpose, procedure, safety, data and observations, discussion and post lab question. The SWH laboratory report is comprised of student generated beginning questions, procedure, safety, data and observations, claims, evidence and a reading and reflection section.[112] The SWH format helps students relate their

laboratory work to concepts and develop meaning from the activity by helping them make connections between ideas and draw inferences.[112]

Our findings reported below are based on the responses given by the students participating in the two formats of the same laboratory exercise. The aim of this project was to determine if upper level undergraduate students in an instrumental analysis course learn optical microscopy more effectively with a traditional approach or an inquiry approach.

Methods

For both groups of students, the pre-laboratory material was given in a traditional format as a set of questions the students were required to answer before they performed the laboratory experiment. The material covered the basics of optical microscopy that students would need to know to understand the concepts in the laboratory experiment. Links to online tutorials were also provided for students to utilize.

The laboratory experiment utilizes a dark field microscope which students manipulate to image multiple samples. In the first part, students observe silver crystal growth on a copper wire as it reacts with silver nitrate. In the remainder of the exercise, students used bandpass filters of various wavelength ranges to image three different types of nanoparticles – 100 nm gold spheres, 100 nm silver spheres, and 200 nm silica spheres. By imaging with filters, students are exposed to the concept of localized surface plasmon resonance in metal nanoparticles. During the experiment students learn about the components of the microscope, and how they work together to create an image. After the data collection is completed, students learn image analysis by measuring the length of crystals over the course of the reaction.

To monitor student learning gains, an optical microscopy assessment was created - named the Chemical Optical Microscopy Assessment (COMA). The assessment consisted of 10 questions that covered basic optical microscopy questions ranging from how the components work together, to imaging and data acquisition. The COMA, found in the Supplemental Information, was used as both a pre and post quiz to the lab experiment.

All statistical analysis was performed with JMP software; a licensed software available to Iowa State University from SAS. Wilcoxon rank sums tests were performed to compare students ACS analytical exam scores, laboratory report scores and COMA scores. The Wilcoxon rank sums test was chosen due to the small number of participants and the non-Gaussian distribution of their ACS analytical exam scores.

Participants

Participants were volunteers from an instrumental analysis course at Iowa State University. The course is meant for junior and senior chemistry majors who have already taken quantitative analysis. A total of 32 participants partook in the study. The study was approved and exempted by the Internal Review Board (IRB) for human research. Even though the study was determined to be exempt students had to sign a consent form.

There were four laboratory sections of the instrumental analysis course. Using the intact laboratory sections, two laboratory sections were randomly assigned the traditional experiment while the other two were assigned the inquiry experiment. Students were divided into two groups; one group performed the traditional experiment while the other performed the inquiry experiment. This study was conducted over a two semester time span.

Results and Discussion

Establishing Equivalency

A shortened version (comprising 18 questions) of the ACS analytical chemistry exam from 2007 was administered to students in order to determine whether the two groups of students had an equal background in chemistry content knowledge. The selected questions covered spectroscopy-related content. Only 18 questions were asked due to time constraints set in the lecture portion of the class. The analytical exam was chosen as the comparison point, because students are required to take quantitative analysis before they are allowed to take Instrumental Analysis at Iowa State University.

The exam was scored as one point per question, for a total of 18 points. The traditional group of students had an average score of 9.94, while the inquiry group of students had an average score of 9.87. The resulting p-value from the Wilcoxon rank sums test is 0.8620, meaning that both groups of students have the same baseline knowledge about analytical chemistry and spectroscopy, specifically.

Laboratory Reports

The students were required to write a laboratory report following the laboratory experiment, which was handed in two weeks after performing the experiment. The lab reports were graded out of 90 points. The traditional students scored slightly higher than the inquiry students, 67 versus 65 points, on average. The p-value shows an insignificant difference between the two groups, with a value of 0.6097.

Assessing Learning Gains

The COMA is a 10 question quiz that covers the fundamentals of optical microscopy. There are two questions per objective and two application questions covering information they

learned in the lab experiment. The COMA was graded with two points per question for a total of 20 points. The COMA was administered to each student twice – before and after the experiment. For each student a pre-score, a post-score and a normalized gain score were calculated.

To establish the validity of the COMA, five doctoral candidates who perform spectroscopy research rook the exam. From their scores, a Cronbach's α value of 0.8156 was calculated. Such a value reveals that the COMA is truly measuring optical microscopy content and the COMA is reliable.

The students participating in the study took the COMA twice: first before performing the experiment and again after they handed in their laboratory reports. The traditional group of students had an average score of 9.53 as a pre-quiz score and an average of 10.46 for their post quiz. This came out to an average normalized learning gain of 0.074 from performing the experiment. The inquiry group of students had a pre-quiz score of 8.33 and an average post quiz score of 11.6 for an average normalized learning gain of 0.283. The higher score for the inquiry group shows that they are learning more about optical microscopy from the laboratory experiment than the traditional students.

There is a large difference between the learning gains scores of both groups. The p-value when comparing both groups is 0.0473, showing that there is definitely a statistical difference between the two groups. The inquiry group had a higher learning gains score most likely because they were forced to make connections to other learning experiences and to defend their data and ideas through the SWH writing process. The traditional group of students was not encouraged to make connections to other learning experiences, as these are not part of the traditional laboratory report. Furthermore, they were not required to argue in defense of their data and conclusions. Their lab experiment was strictly verification; there was no active learning involved.

Conclusions and Implications

Optics is considered important to basic science research, according to the Department of Energy.[113] Even though it is a part of the basic sciences, it is rarely discussed in lecture or laboratory for undergraduate chemistry students. To aid in filling this gap, an optical microscopy laboratory experiment was created utilizing a dark field microscope to image nanoparticles and silver crystal growth.

The laboratory experiment was created in two different formats – a traditional verification style and a structured inquiry style. The laboratory report scores, and normalized learning gains on the Chemical Optical Microscopy Assessment were compared. Students in both groups were able to learn from the laboratory experiment, and this was obvious from the similar lab report scores in the two groups of students, but the students in the inquiry group achieved higher learning gains on the COMA assessment. This is due to the students writing their lab reports in the SWH format, where they were forced to make connections to other learning experiences and create and defend their own ideas from the laboratory experiment.

SWH and inquiry based laboratory are excellent instructional tools for teaching science concepts. They not only help students gain a deeper understanding of science, but also to think like a scientist. The SWH forces students to create claims based on their data and use their data as evidence to support their claims. Students are also required to reference their textbook and find literature that supports their ideas as well as reflect on how their ideas have changed.[50,61] Because students are more engaged with the experiment they create a deeper understanding and ultimately have higher learning gains.

While it is important to create innovative curriculum, it is important to monitor how we teach. Structuring lab experiments effectively is critical to student learning. It is important to

create innovate curriculum, but more importantly how we teach is critical to student learning outcomes. The present study provides some evidence that students who experience optical microscopy with an SWH approach have higher learning gains compared to students who have a traditional style approach with optical microscopy.

REFERENCES

(1)   Fahey, A.; Tyson, J. *Anal Chem* **2006**, *78*, 4249.

(2)   Tyson, J. F. *Management of Modern Laboratories* **1996**, *2*, 55.

(3)   Barclay, G. F.; Clifford, P. e. *The American Biology Teacher* **1991**, *53*, 285.

(4)   Gray, R.; Gray, A.; Fite, J. L.; Jordan, R.; Stark, S.; Naylor, K. *CBE life sciences education* **2012**, *11*, 180.

(5)   Omoto, C. K.; Folwell, J. A. *The American Biology Teacher* **1999**, *61*, 621.

(6)   Winokur, R.; Monroe, M. *Journal of Chemical Education* **1985**, *62*, 157.

(7)   Thiessen, G. W.; Beste, L. F. *Journal of Chemical Education* **1942**, *11*, 331.

(8)   Benedetti-Pichler, A. A.; Vikin, J. *Journal of Chemical Education* **1966**, *42*, 421.

(9)   Lam-Erwin, C.-Y.; Sprague, J. *Journal of Chemical Education* **1992**, *69*, 855.

(10)   Flowers, P. A. *Journal of Chemical Education* **2011**, *88*, 1716.

(11)   Augspurger, A. E.; Stender, A. S.; Marchuk, K.; Greenbowe, T. J.; Fang, N. *Journal of Chemical Education* **2014**, *91*, 908.

(12)   Lawson, A. E.; Abraham, M. R.; Renner, J. W. *A theory of instruction: Using the learning cycle to teach science concepts and thinking skills*; National Association for Research and Science Teaching: Kansas State University, 1989.

(13)   Abraham, M. R. In *Chemists' Guide to Effective Teaching*; Pienta, N. J., Cooper, M. M., Greenbowe, T. J., Eds.; Pearson: New Jersey, 2005; Vol. 1.

(14)   Lawson, A. E.; Abraham, M. R.; Renner, J. W. *A Theory of Instruction: Using the Learning Cycle To Teach Science Concepts and Thinking Skills*; National Association of Reasearch in Science Teaching, 1989.

(15)   I, J. A. R.; Greenbowe, T. J.; Hand, B. M.; Legg, M. J. *Journal of College Science Teaching* **2001**, *12*, 1680.

(16)   Burke, K. A.; Greenbowe, T. J.; Hand, B. M. *Journal of Chemical Education* **2006**, *83*, 1032.

(17)   Fay, M. E.; Grove, N. P.; Towns, M. H.; Bretz, S. L. *Chemistry Education Research and Practice* **2007**, *8*, 212.

(18)   Fay, M. E.; Bretz, S. L. *The Science Teacher* **2008**, 38.

(19)   Burke, K. A.; Poock, J.; Greenbowe, T. J.; Hand, B. M. In *National Meeting of the American Chemical Society* New Orleans, LA, 2004.

(20)   Energy, U. S. D. o. *Basic Sciences Summary Report*, 2014.

(21)   Prain, V.; Hand, B. *Teaching and Teacher Education* **1996**, *12*, 609.

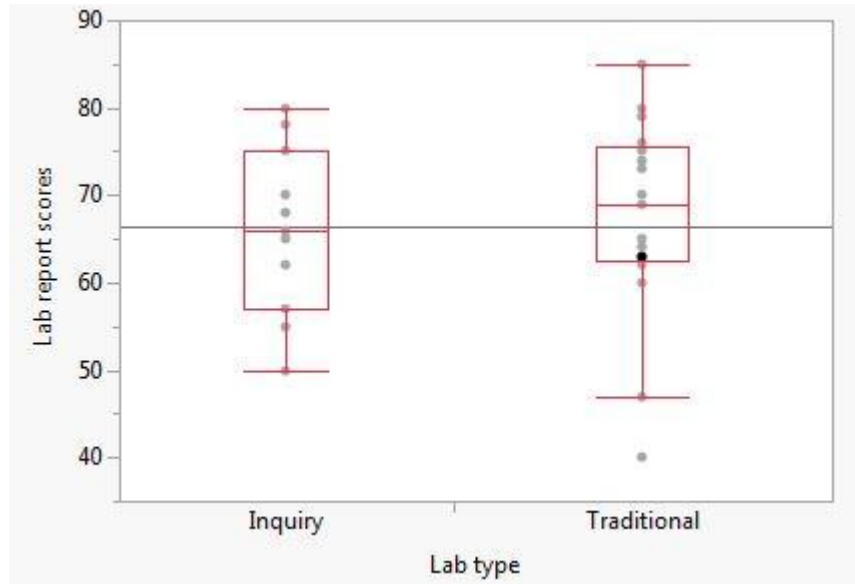**TABLES & FIGURES**
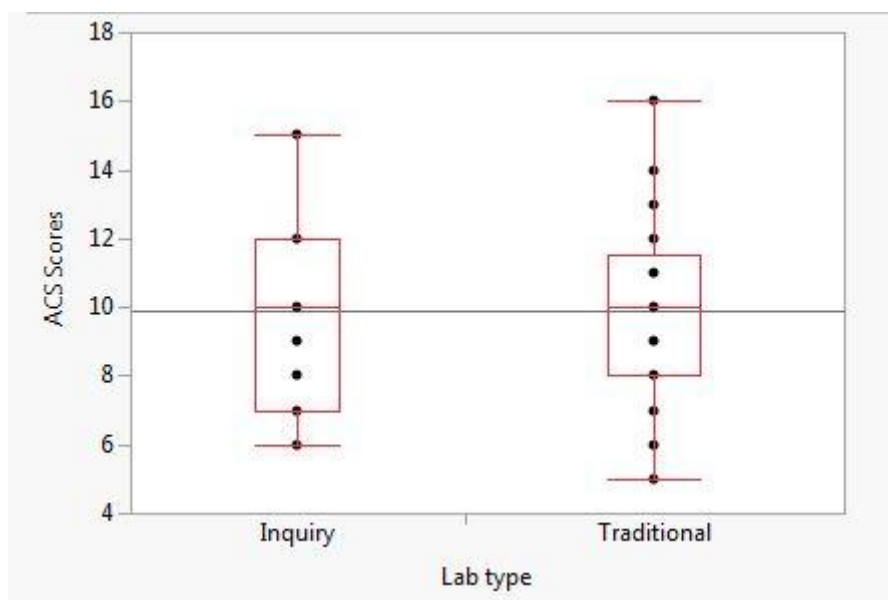
	Exam Score	P-value
Traditional	9.94 ± 2.79	0.8620
Inquiry	9.87 ± 2.75	

Table 1 Wilcoxon rank sum p value of ACS analytical exam scores and means and standard deviations of exam scores.

	Lab Report Score	P-value
Traditional	67.35 ± 11.52	0.6097
Inquiry	65.53 ± 10.21	

Table 2. Wilcoxon rank sum p value of laboratory report scores and means and standard deviations of scores.
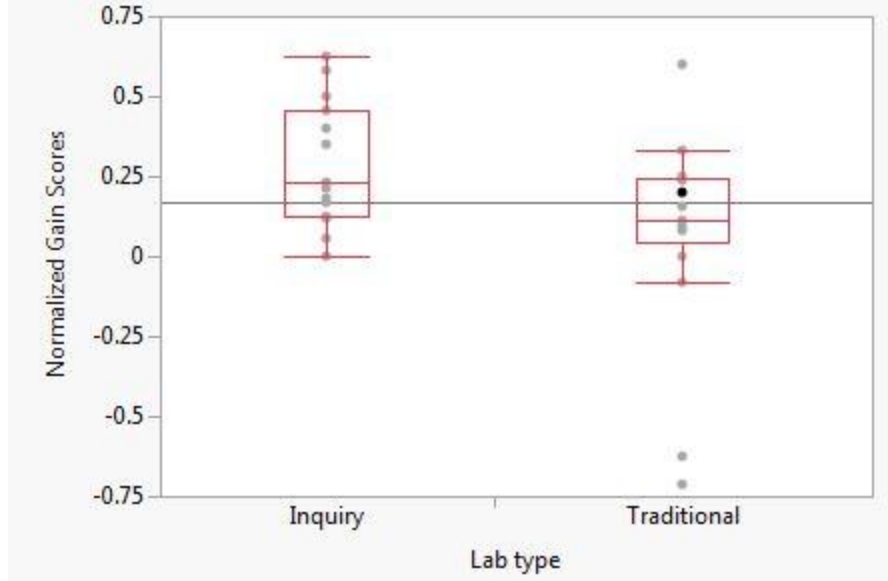
	Pre-quiz	Post quiz	Normalized gain
Wilcoxon test	p < 0.4034	P < 0.2471	p < 0.0473
Traditional	9.53 ± 3.84	10.47 ± 3.64	0.074± 0.32
Inquiry	8.33 ± 3.90	11.6 ± 3.96	0.283 ± 0.19

Table 3. Wilcoxon rank sum p-value of COMA scores and means and standard deviations of scores with normalized learning gains.

APPENDIX. SUPPORT. INFORMATION

Optical Microscopy Experiment, Traditional Format

Introduction

Dark field microscopy is a common optical microscopy technique used in laboratories today. It is used to study thin samples including cells, tissue cultures and various types of surfaces. This microscopic technique utilizes light at oblique angles (large angles) to illuminate the sample and create a dark background. The sample will then appear as a bright image against the dark background, similar to stars in the night sky[42].

The incident light originates from the light source and enters a dark field condenser. The dark field condenser contains an opaque disk, known as an annular stop, which is located in the middle of the condenser's opening or "aperture." The annular stop prevents light from going directly through the condenser and to the sample, but it does allow light to illuminate the sample from large angles. To see this better, below are two images of a dark field condenser when looking at it from the top.
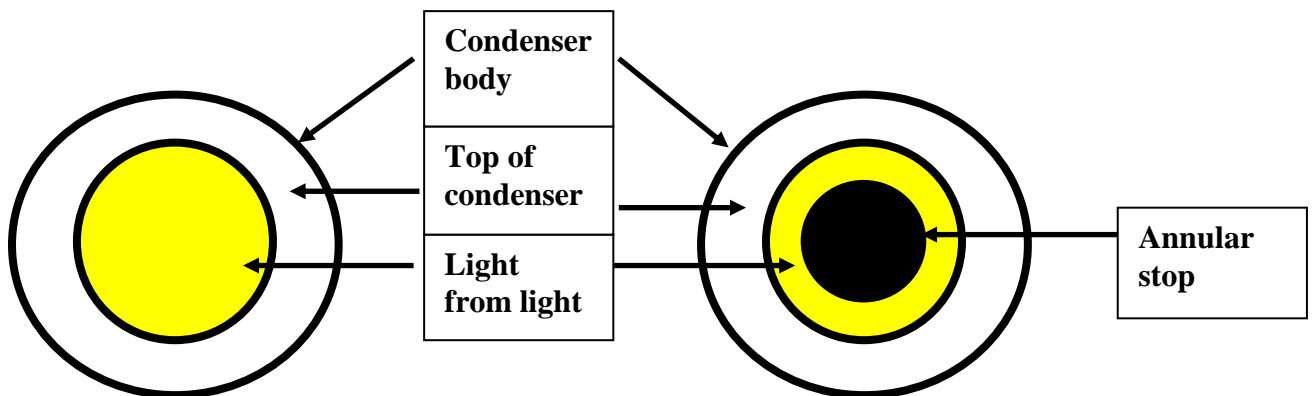
The condenser on the left is a typical condenser used in optical microscopy, while the condenser on the right is a dark field condenser. If no sample is present, none of the light will pass into the objective, and the entire imaging area will look black. However, when a proper sample is present (anything that is able to scatter light), some of the light will become scattered toward the direction of the objective, where the light is collected and an image is generated. Below is an image of a dark field microscope.
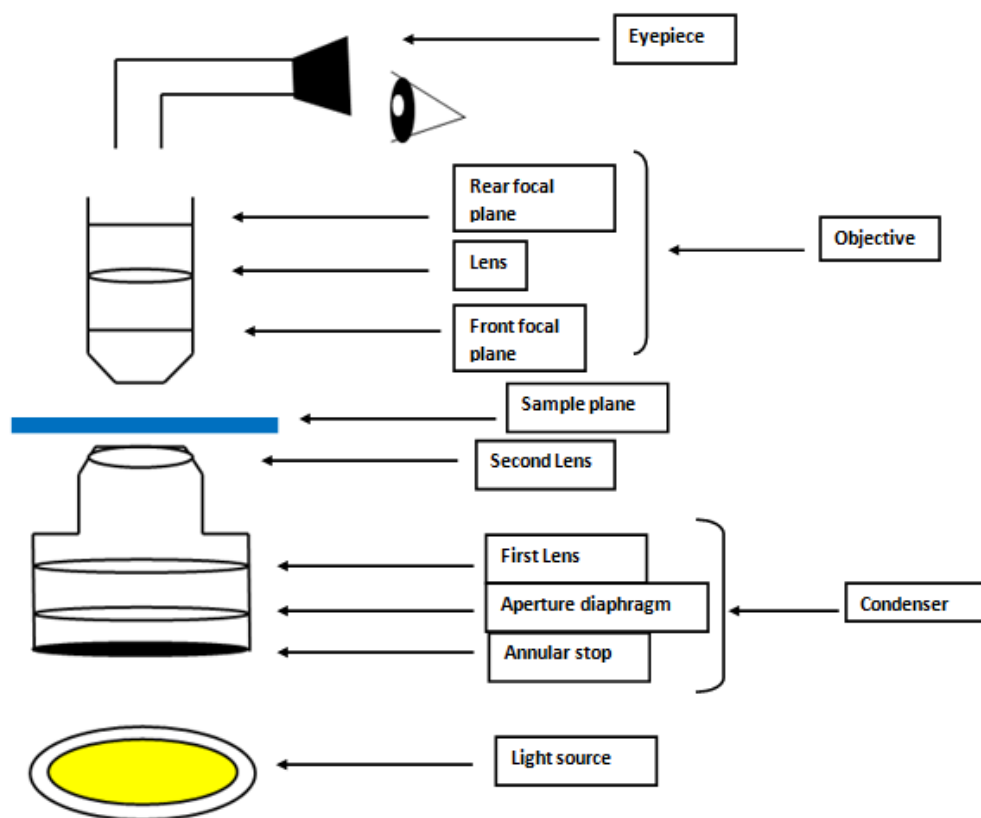
The dark field microscope you will be using in the lab experiment is pictured below with the components labeled.

92

Eyepiece

Condense

Light

Tuning knob
(adjusts focus
and move
stage)

Objective

Stage (sample plane)
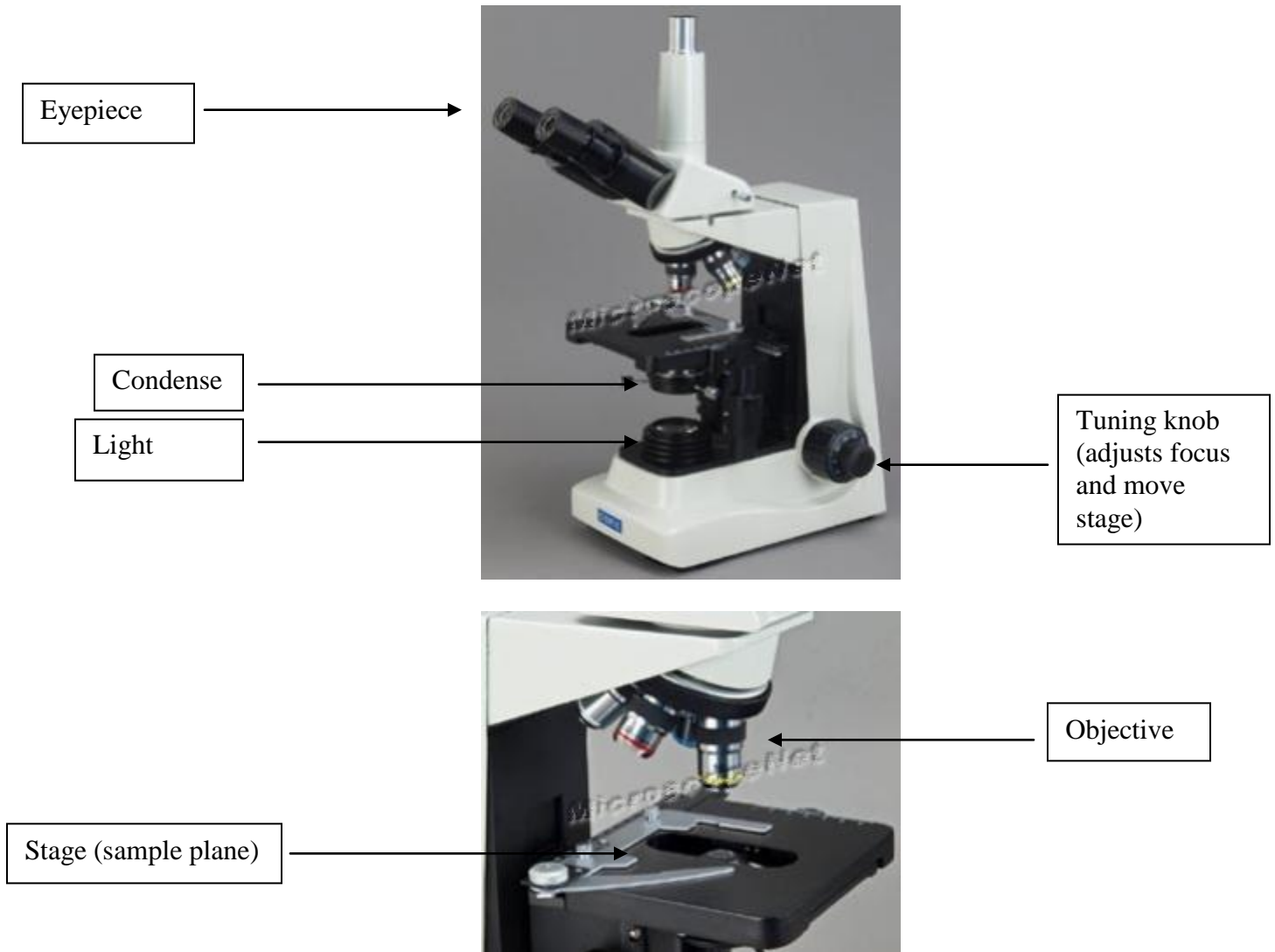
Oftentimes, dark field microscopy utilizes a spectrophotometer in order to measure the radiation intensity of light after interacting with the sample as a function of wavelength. If a spectrophotometer is not available a diffraction grating, or bandpass filters can be used. The grating is placed between the objective and the detector, and it diffracts the light that is scattered by the sample. This allows for the scattering signal at all wavelengths to be measured, just as with a spectrophotometer. In this experiment filters will be used. Filters are different than gratings and spectrophotometers as they only allow specific wavelengths of light to pass from the light source to the sample. This means that multiple filters have to be utilized in order to collect

the same wavelength spectrum as would be collected with a grating; which can add time to data collection. But, because filters have specific wavelength ranges, if only a portion of the light spectrum is of interest, filters can be more advantageous than a grating.

In the laboratory experiment you will be investigating nanoparticles and some of their optical properties. Noble metal nanoparticles can be fabricated in all shapes and sizes, depending on what properties are desired; common shapes of nanoparticles include rods, cubes and triangles. Nanoparticles are quite small, by definition they are between 10 – 100 nm in diameter. To put this in perspective of other 'small items' a pictorial comparison of nanoparticles compared to cells and a carbon – carbon bond. The cells typically range between tens and hundreds of μm in length (in the image the cell has nanorods on the surface, these rods are 25nmx73nm). The image of the nanoparticles was taken with transmission electron microscopy (TEM); there are different shapes – rods, triangles and spheres – the spheres are 20nm in diameter. A carbon – carbon bond ranges between 120 – 154 pm, below is an ethane molecule.
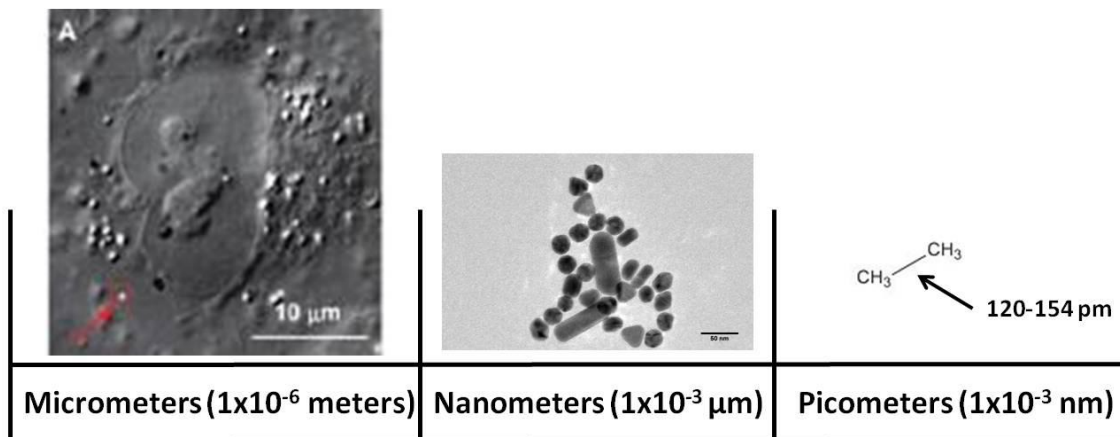

Figure 12 A549 lung cancer cell from Yan Gu[114]; TEM image by Anthony Stender.

The origin of optical properties of metals of any size is the ability of the conductive electrons to oscillate collectively when they are excited by incident light. The movement of electrons is known as a surface plasmon.. A plasmon is dependent on the polarizability of the

nanoparticle. Below is a diagram of nanoparticles' electrons being excited by incident light (i.e. electric field).
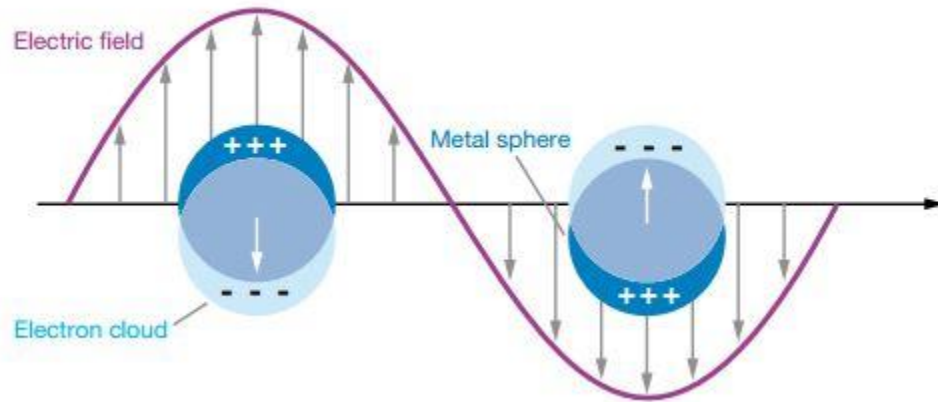
Figure 13. Incident light hitting a nanoparticle and exciting the conducting electrons; when electrons are excited the electron cloud of the nanoparticle shifts and creates a dipole[115].

As incident light hits a bulk metal the conduction electrons begin to collectively oscillate at the surface of the metal. The oscillation creates a wave across the surface of the metal film. In the case of a nanoparticle that is irradiated with light, the conduction electrons collectively oscillate as well, but rather than create a wave across the surface the oscillating electrons create a dipole. Plasmons are found in metals such as copper, silver and gold, among others; plasmons can occur in bulk metal, small metal nanoparticles, and on metal surfaces. In this lab experiment, we will be focusing on gold and silver nanoparticles. When the electrons are excited and oscillate in metal nanoparticles, the plasmon is referred to as a localized surface plasmon resonance (LSPR). From the absorption or scattering spectrum, the wavelengths that excite the LSPR can be determined. The spectral location of the LSPR peak is influenced by many factors, but the most important are the type of metal, size, shape and the solvent's refractive index. Silver spheres will have a LSPR peak in 400-500nm range while gold spheres have a LSPR peak between 500-600nm.
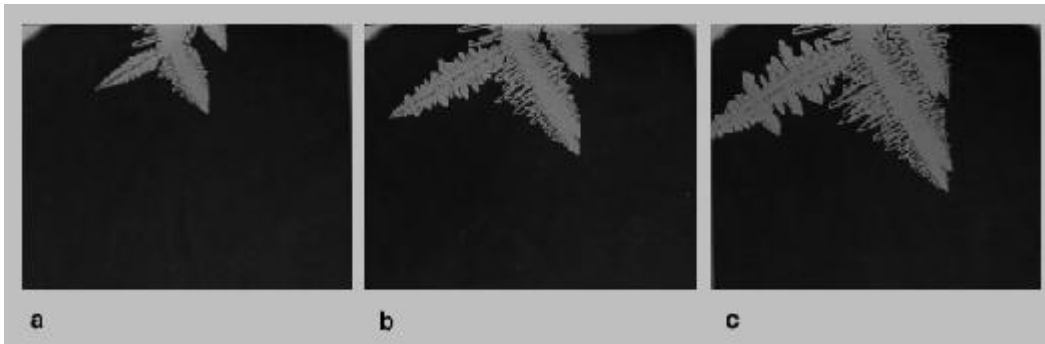
Nanoparticles can absorb and scatter light due to their plasmonic properties. Absorption or scattering can be detected depending on what type of instrument is being used. Dark field microscopy is only able to collect the scattered light; therefore, anything on the sample plane that is able to scatter light will be seen with a dark field microscope. There are different types of scattering that can occur – Raman, Rayleigh, Mie, and Debye. Dark field microscopy collects Rayleigh scattering, which takes place when a particle is much smaller than the incident light[116]. (It's because of Rayleigh scattering that the sky is blue). In today's experiment you will be investigating the scattering of three types of nanospheres.

The silica spheres are able to scatter light and will have a scattering spectrum because they interact with light, but they do not have plasmonic properties. Silica spheres, as well as other polymeric nanostructures, often serve as controls for nanotechnology experiments.

Nanoparticles have been used as biological sensors to examine biological processes in cells such as cell apoptosis[39] and as chemical sensors to detect explosive materials such as 2-4-6-trinitrotoluene[37] (TNT). Nanoparticles have also been utilized in the miniaturization of electronics, in high performance polymers, catalysis, and drug delivery[117]. Nanoparticles are widely used to enhance signals of fluorescent molecules in fluorescence resonance energy transfer. These applications exploit the optical properties that are unique to nanoparticles *i.e.* surface plasmons.

In today's experiment, you will look at two of types of nanoparticles – silver spheres and gold spheres, you will also be growing your own silver crystals. When crystals grow at rapid rates dendrite crystals are formed; the branches that form are the preferred growth direction. They resemble multi-branched trees. Dendrite crystals can grow during solidification,

electrochemical deposition, or growth from a vapor. They are a classic example of pattern

formation in non-equilibrium systems[118]. Below are images of a dendrite crystal growth system.
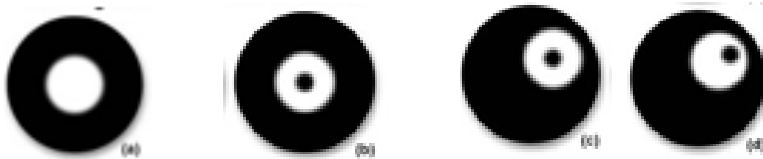
Equipment and materials:
1. Nanoparticles
   a. 100nm Gold spheres
   b. 100nm Silver spheres
   c. 200nm mesoporous silica spheres
   d. Silver crystals
2. Solution of silver nitrate, 0.0125M
3. Equipment
   a. 0.5 cm of copper wire
   b. Plastic dropper
   c. 10mL graduated cylinder
   d. 10mL beaker
   e. Glass slides with etched rings
   f. Plane glass slides
   g. Glass coverslips
   h. 100μL pipette
   i. Clear nail polish

Software:
1. The software you will be using for the experiment is Toupview.
2. Double click on the Toupview icon on the desktop to open up the program.
3. Click on the link to the camera in the top left corner of the screen when the program is open. There should be one link in the camera list.
4. To take a picture click on "snap".
5. To go to a live view after taking an image click on the video tab at the top of the images.
6. To adjust the gain and exposure settings, make sure the "auto" setting is un-clicked. Then move the bar on the scales to the setting of your choice.

Procedure:

Part I: Setting microscope alignment (Köhler Illumination)

1. Once you have a slide ready and it is on the microscope stage, you need to make sure the Köhler illumination is set. Setting the Köhler illumination insures that the condenser and objective are properly aligned. You will have to do this only once.

2. To set the Kohler illumination, take the eyepiece lens off the microscope. Be sure not to touch any of the lens glass on the eyepiece, or you will leave oils from your fingers which will obstruct your view of the sample.

3. After the eyepiece is off look down the rest of the eyepiece tunnel. You should see any one of the following images:

(http://www.olympusmicro.com/primer/techniques/darkfieldsetup.html accessed 8/10/2012)

4. Move the condenser position with the screws located on the condenser's front until you see something similar to image a. The bright disk in the middle will be bigger than the dark ring on the outer edges.

Part II: Copper crystal growth

1. Make a 0.0125M solution of silver nitrate in 1mL of DI water.

2. Cut a 0.5cm length of copper wire.

3. On the computer adjust the gain setting of 1.5 and exposure time to 500ms.

4. On the stage of the microscope put the glass slides with the depressions facing upward and place your copper wire sample.

5. Using the 10x objective bring the sample into focus. As the reaction proceeds focus on the crystals growing not the copper wire.

6. Add a few drops of the silver nitrate solution you made.

7. Take images every 30 seconds as the reaction proceeds.

8. Run the reaction again at different gain or exposure time settings of your choosing.

Analysis questions:

1. Why did you change the gain and exposure settings in the way that you did?

2. When you increased, or decreased, the gain setting, did you have to increase or decrease the exposure time?

3. Is there a relationship between gain and exposure time?

4. What type of chemical reaction is this? Write the equation below.

5. If you had a higher or lower concentration of silver nitrate how would that affect the crystal growth rate?

6. Would the reaction be as spontaneous if magnesium chloride were used instead of silver nitrate? Why or why not?

Part III: Investigation of plasmon resonances in prefabricated nanoparticles

1. Prepare three samples of prefabricated nanoparticles (you are going to make one of each type of sphere).

2. Deposit between 5 and 7 μl of your diluted nanoparticle sample onto the slide.

3. Over the aliquot on the slide, add a coverslip and seal the edges with clear nail polish. Be sure not to get the polish anywhere but on the edges of the coverslip.

4. Once the nail polish has dried, place the slide on the stage of the microscope and position the stage to get the particles in focus; use the 40x objective.
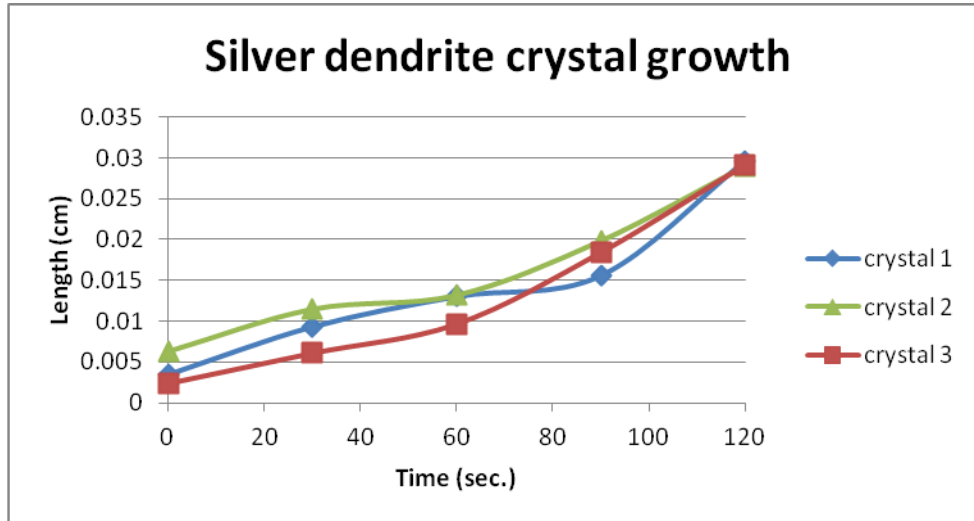
5. Check the Köhler illumination to make sure the objective and condenser are still properly aligned.

6. Use the 40x objective and bring your sample into focus.

7. Adjust the exposure time to 300ms and gain setting of 2.

8. Take an image and save it to the computer. Make a folder with your name in the 316L folder. Be sure to label your images with the sphere type (i.e. gold, silver or silica), gain and exposure settings.

9. Once you have taken an image of one of your samples, you will take another 5 images of the same sample with bandpass filters. You will have to adjust the gain and exposure settings to obtain an image with the highest spatial resolution that you can. Be sure to label the images with the type of sphere, filter wavelength, gain and exposure settings.

10. There are five filters that each allow different wavelengths of light through. Each filter is labeled with its transmission peak and the range of wavelengths on either side of the peak (e.g. 550 nm ±10 allows light to pass from 540 nm to 560 nm).

11. Repeat this procedure with all three samples.

Analysis questions:

1. Which filter gave the cleanest image for each sample?

2. Look at the absorption spectra of the sphere samples; do the filter transmission wavelengths match the sphere absorption wavelengths? What are they for each sample?

3. The filters are labeled with the wavelengths that pass, but how accurate is this? How can the wavelength ranges be verified? Hint: When absorption or transmission of a chemical needs to be known a UV-Vis spectrum is taken; this is can also be performed with filters

to verify the wavelength transmission range. Take a UV-Vis of the filter that gave the cleanest images for each sample.

Sample data

Data analysis

1. Measure the crystal growth rate of the silver crystals that you grew and graph the distance per time in nanometers per second. Graph more than one crystal.

Data analysis tools

You can calculate the length of the crystal using the computer program ImageJ. ImageJ is a free download from NIH (http://rsbweb.nih.gov/ij/) and is a common program to analyze images in microscopy. It can be used to analyze still images such as nanoparticles on a glass slide and cells, as well as movies to track moving nanoparticles in live cells. The data that you collect today will be analyzed with ImageJ.

The tools you may need in the program include

1. Straight tool - ◹ used to measure intensity, length, spectrum of object in image
2. Control m – take a measurement when using the straight tool, or any tool
3. To change the contrast of the image, go to image ⟶ adjust ⟶ contrast/brightness
4. To add a scale bar go to analyze ⟶ tools ⟶ scale bar
5. To stack images (i.e. make a movie) go to image ⟶ stacks ⟶ images

To measure the length of the crystals
1. Use the straight tool and measure from the copper wire to the end of the crystal.
2. Hit control-m to take a measurement
3. You will get the length in pixels
4. One pixel is 1.4μm at 1x magnification, but remember you used 10x magnification.

Post lab questions

1. Draw a dark field microscope set up and show the light path through the microscope.
2. What are a few advantages and disadvantages of dark field microscopy? Name two of each.
3. Dark field microscopy collects Rayleigh scattering, but Raman scattering is commonly measured with other analytical instruments. Compare and contrast Rayleigh and Raman scattering.

References

1.   Wang, G.; Stender, A. S.; Sun, W.; Fang, N., Optical imaging of non-fluorescent nanoparticle probes in live cells. *Analyst* **2010,** *135* (2), 215-221.

2.   Yan Gu, W. S., Gufeng Wang, Ning Fang, Single Particle Orientation and Rotation Tracking Discloses Distinctive Rotational Dynamics of Drug Delivery Vectors on Live Cell Membranes. *Journal of the American Chemical Society* **2011,** *133*, 5720-5723.

3.   Van Duyne, R. P.; Willets, K. A., ANYL 41-Localized surface plasmon resonance spectroscopy and sensing. *Abstr. Pap. Am. Chem. Soc.* **2007,** *234*.

4.   Ball, D. W., Rayleigh and Raman Scattering. *Spectroscopy* **2001,** *16* (2), 29-30.

5.   Choi, Y.; Kang, T.; Lee, L. P., Plasmon Resonance Energy Transfer (PRET)-based Molecular Imaging of Cytochrome c in Living Cells. *Nano Letters* **2009,** *9* (1), 85-90.

6.   Qu, W.-G.; Deng, B.; Zhong, S.-L.; Shi, H.-Y.; Wang, S.-S.; Xu, A.-W., Plasmonic resonance energy transfer-based nanospectroscopy for sensitive and selective detection of 2,4,6-trinitrotoluene (TNT). *Chemical Communications* **2011,** *47* (4), 1237-1239.

7.   Hayden, C. O. C. a. H., Contextualising nanotechnology in chemistry education. *Chemistry Education Research and Practice* **2008,** *9*, 35-42.

8.   David A. Kessler, J. K. a. H. L., Steady-state dendritic crystal growth. *Physical Review A* **1986,** *33* (5), 3352-3357.

Optical Microscopy Experiment, Inquiry Format

Introduction

You've already been introduced to the basics of optical microscopy in the pre-lab activity – what the components are, how they work together with the light path to create an image and how the image is detected. In today's experiment you will be working with a dark field microscope; a dark field microscope has the same components as any other optical microscope. Below are images of the microscope you will be using in the experiment; label the parts of the microscope, the components have arrows pointing to them and there is a word bank with the names of the components.

Stage (sample plane)
Objective
Light source
Tuning knob (adjusts
focus and move stage)
Condenser
Eyepiece
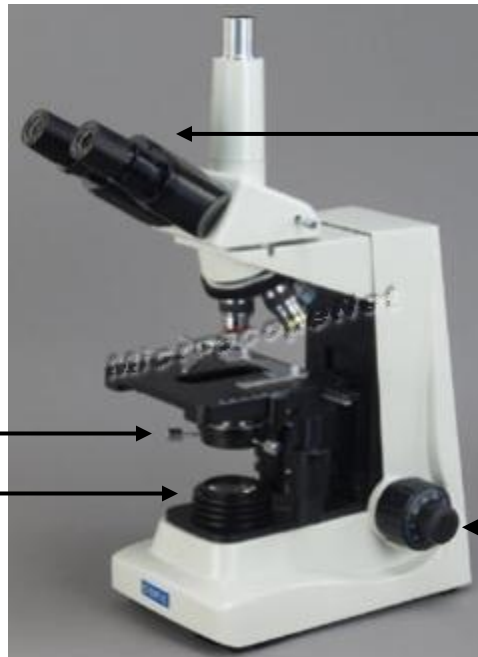
Model 1: An introduction to dark field microscopy

Dark field microscopy is a common optical microscopy technique used in laboratories today. It is used to study thin samples including cells, tissue cultures and various types of surfaces. A dark field microscope is named so because it produces images that have a dark background; anything that's on the sample plane will appear bright, similar to a night sky with stars.[42] How is the dark background created? Below is a comparison of a typical condenser used in optical microscopy and a dark field condenser; the components are labeled.
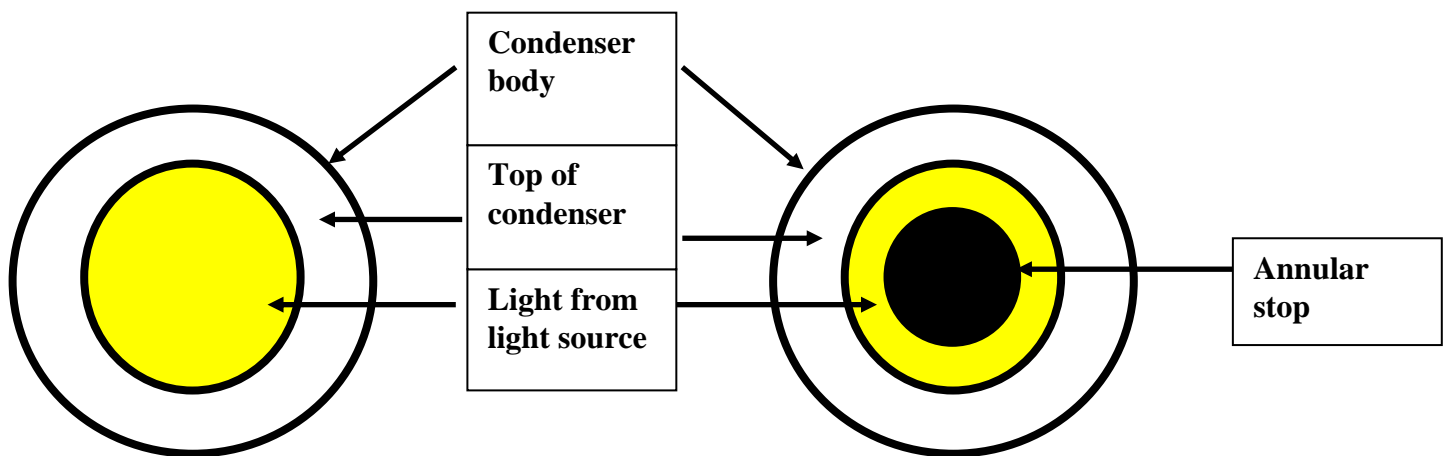
Dark field microscopy is only able to collect scattered light; therefore, anything on the sample plane that is able to scatter light will be detected. There are diferent types of scattering – Rayleigh, Raman and Mie are the most common types of scattering studied. Dark field

microscopy collects Rayleigh scattering, which takes place when a particle is much smaller than the incident light[116]. (It's because of Rayleigh scattering that the sky is blue).

Questions:

1. Do both condensers have the same components?
2. Does the same amount of light seem to pass through the condenser?
3. What is the function of the annular stop?
4. Dark field microscopy collects Rayleigh scattering, another type of scattering discussed in this course is Raman scattering; compare and contrast Rayleigh and Raman scattering.
5. What are a few advantages and disadvantages of dark field microscopy? Name two of each.
6. Come up with a hypothesis on how the black background is created.

Now that you understand the basic operating principle of dark field microscopy, how do all of the components work together? Below is an image of a microscope, like the one in the pre-lab material, with a dark field condenser. Draw the light path through the microscope to see how the components work together; remember that the annular stop is present and what that does to the light path.
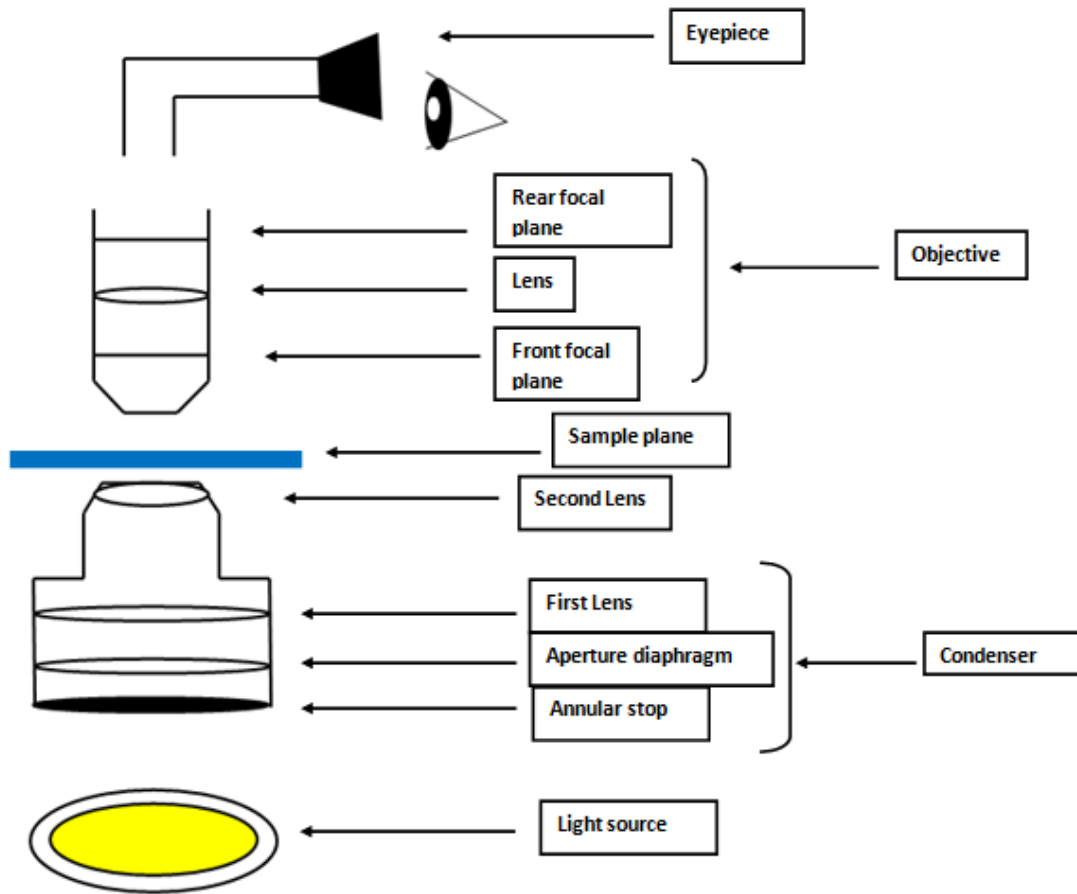
Dark field microscopy collects light at all wavelengths therefore, it is often necessary to separate the light to measure the signal at separate wavelengths. To do this there are a few different techniques that can be utilized. The most common are spectrophotometers, diffraction gratings and filters. Spectrophotometers measure the radiation intensity of light after interacting with the sample as a function of wavelength. If a spectrophotometer is not available a diffraction grating, or bandpass filters can be used. A diffraction grating is placed between the objective and the detector; it diffracts the light that is scattered by the sample. This allows for the scattering signal at all wavelengths to be measured, just as with a spectrophotometer. In this experiment filters will be used. Filters are different than gratings and spectrophotometers as they only allow specific wavelengths of light to pass from the light source to the sample. Individual filters are

placed between the light source and condenser. This means that multiple filters have to be utilized in order to collect the same wavelength spectrum as would be collected with a grating; which can add time to data collection. Because filters have specific wavelength ranges, if only a few wavelengths of light are of interest, filters can be more advantageous than a grating.

Model 2: Nanoparticles and plasmons

In today's experiment, you will be working with nanoparticles. Nanoparticles can be fabricated in all different shapes and materials. Common nanoparticle shapes include spheres, rods, cubes, triangles and stars; which are most often synthesized from noble metals such as gold and silver. Nanoparticles are defined as a small particle between 10 – 100 nm in diameter. But, how small is this? To get a better understanding of their small size below is a scale comparing a nanoparticle to a cell and a carbon – carbon bond length.

| Micrometers (1x10^{-6} meters) | Nanometers (1x10^{-3} μm) | Picometers (1x10^{-3} nm) |
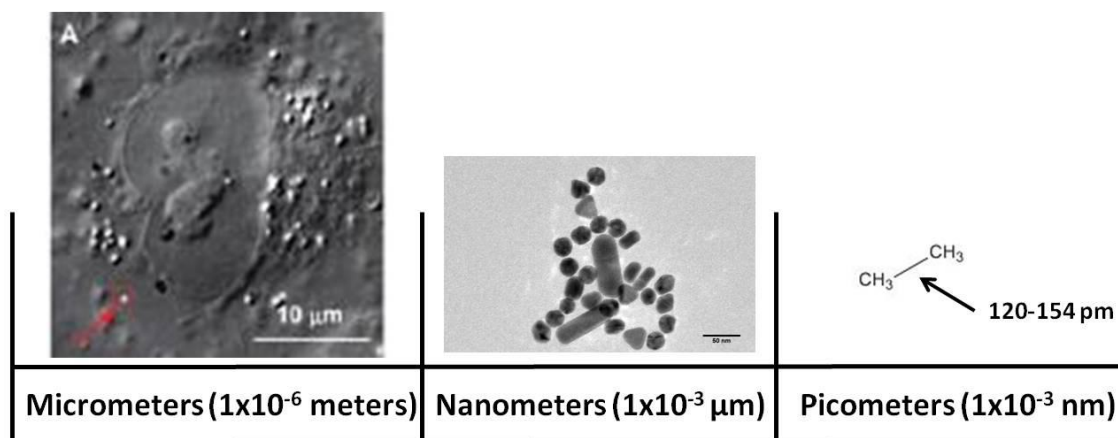
Figure 14. A549 lung cancer cell with gold nanorods on the membrane[114]; TEM image of various nanoparticles by Anthony Stender; Ethane molecule.

Noble metal nanoparticles are commonly used in chemistry, biological and materials research. Nanoparticles have been used as biological sensors to examine biological processes such as cell apoptosis[39] and as chemical sensors to detect explosive materials such as 2-4-6-trinitrotoluene[37] (TNT). Nanoparticles have also been utilized in the miniaturization of

electronics, in high performance polymers, catalysis, and drug delivery[117]. Nanoparticles are widely used to enhance signals of fluorescent molecules in fluorescence resonance energy transfer. These applications exploit the optical properties that are unique to nanoparticles. The optical properties of nanoparticles originate from a phenomenon known as plasmons, described in the next section. Below is a depiction of one nanoparticle as it is being irradiated with incident light over time.
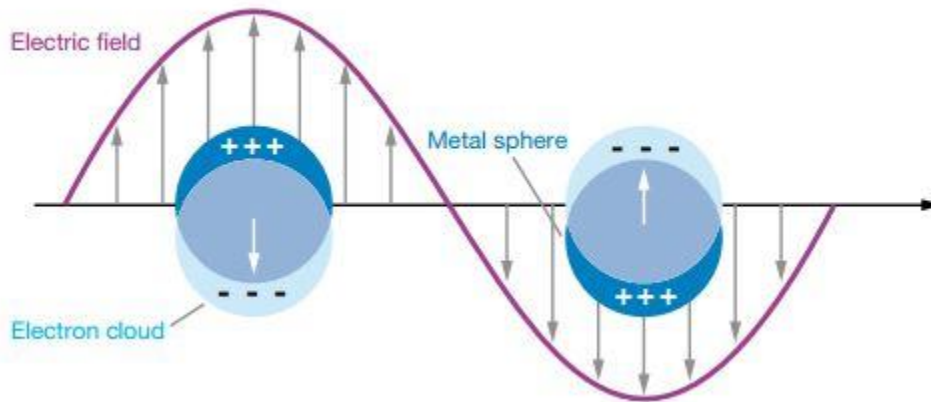
Figure 15. A depiction of one nanoparticle as it is being irradiated with incident light over time.[115]

Questions:
1. As the electric field (incident light) hits the nanoparticle what happens to the conducting electrons (electron cloud)?
2. What do the positive and negative charges indicate?
3. How is the dipole created?
4. Is the dipole permanent, or oscillating?

It is because of plasmons that nanoparticles can interact with light; they are able to absorb and scatter light. The scattering and absorption of light is why nanoparticles are able to be detected with optical microscopy. Metal nanoparticles have different optical properties than their bulk counterparts mainly due to the size. A metal film will have a surface plasmon that creates a wave that moves across the surface of the film, while a nanoparticle will have a plasmon that creates a dipole rather than a wave. The size, shape and type of metal can have an effect on the

plasmons of the nanoparticle. Just as with any other absorbing material, there are wavelengths that are better absorbed than others. When discussing plasmons, the wavelengths that excite the conducting electrons best is termed the localized surface plasmon resonance (LSPR). In today's experiment, you will be working with gold and silver 100 nm spheres.
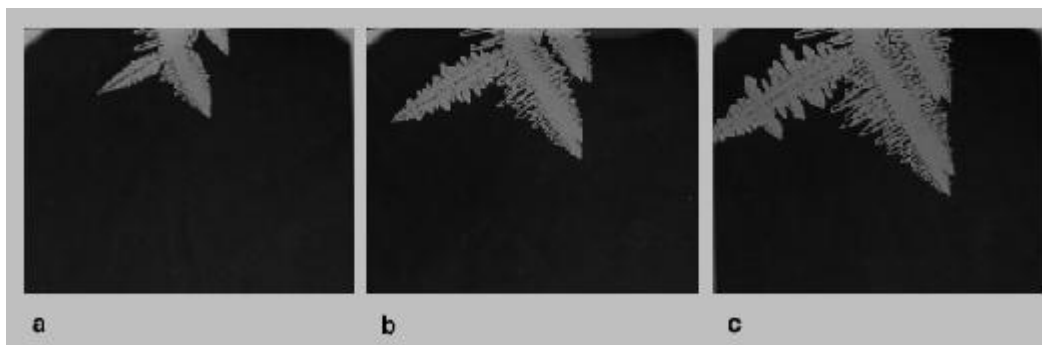
There are other materials that are able to interact with light even though they are not plasmonic. These materials are often used as controls in microscopy and nanoparticle research. Such materials include polystyrene and silica. In today's experiment you will not only be working with gold and silver nanospheres, but also 200 nm mesoporous silica nanospheres (mesoporous means that there are pores in the silica spheres).

Questions:
1. Do you think there are wavelengths of light that will excite the conducting electrons in a nanoparticle better than others? Why or why not?
2. Will gold and silver have their plasmon peaks at the same wavelengths? Why or why not?
3. Why do you think that non plasmonic materials are used as controls in experiments?

Model 3: A reaction between copper and silver

Nanoparticles are not the only type of sample that can be studied with dark field microscopy. Dark field microscopy is used to study thin samples such as cells, tissue cultures and various types of surfaces. Another sample you will be studying is a copper wire reacting with silver nitrite. As the reaction proceeds, silver crystals begin to grow on the surface of the wire. When crystals grow at rapid rates dendrite crystals are formed; the branches that form are the preferred growth direction. Dendrite crystals can grow during solidification, electrochemical deposition, or growth from a vapor; they are a classic example of pattern formation in non-equilibrium systems[118]. Below are images of a dendrite crystal growth system over time.

Equipment and materials:

1. Nanoparticles
    a. 100nm Gold spheres
    b. 100nm Silver spheres
    c. 200nm mesoporous silica spheres
    d. Silver crystals
2. Solution of silver nitrate, 0.0125M
3. Equipment
    a. 0.5 cm of copper wire
    b. Plastic dropper
    c. 10mL graduated cylinder
    d. 10mL beaker
    e. Glass slides with etched rings
    f. Plane glass slides
    g. Glass coverslips
    h. 100μL pipette
    i. Clear nail polish

Software:

1. The software you will be using for the experiment is Toupview.
2. Double click on the Toupview icon on the desktop to open up the program.
3. Click on the link to the camera in the top left corner of the screen when the program is open. There should be one link in the camera list.
4. To take a picture click on "snap".
5. To go to a live view after taking an image slick on the video tab at the top of the images.
6. To adjust the gain and exposure settings, make sure the "auto" setting is unclicked. Then move the bar on the scales to the setting of your choice.

Procedure:
Part I: Setting microscope alignment (Köhler Illumination)

1. Once you have a slide ready and it is on the microscope stage, you need to make sure the Köhler illumination is set. Setting the Köhler illumination insures that the condenser and objective are properly aligned. You will have to do this only once.

2. To set the Kohler illumination, take the eyepiece lens off the microscope. Be sure not to touch any of the lens glass on the eyepiece, or you will leave oils from your fingers which will obstruct your view of the sample.

3. After the eyepiece is off look down the rest of the eyepiece tunnel. You should see any one of the following images:

(http://www.olympusmicro.com/primer/techniques/darkfieldsetup.html accessed 8/10/2012)

4. Move the condenser position with the screws located on the condenser's front until you see something similar to image a. The bright disk in the middle will be bigger than the dark ring on the outer edges.

Part II: Copper crystal growth

1. Make a 0.0125M solution of silver nitrate in 1mL of DI water.

2. Cut a 0.5cm length of copper wire.

3. On the computer adjust the gain setting of 1.5 and exposure time to 500ms.

4. On the stage of the microscope put the glass slides with the depressions facing upward and place your copper wire sample.

5. Using the 10x objective bring the sample into focus. As the reaction proceeds focus on the crystals growing not the copper wire.

6. Add a few drops of the silver nitrate solution you made.

7. Take images every 30 seconds as the reaction proceeds.

8. Run the reaction again at different gain or exposure time settings of your choosing.

Analysis questions:
1. Why did you change the gain and exposure settings in the way that you did?
2. When you increased, or decreased, the gain setting, did you have to increase or decrease the exposure time?
3. Is there a relationship between gain and exposure time?
4. What type of chemical reaction is this? Write the equation below.
5. If you had a higher or lower concentration of silver nitrate how would that affect the crystal growth rate?
6. Would the reaction be as spontaneous if magnesium chloride were used instead of silver nitrate? Why or why not?

Part III: Investigation of plasmon resonances in prefabricated nanoparticles
1. Prepare three samples of prefabricated nanoparticles (you are going to make one of each type of sphere).
2. Deposit between 5 and 7 μl of your diluted nanoparticle sample onto the slide.
3. Over the aliquot on the slide, add a coverslip and seal the edges with clear nail polish. Be sure not to get the polish anywhere but on the edges of the coverslip.
4. Once the nail polish has dried, place the slide on the stage of the microscope and position the stage to get the particles in focus; use the 40x objective.
5. Check the Köhler illumination to make sure the objective and condenser are properly aligned.
6. Use the 40x objective and bring your sample into focus.
7. Adjust the exposure time to 300 ms and gain setting of 2.
8. Take an image and save it to the computer. Make a folder with your name in the 316L folder. Be sure to label your images with the sphere type (i.e. gold, silver or silica), gain and exposure settings. Example: Ag; 3; 350ms; no filter.
9. Once you have taken an image of one of your samples, you will take another 5 images of the same sample with bandpass filters. You will have to adjust the gain and exposure settings to obtain an image with the highest spatial resolution that you can. Be sure to label the images with the type of sphere, filter wavelength, gain and exposure settings.

10. There are five filters that each allow different wavelengths of light through. Each filter is labeled with its transmission peak and the range of wavelengths on either side of the peak (e.g. 550 nm ±10 allows light to pass from 540 nm to 560 nm).
11. Repeat this procedure with all three samples.
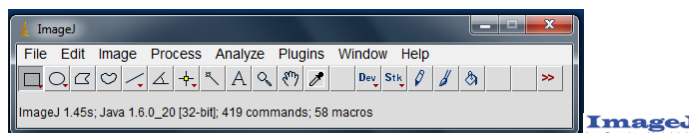
Analysis questions:
1. Which filter gave the cleanest image for each sample? Was it the same filter for each sample?
2. Why doesn't the same filter produce the same clean image with all three samples?
3. If you look at the absorption spectra of the sphere samples, does this give you an idea why the filter that gave the cleanest image that did? Explain.
4. The filters are labeled with the wavelengths that pass, but how accurate is this? How can the wavelength ranges be verified? Hint: When absorption or transmission of a chemical needs to be known a UV-Vis spectrum is taken; this is can also be performed with filters to verify the wavelength transmission range. Take a UV-Vis of the filter that gave the cleanest images for each sample.

Data analysis
1. Measure the crystal growth rate of the silver crystals that you grew and graph the distance per time in nanometers per second. Graph more than one crystal.

Data analysis tools

You can calculate the length of the crystal using the computer program ImageJ. ImageJ is a free download from NIH (http://rsbweb.nih.gov/ij/) and is a common program to analyze images in microscopy. It can be used to analyze still images such as nanoparticles on a glass slide and cells, as well as movies to track moving nanoparticles in live cells. The data that you collect today will be analyzed with ImageJ.

The tools you may need in the program include

1. Straight tool - used to measure intensity, length, spectrum of object in image.
2. Control m – take a measurement when using the straight tool, or any tool.
3. To change the contrast of the image, go to image ⟶ adjust ⟶ contrast/brightness.
4. To add a scale bar go to analyze ⟶ tools ⟶ scale bar
5. To stack images (i.e. make a movie) go to image ⟶ stacks ⟶ images

To measure the length of the crystals

1. Use the straight tool and measure from the copper wire to the end of the crystal.
2. Hit control-m to take a measurement.
3. You will get the length in pixels.
4. One pixel is 1.4µm at 1x magnification, but remember that you used 10x magnification.

REFERENCES

1. Wang, G.; Stender, A. S.; Sun, W.; Fang, N., Optical imaging of non-fluorescent nanoparticle probes in live cells. *Analyst* **2010,** *135* (2), 215-221.

2. Yan Gu, W. S., Gufeng Wang, Ning Fang, Single Particle Orientation and Rotation Tracking Discloses Distinctive Rotational Dynamics of Drug Delivery Vectors on Live Cell Membranes. *Journal of the American Chemical Society* **2011,** *133*, 5720-5723.

3. Van Duyne, R. P.; Willets, K. A., ANYL 41-Localized surface plasmon resonance spectroscopy and sensing. *Abstr. Pap. Am. Chem. Soc.* **2007,** *234*.

4. Ball, D. W., Rayleigh and Raman Scattering. *Spectroscopy* **2001,** *16* (2), 29-30.

5. Choi, Y.; Kang, T.; Lee, L. P., Plasmon Resonance Energy Transfer (PRET)-based Molecular Imaging of Cytochrome c in Living Cells. *Nano Letters* **2009,** *9* (1), 85-90.

6. Qu, W.-G.; Deng, B.; Zhong, S.-L.; Shi, H.-Y.; Wang, S.-S.; Xu, A.-W., Plasmonic resonance energy transfer-based nanospectroscopy for sensitive and selective detection of 2,4,6-trinitrotoluene (TNT). *Chemical Communications* **2011,** *47* (4), 1237-1239.

7. Hayden, C. O. C. a. H., Contextualising nanotechnology in chemistry education. *Chemistry Education Research and Practice* **2008,** *9*, 35-42.

8. David A. Kessler, J. K. a. H. L., Steady-state dendritic crystal growth. *Physical Review A* **1986,** *33* (5), 3352-3357.

Chemical Optical Microscopy Assessment (COMA)

This is an assessment about optical microscopy; it will test your knowledge of optical microscopy. You will be asked to take this assessment before you perform the optical microscopy lab experiment and two weeks after you have performed the lab experiment. This will aid in monitoring your learning gains about optical microscopy.

1. If the light intensity from the light source was lowered, what affects would that have on the optical system?

2. When you are imaging with an optical microscope and are having an issue with low signal, what can be adjusted to increase signal intensity? Name two components that affect light intensity and what can be adjusted.

3. If you have two objectives with different numerical apertures: 0.75 and 1.0. Which objective will give you a higher spatial resolution image? Explain why you chose the objective you did.

4. When changing between objectives with different NA, why is it a good idea to adjust the NA on the condenser?

5. Other than the NA of the optical system, what affects spatial resolution? Name two variables.

6. What are changing the magnification of the objective, properly aligning the objective and condenser, and imaging with oil optics rather than air optics all methods used to accomplish.

7. Would you see a difference in resolution between an image taken with an air objective and one taken with an oil immersion objective if all other variables are the same, why? (Hint: think about refractive index)

8. The sample's substrate can have an effect on imaging. If a quartz slide were used instead of a glass slide with the same objective, why would the amount of light collected change? (Hint: $NA = n \times sin\alpha$; quartz has a refractive index of 1.5 and glass has a refractive index of 1.33.)

9. Application: A polarizer is a device that is often used with un-polarized light to create polarized light. A polarizer is placed between the light source and the condenser. If a linear polarizer were used, what would happen to the light that passed through the microscope? Would the use of a polarizer have an effect on the signal intensity?

10. Application: Filters can be to investigate specific regions of the light spectrum, when only those regions are of interest. However, using filters can add time to data acquisition and analysis. Another technique to separate light is a diffraction grating. What would be the advantages to using a grating? Name two.

Chemical Optical Microscopy Assessment (COMA) Answers

This is an assessment about optical microscopy; it will test your knowledge of optical microscopy. You will be asked to take this assessment before you perform the optical microscopy lab experiment and two weeks after you have performed the lab experiment. This will aid in monitoring your learning gains about optical microscopy.

1. If the light intensity from the light source was lowered, what affects would that have on the optical system?

There would be a lower signal and lower resolution of the image. A longer exposure time would be needed therefore data acquisition time would increase.

2. When you are imaging with an optical microscope and are having an issue with low signal, what can be adjusted to increase signal intensity? Name two components that affect light intensity and what can be adjusted.

Increase gain and exposure time or increase light source. Increase NA on condenser and objective, if possible. Changing sample substrate material would also be an option.

3. If you have two objectives with different numerical apertures – 0.75 and 1.0. Which objective will give you a higher spatial resolution image? Explain why you chose the objective you did.

A NA of 1.0 would give a higher spatial resolution. Increasing NA would decrease the distance between two discernible objects according to Abbe's limit.

Also, a higher NA allows for more light to be collected allowing for a higher resolution.

4. When changing between objectives with different NA, why is it a good idea to adjust the NA on the condenser?

Matching NA on condenser and objective lets the maximum amount of light to be collected. This gives a better signal, able to conserve light.

5. Other than the NA of the optical system, what affects spatial resolution? Name two variables.

Wavelength of incoming light; imaging medium RI; magnification of objective; amount of pixels (more pixels allows for a clearer picture)

6. What can be used or altered on the microscope to improve spatial resolution? Name two methods.

Increasing NA; setting Köhler illumination if possible; incoming wavelength; RI of imaging medium; longer exposure time; magnification of objective; pixel number.

7. Would you see a difference in resolution between an image taken with an air objective and one taken with an oil immersion objective if all other variables are the same, why? (Hint: think about refractive index)

Oil will have a higher resolution because it has a higher RI (NA= n sin (α))

Having an RI mismatch will negatively affect NA and thus spatial resolution distance.

8. The sample's substrate can have an effect on imaging. If a quartz slide were used instead of a glass slide with the same objective, why would the amount of light collected change? (Hint: $NA = n \times sin\alpha$; quartz has a refractive index of 1.5 and glass has a refractive index of 1.33.)

Different RI will cause the speed of light to change. NA will be larger if you use quartz.

9. Application: A polarizer is a device that is often used with un-polarized light to create polarized light. A polarizer is placed between the light source and the condenser. If a linear polarizer were used, what would happen to the light that passed through the microscope? Would the use of a polarizer have an effect on the signal intensity?

Linearly polarized light will only be allowed to pass thus lowering the amount of light that is able to pass through the optical system. This will affect the image resolution.

10. Application: Typically the source used in optical microscopy is considered to produce white or polychromatic light, but often only a few wavelengths of light are of interest. This is accomplished by placing a filter after the light source. What would be the disadvantages of using filters? Name two disadvantages.

Light intensity will be decreased; wavelength of incoming light will be narrowed.

Gain and exposure times will need to be changed between each filter if more than one is being used.

Many filters will need to be used if a broad wavelength of light is of interest. This can get expensive.

Working with one filter or a grating is quick to collect. Only requires one image. Working with multiple filters requires multiple images to be collected.

CHAPTER 6. CONCLUSIONS

It has been shown in the previous chapters that nanoparticles can be used for chemical sensing and cellular imaging with minimal interruption of normal cellular activity. The optical responses of nanoparticles were monitored as they were used for chemical and biological sensing using DIC microscopy.

Gold nanospheres were used to detect cytochrome c in microchannels and cancer cells undergoing ethanol induced apoptosis with PRET. As cytochrome c conjugated to the surface of the gold spheres, the DIC contrast spectra of the spheres showed spectral dips. These spectral dips were located where the extinction spectra of the gold spheres and absorption spectrum of cytochrome c overlap.

Gold-capped mesoporous silica nanoparticles were uncapped with dithiothreitol in flow cells and glutathione in lung cancer cells. It was shown that the uncapping process of gold-capped MSNs could be monitored with DIC microscopy by measuring the contrast changes as gold was cleaved from the MSNs. This allows the entire process of drug delivery to now be monitored, rather than merely monitoring fluorescent dye diffusion. It is essential to understand the entire drug delivery process to design an ideal drug delivery vector.

Nanoparticles are great as contrast agents to understand cellular processes, understand cellular mechanisms, and to understand drug delivery at the cellular level. They are ideal probes because they offer high signal to noise ratios, can be imaged for long periods of time and have easy synthesis and surface modification. However, there are a few drawbacks to using gold nanoparticles for cellular imaging diagnostics in the medical community.

The biggest issue facing nanoparticles is their toxicity *in vivo* and biodistribution. On the whole, gold can induce a high production of ROS in cells which can lead to inflammation and

eventually kill the cell through ROS induced apoptosis.[119] Gold can also cause respiratory issues when they are in the lungs.[120] One method to circumvent this would to have biodegradable nanoparticles that do not interfere with the biological system and do not stick around in the body for years to come. To date, there are very few commercially available biodegradable drug or gene delivery vectors, such as poly-D,L-lactide-co-glycolide (PLGA), poly-ε-caprolactone (PCL), and polylactic acid (PLA).[121] Yet they are highly cytotoxic when they degrade.[122]

The toxicity and biodistribution of drug delivery vectors needs to be studied more *in vivo*, not in vitro as the nanoparticles will be interacting with different environments *in vivo* versus *in vitro*. The different biological environments can lead to varying surface chemistry of nanoparticles, as seen with the recent studies of the protein corona on nanoparticles. The overall biocompatibility of gold nanoparticles and drug delivery vectors needs to be improved, or an efficient method to retrieve non-degradable nanoparticles after they have delivered the drug. An ideal delivery agent would have a high loading efficiency, have reproducibility and stability, while also being biodegradable to benign compounds to lessen the cytotoxic effects after degradation.[122] Delivery systems should also have targeting ability in order to alleviate negative interactions with non-targeted areas of the body and increase efficacy so drugs are not delivered to areas that are not affected by the disease being treated.[123]

The other portion of this dissertation includes research in analytical chemical education. An optical microscopy laboratory experiment was created that utilized a dark field microscope to image reactions and nanoparticles. The student learning gains were monitored through laboratory reports and the Chemical Optical Microscopy Assessment. Based upon this study, students studying optical microscopy learn best from an inquiry approach rather than a traditional instruction method. The optical microscopy experiment was created in an effort to update

instrumental analysis curriculum to engage students with current analytical chemistry research methods and prepare them for future careers in STEM.

Analytical chemistry curriculum needs to be updated to reflect current analytical chemistry research methods. The instruction of upper division undergraduate education needs to be improved because there is little going on in analytical chemical education in terms of inquiry based instruction or other alternative methods to traditional lab and lecture. There is also very little research being done in how students comprehend analytical chemistry and instrumental analysis, common misconceptions and how to circumvent these.

One obstacle in analytical chemical education is the lack of consistency in the curriculum of quantitative analysis and instrumental analysis, unlike other disciplines in chemistry such as general chemistry and organic chemistry. In general chemistry all students learn about moles and stoichiometry and all students learn about synthesis in organic chemistry. Analytical chemistry should be held to the same standards as the other chemistry disciplines.

It was Alexander Smith in 1902 who said that the chemistry lab should play two central roles 1) verification of chemical principles and 2) independent discovery of knowledge.[45] It is one of my career goals to help chemistry students become independent discoverers in the chemistry laboratory.

REFERENCES

(1) Naik, E.; Dixit, V. M. *The Journal of Experimental Medicine* **2011**, *208*, 417.

(2) De Jong, W. H.; Borm, P. J. *Int J Nanomedicine* **2008**, *3*, 133.

(3) Kumari, A.; Yadav, S. K.; Yadav, S. C. *Colloids and surfaces. B, Biointerfaces* **2010**, *75*, 1.

(4)	Du, J.; O'Reilly, R. K. *Soft Matter* **2009**, *5*, 3544.

(5)	Brewer, E.; Coleman, J.; Lowman, A. *Journal of Nanomaterials* **2011**, *2011*, 1.

(6)	Abraham, M. R. In *Chemists' Guide to Effective Teaching*; Pienta, N. J., Cooper,

M. M., Greenbowe, T. J., Eds.; Pearson: New Jersey, 2005; Vol. 1.